General Disclaimer

One or more of the Following Statements may affect this Document

- This document has been reproduced from the best copy furnished by the organizational source. It is being released in the interest of making available as much information as possible.

- This document may contain data, which exceeds the sheet parameters. It was furnished in this condition by the organizational source and is the best copy available.

- This document may contain tone-on-tone or color graphs, charts and/or pictures, which have been reproduced in black and white.

- This document is paginated as submitted by the original source.

- Portions of this document are not fully legible due to the historical nature of some of the material. However, it is the best reproduction available from the original submission.

D6-60105-3

EXPERIMENTAL L-BAND SST SATELLITE COMMUNICATIONS/SURVEILLANCE TERMINAL STUDY

VOLUME IV

AIRCRAFT ANTENNA STUDIES

by

W. V. Kiskaddon and Duncan M. Carman

November 1968

Prepared under Contract No. NAS 12-621 by

BOEING

COMMERCIAL AIRPLANE DIVISION
RENTON, WASHINGTON

for

Electronics Research Center

NATIONAL AERONAUTICS AND SPACE ADMINISTRATION

EXPERIMENTAL L-BAND SST SATELLITE COMMUNICATIONS/SURVEILLANCE TERMINAL STUDY

VOLUME IV

AIRCRAFT ANTENNA STUDIES

by

W. V. Kiskaddon and Duncan M. Carman

November 1968

Prepared under Contract No. NAS 12-621 by

BOEING

COMMERCIAL AIRPLANE DIVISION
RENTON, WASHINGTON

for

Electronics Research Center

NATIONAL AERONAUTICS AND SPACE ADMINISTRATION

EXPERIMENTAL L-BAND SST SATELLITE
COMMUNICATIONS/SURVEILLANCE TERMINAL STUDY

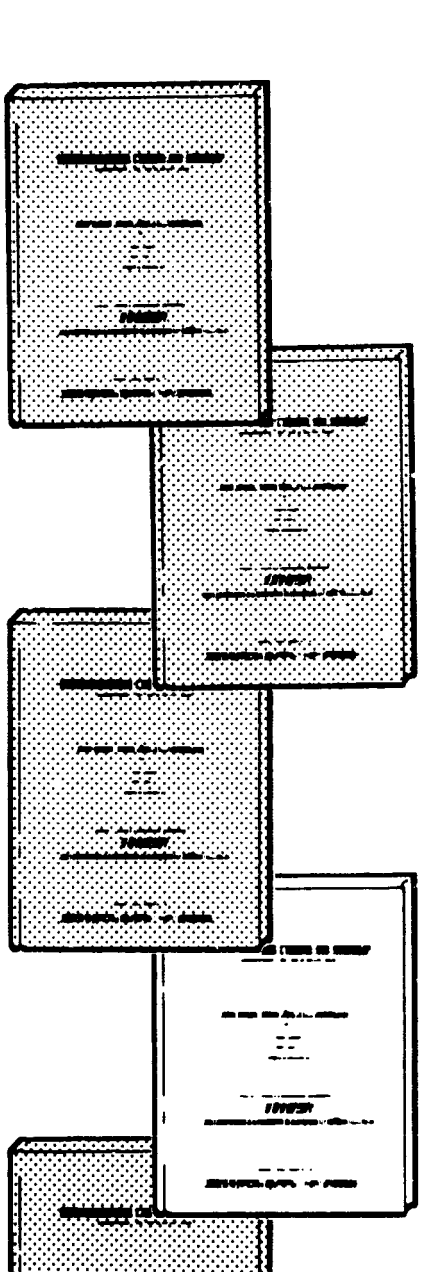

VOLUME I
STUDY SUMMARY

VOLUME II
OPERATIONAL REQUIREMENTS STUDY

VOLUME III
COMMUNICATIONS/SURVEILLANCE ANALYSIS

VOLUME IV
AIRCRAFT ANTENNA STUDIES

VOLUME V
AIRCRAFT TERMINAL DEFINITION

CONTENTS

CONTENTS—Concluded

FIGURES

FIGURES–Concluded

TABLES

EXPERIMENTAL L-BAND SST SATELLITE COMMUNICATIONS/SURVEILLANCE TERMINAL STUDY

VOLUME IV: AIRCRAFT ANTENNA STUDIES

By W. V. Kiskaddon and Duncan M. Carman
The Boeing Company

SUMMARY

The L-band antenna system considered for the SST for satellite communications must satisfy gain requirements imposed by power-limited voice links between the satellite and aircraft and also meet the flush-mounted constraint imposed by the aerodynamics of the SST. The results are presented of an analytic and experimental evaluation carried out as part of NASA/ERC contract NAS 12-621 to develop antenna requirements for the SST aircraft terminal..

Antenna coverage and gain criteria, multipath rejection requirements, and environmental limits of the antenna system are described for an experimental terminal capable of demonstrating surveillance and voice communications in the 1540- to 1660-MHz (L-band) frequency range. Data on low-gain antennas, mechanically steered antennas, phased arrays, and possible antenna locations on the SST are provided. Selection of possible antenna systems is discussed for an airplane experimental terminal capable of operation with satellites having EIRP's between 24 and 40 dBW.

Experimental patterns of a circularly polarized orthogonal-mode-cavity antenna mounted on a cylinder simulating the SST are used as the basis for the low-gain antenna discussion. Different antenna systems are then described that are capable of providing minimum gains of -1 dB, 3 to 6 dB, 7 to 10 dB, and 13.5 to 18 dB over the upper hemisphere for the SST experimental system, and a recommended system antenna implementation is described. Operational satellite capability is discussed in describing the growth of the aircraft antenna system to an operational configuration permitting full-time ATC communications/surveillance operation for North Atlantic air traffic.

1.0 INTRODUCTION

It has been recognized from the inception of this program that the requirements established for an airborne terminal antenna would be one of the most significant results of the study. To establish the airborne terminal requirements, a detailed operations study was performed with the goal of identifying the quantitative information transfer requirements between a typical airborne terminal and the ground terminal. Concurrently, a study aimed at optimizing the methods of information transfer between the airborne and ground terminals was pursued. Included in this study was an analysis of surveillance schemes, voice and digital modulation techniques, methods of access and control, the effects of the propagation medium on system performance, and the limitations imposed by the external and internal noise environments at the airborne terminal.

The ultimate goal of these two major studies was to establish the overall system requirements so that the tradeoffs between the airborne terminal characteristics and those of other elements of the system could be identified. A range of terminal antenna performance requirements was established on the basis of these tradeoff studies and was used as a guide for the antenna studies and experimental efforts.

This document describes the analytical and experimental efforts on the airborne antenna performed during this study. A preliminary analysis of the system requirements led to the conclusion that both low-gain, fixed-beam antennas and steerable, medium-gain antennas should be considered for the airborne terminal. Because weight and drag on a supersonic airplane are critically important, a study of flush-mounted antenna configurations was made.

The basic antenna system requirements are discussed in Sec. 2.0. Sections 3.0 through 5.0 describe candidate low-gain, mechanically steered, and phased-array antennas. Potential locations for the various categories of antennas are considered in Sec. 6.0. The antenna systems applicable to the experimental terminal are described in Sec. 7.0, and specific recommendations are given for the experimental terminal in Sec. 8.0. The growth of the antenna system to an operational terminal concept is considered in Sec. 9.0. Also described in Sec. 9.0 is a Boeing concept of a steerable satellite antenna; this type of antenna is an implicit requirement in some of the low-gain airborne terminal concepts considered.

A state-of-the-art antenna survey trip was made as part of this program. Information resulting from the survey appears throughout the volume where applicable.

The antenna analysis and developmental studies reported in this volume were conducted in close liaison with the system requirements analysis. The following personnel made significant contributions to the antenna study:

Technical direction and high-gain-antenna studies	W. V. Kiskaddon
Low-gain antenna and mechanically steerable antenna studies	D. Hutchinson
Multipath considerations	D. M. Carman
Range pattern measurements	J. Hyde

2.0 ANTENNA SYSTEM REQUIREMENTS

Determination of the specific airborne-terminal antenna requirements have resulted, in part, from systems analyses and tradeoff studies that were not completed until the second half of phase I. For the antenna system studies and the developmental effort conducted at the beginning of the program, certain requirements were assumed. It was believed that these requirements would be included in the range of requirements resulting from the system studies. In particular, an initial assumption was that antenna gain requirements might range from a low of zero dB to as much as 20 dB; accordingly, antenna configurations with gains in this range were studied. Similarly, an assumption was made and studies directed toward a power-handling capability for the terminal antenna ranging from 100 to 1000 watts.

These two critical assumptions have proven valid. The terminal description in vol. V required an antenna gain and power-handling capability that fell within these assumed limits.

2.1 Basic Parameters

Although the specific antenna requirements were not available at the beginning of the program, there were several parameters that could be identified before completion of the system studies. These parameters are operating frequency range, impedance, polarization, and environmental requirements.

2.1.1 Operating frequency.– The operating frequency of the system is in the 1540- to 1660-MHz aeronautical communications band. The choice of this band was a basic condition established by NASA/ERC; hence, no frequency tradeoff studies were performed during the program.

The airborne terminal antenna will transmit in the 1640- to 1660-MHz band and receive at 1540 to 1560 MHz. This is in agreement with the recommendations of the FAA.

2.1.2 Impedance. - The impedance of the terminal antenna will be such that the voltage standing-wave-ratio (VSWR) does not exceed 1.5:1 at any frequency in the transmit or receive band. This ensures that the system loss attributable to mismatch between the antenna and its transmission line does not exceed 0.2 dB.

2.1.3 Polarization.– The relative-attitude variations between the aircraft and a satellite and the possibility of Faraday rotation effects require that circular polarization be used on either the satellite or the aircraft, or both, to ensure no complete loss of signal. The effect of noncircularity (ellipticity) on polarization loss between two terminals is discussed by Hartop (ref. 1) and must be considered in the antenna design. Since there is an inherent 3-dB loss in the link if one terminal is circularly polarized and the other is linearly polarized, circularly polarized antennas were emphasized during the study.

2.1.4 Environmental requirements.– Environmental criteria described in ref. 2 are typical of those to which the SST will be developed. Parameters applicable to the terminal antenna system are shown in table 1. Specifically, the terminal, including the antenna system, must be capable of operation at altitudes up to 75 000 feet and satisfy requirements similar to those in table 1. Although this environment is considerably more severe than that experienced by present commercial aircraft, flush-mounted, L-band annular slot antennas have been qualified for similar environments for military aircraft.

TABLE 1.– TYPICAL SST ENVIRONMENTAL CRITERIA

Parameter	Extreme values
External acoustic environment – maximum noise level	165 dB
External acoustic environment (spectra at takeoff)-peak level	144 dB at 42.5 Hz
Acoustic noise environment in unconditioned compartments	min.: 80 dB at 53 Hz max.: 143 dB at 425 Hz
Acoustic noise environment in conditioned compartments	min.: 75 dB at 53 Hz max.: 128 dB at 850 Hz
Vibration envelope– power spectral density (g^2/Hz) vs frequency	min.: 1.8×10^{-4} at 53 Hz max.: 10 at 150 Hz
Flight ambient temperatures	min.: -123° F max.: 102° F
Equilibrium skin temperature	min.: 410° F max.: 480° F stagnation: 500° F
Temperature in unconditioned compartments	min.: -50° F max.: 480° F

2.2 Antenna-Coverage Requirements

Determination of the antenna look-angle profile from a moving airplane to one or more geostationary satellites is essentially a geometrical problem. Families of antenna look-angle profiles can be established as functions of the number of satellites and their locations and of the flight path, attitude, and altitude of the airplane. This analysis, because it is geometric, is performed independently of studies on antenna gain requirements or any of the basic rf parameters discussed in Sec. 2.1. However, it is apparent that if the basic parameters of polarization and frequency are known and if the airplane antenna-gain requirement is established by an appropriate rf link analysis, a specific pointing-angle profile is the only remaining information needed to define the antenna requirements for the flight path associated with the specific profile.

The propagation analysis model described in Sec. 6.0 of vol. III has a subroutine that performs calculations of the look-angle profile. This subroutine, which is programmed for a CDC 6600 computer, was used to calculate look-angle profiles for a series of typical flight paths.

2.2.1 Antenna look-angle profiles for typical airline routes.– Examples of the bearing and elevation angles to the satellite from the airplane are shown in figs. 1 through 6 for the New York-to-London, Chicago-to-Copenhagen, and Buenos Aires-to-Dakar great-circle routes. Satellite locations are shown parametrically, ranging from 0° to 70° W longitude.

No airplane maneuvers are considered in figs. 1 through 6, because it is assumed that the airplane does not deviate from the prescribed great-circle route. The subroutine can, however, include attitude excursions if inputs describing these excursions are made.

2.2.2 Antenna-pointing requirements: New York to London.– The antenna-pointing profile for the New York-to-London route may be determined by referring to figs. 1 and 2. Assume that there are two satellites, one located at longitude 10° W and the other at longitude 50° W and that the airplane must look at both simultaneously for a surveillance mode and at either one for a communications mode. This configuration is typical of what might be established for an advanced pre-operational test.

For surveillance, the antenna system must look from the right side of the airplane simultaneously at: (1) 14° elevation, 31° forward of broadside, and (2) 36° elevation, 10° aft of broadside when near New York, and from (1) 29° elevation, 10° forward of broadside, and (2) 19° elevation, 33° aft of broadside, when near London. The voice communications antenna can look at either satellite, but only one at a time is required. On the return trip, corresponding coverage on the left side of the airplane is necessary. The resulting minimum-sector-coverage requirements for the terminal antenna using the range coordinate system described in Sec. 3.1 are $52° < \theta < 78°$ in elevation and both $57° < \phi < 123°$ and $237° < \phi < 303°$ in azimuth. That is, a minimum sector width of 26° in elevation and 66° in azimuth is required.

FIGURE 1.– ELEVATION ANGLE TO SATELLITE: NEW YORK-LONDON

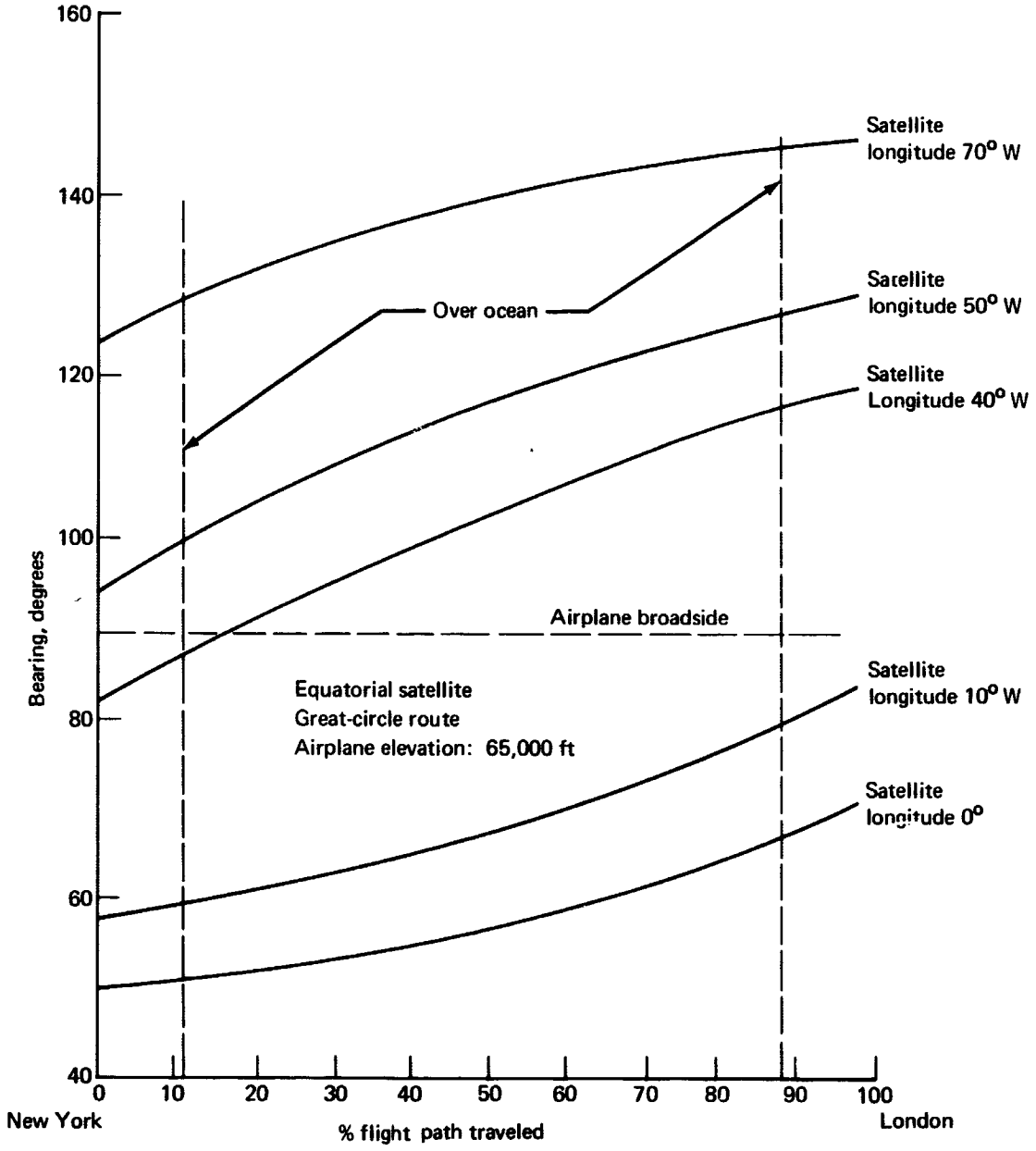

FIGURE 2.– BEARING TO SATELLITE: NEW YORK-LONDON

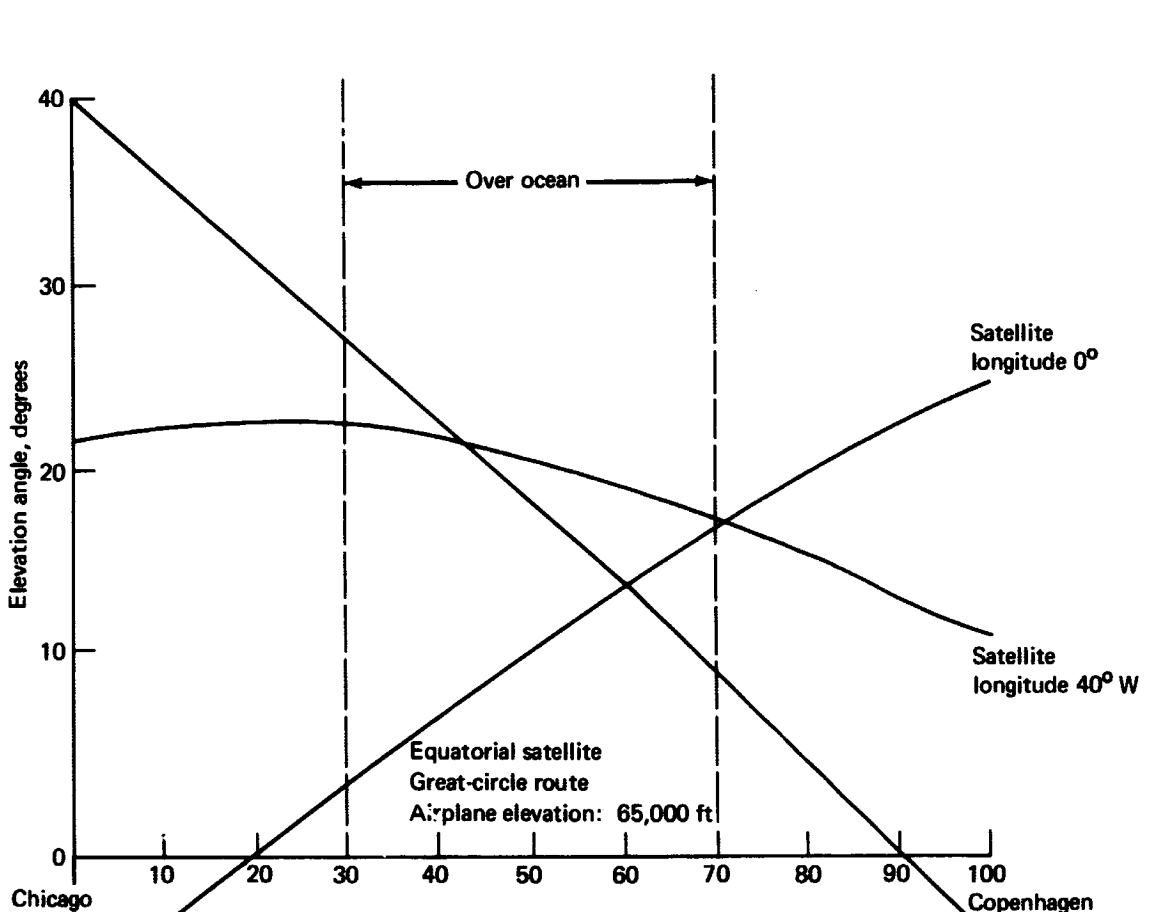

FIGURE 3.– ELEVATION ANGLE TO SATELLITE: CHICAGO-COPENHAGEN

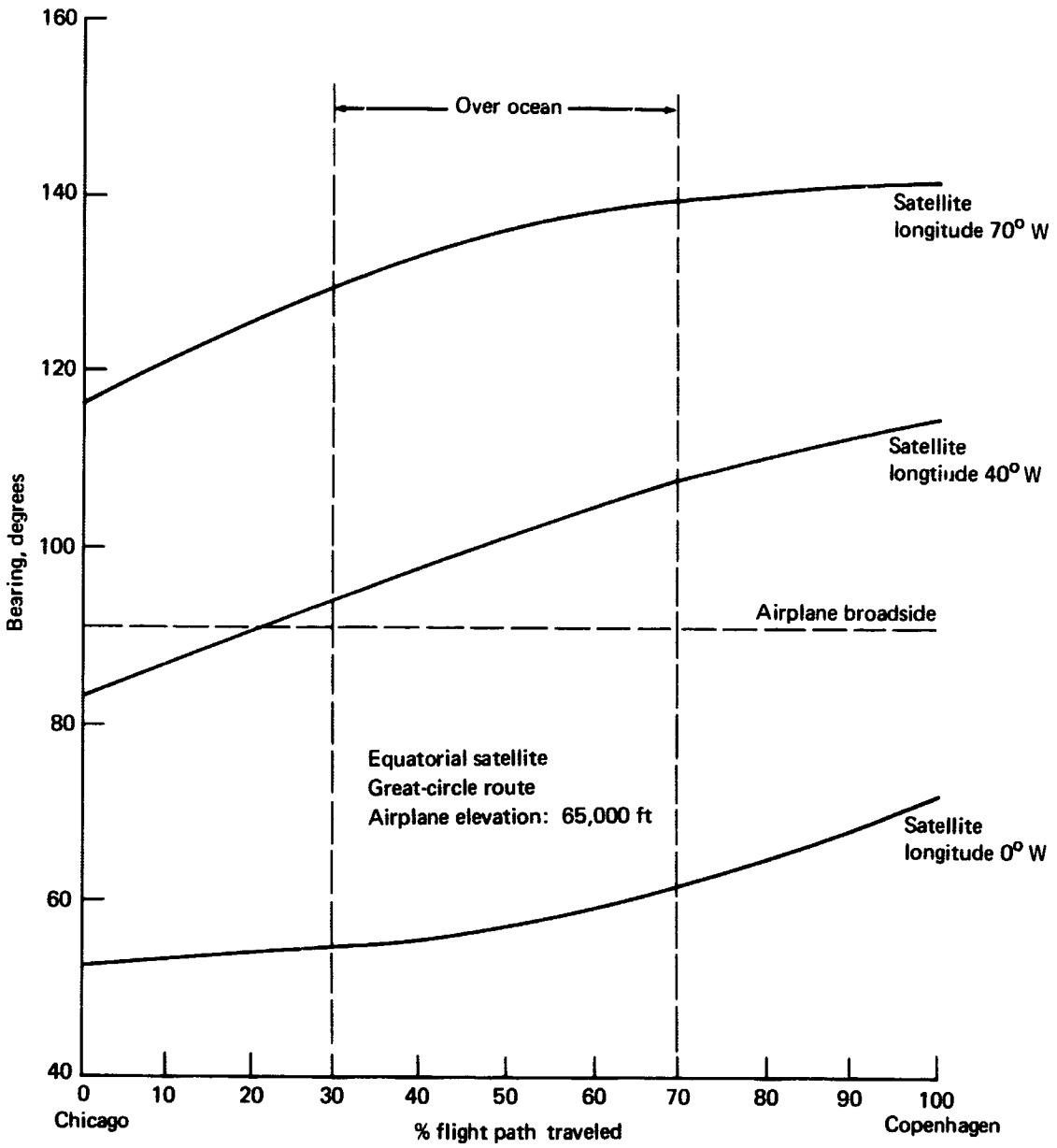

FIGURE 4.– BEARING TO SATELLITE: CHICAGO-COPENHAGEN

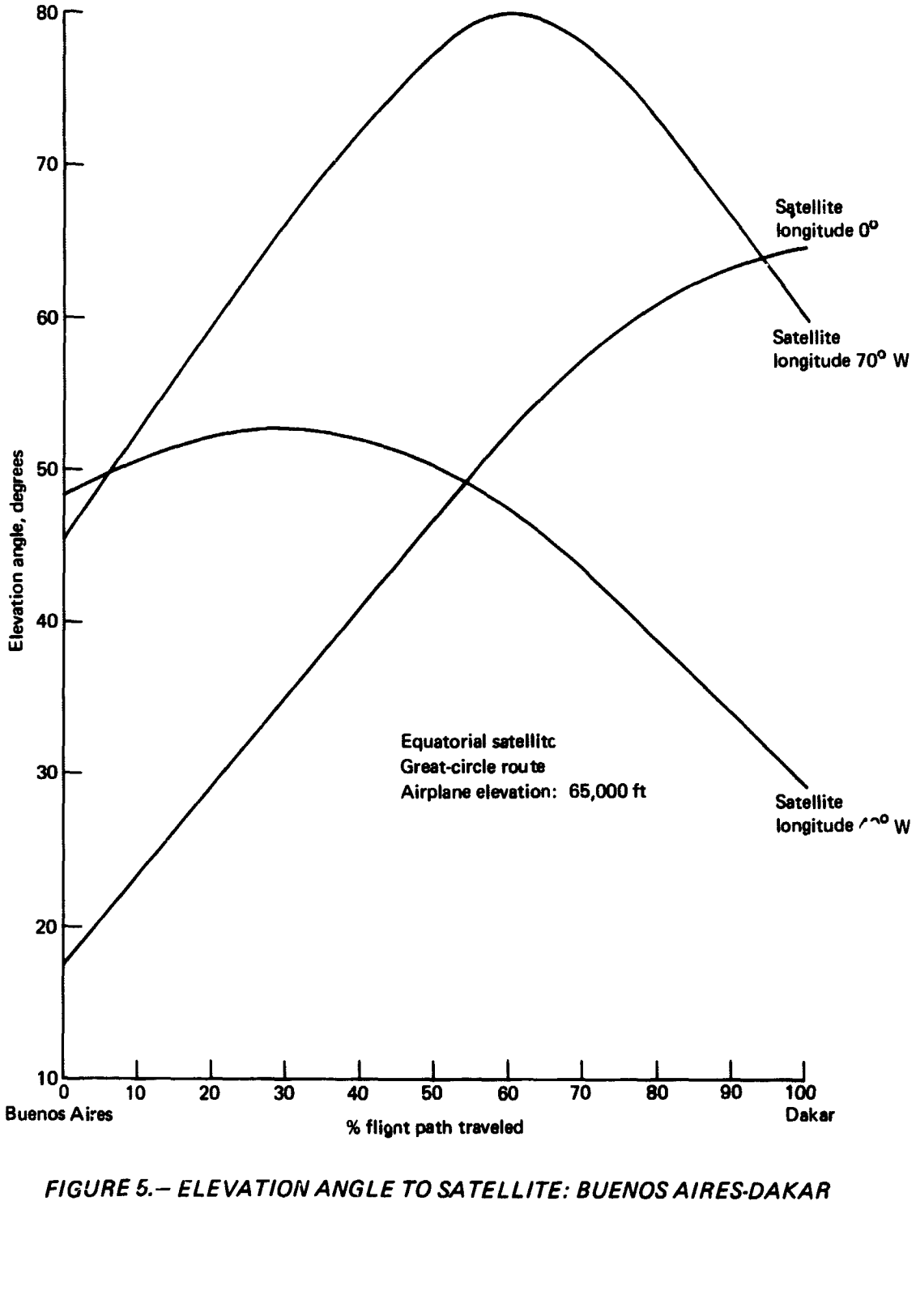

FIGURE 5.– ELEVATION ANGLE TO SATELLITE: BUENOS AIRES-DAKAR

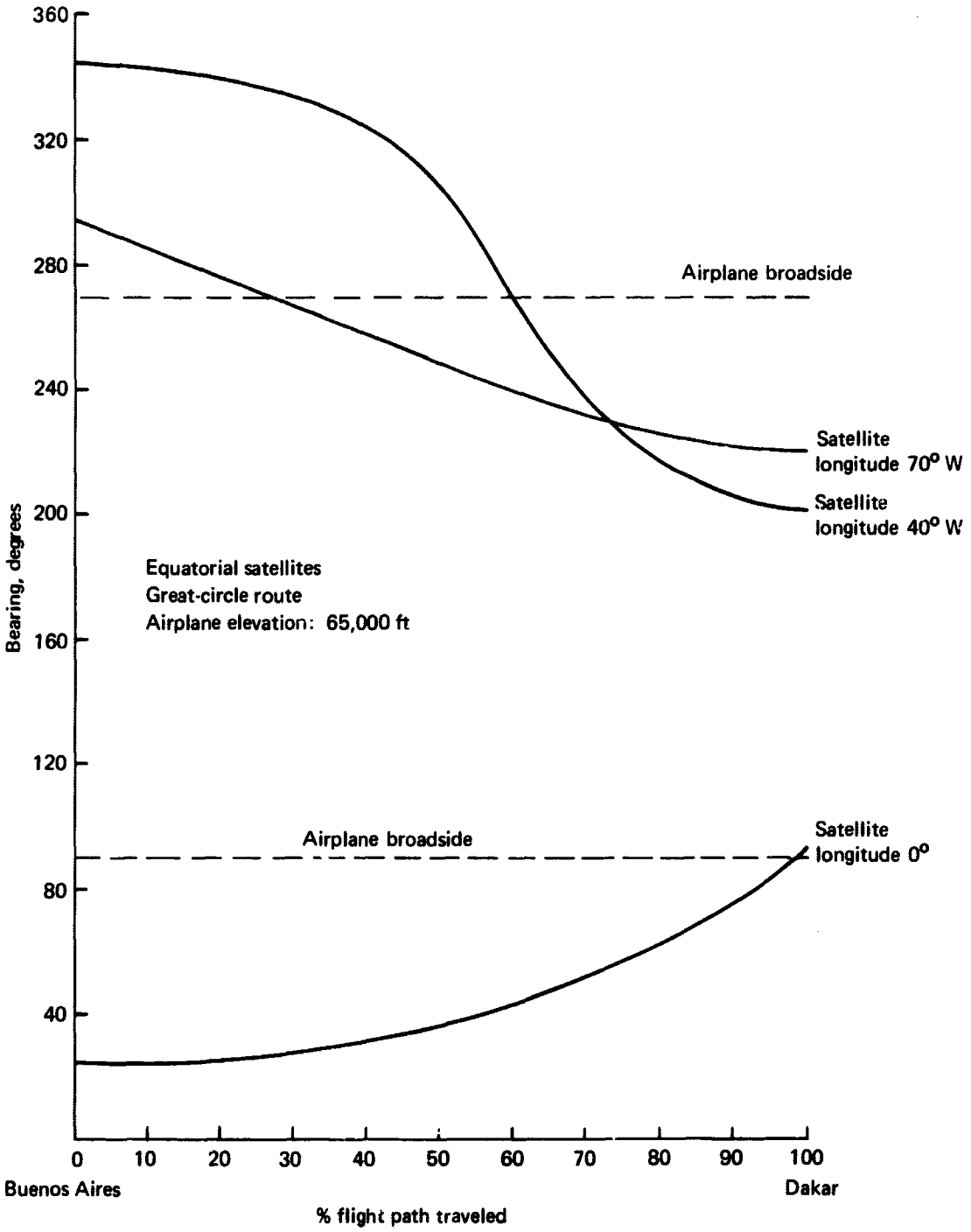

FIGURE 6.– BEARING TO SATELLITE: BUENOS AIRES-DAKAR

2.3 Experimental-Terminal Satellite-To-Airplane Link Performance

The communications and surveillance systems analysis described in vol. III generated, as a part of that study, a series of link tradeoff charts. Figures 7 and 8 show the two graphs that are of most significance in establishing requirements for the airplane antenna. They show the interrelationship of satellite EIRP, airplane antenna gain, and airplane transmitter power for a single-channel experimental voice link and a tone surveillance link. This information was developed during the latter half of the program and has been used in the antenna pointing-profile studies to develop the antenna requirements for the experimental terminal, as described in vol. V. All conditions and qualifications applying to the charts are stated, except the multipath fade margin, which is discussed in Sec. 2.4.

In particular, the voice-link chart (fig. 7) shows the significant tradeoffs that can be made between satellite EIRP and aircraft antenna gain. Although these tradeoffs are discussed in detail in vols. III and V, it is worth noting again that simple, switchable aircraft antennas are feasible for use with a multichannel voice-surveillance system if a limited coverage and/or a steerable satellite antenna is used.

2.4 Multipath Rejection Requirements

In Sec. 2.2, it was stated that if the antenna pointing profile is known and the antenna gain requirement is established, then the antenna requirements are completely defined. Implicit in that statement is that in determining the antenna gain requirement, a multipath fade margin was considered that would ensure a specified link-continuity exceedance level, generally 99%. For antenna pointing-angles near the horizon ($<5°$), the required fade margin, in general, increases for a given exceedance level; hence, the difference must be accounted for by increased antenna gain or improved multipath rejection, or both. Thus, antenna pointing profile and antenna gain are not independent, but are related at low angles by the multipath problem.

Any antenna design should attempt to maximize response to the direct signal between the airplane and the satellite and exhibit a minimum response to the signal reflected from the earth's surface.

The ratio of the direct-wave gain to the reflected-wave gain at a particular angle of arrival is defined as the multipath discrimination factor. For a circularly polarized system, this multipath discrimination factor is maximized by an aircraft antenna pattern that is nearly circularly polarized for the direct path and has a high axial ratio for the reflected-wave path.

A complete discussion of multipath is presented in Sec. 6.2.3 of vol. III. The antenna radiation-pattern effects are discussed in detail in Sec. 6.2.4. Included is an example of the discrimination factor of the orthogonal-mode cavity antenna for the antenna mounted on a cylinder simulating the SST. The gain of the antenna (shown in Sec. 3.2, fig. 13) at 10° above the horizon for the top-mounted antenna is -1.5 dB. Mounted 30° from the top of the aircraft, the gain at 10° above the horizon is +3 dB. The ellipticity ratio of the top-mounted antenna is 11 dB at 10° above the horizon and 22 dB at 10° below the horizon. For the antenna mounted 30° from the top of the aircraft, the ellipticity is 5 dB for 10° above the horizon and 7 dB for 10° below the horizon. For 99% time availability of communications when flying over a smooth sea (sea state 1 as defined in vol. III), the necessary fade margin allowance in the link budget calculation for the antenna mounted on top of

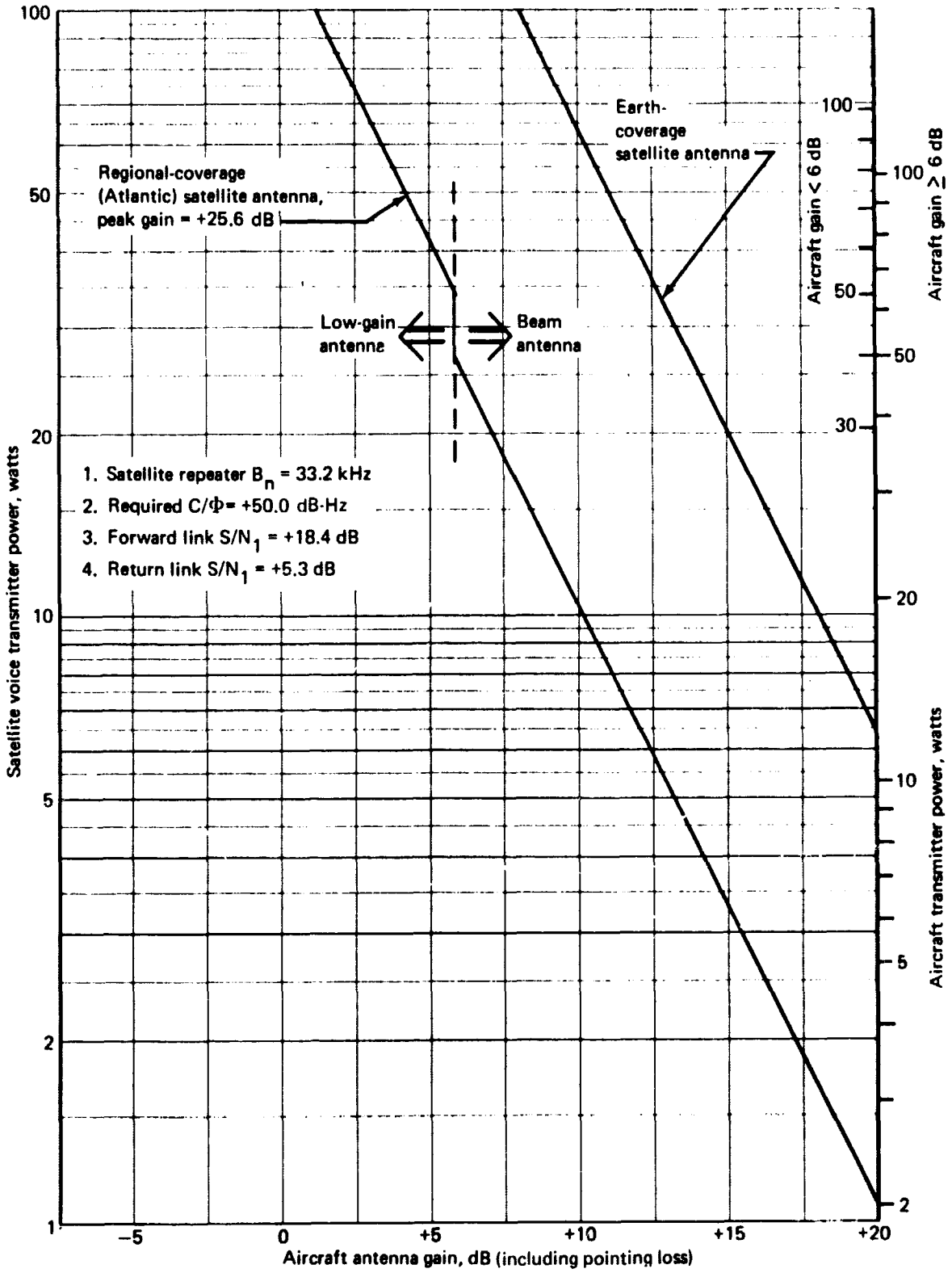

FIGURE 7.– EXPERIMENTAL-TERMINAL SINGLE-CHANNEL VOICE LINK PERFORMANCE

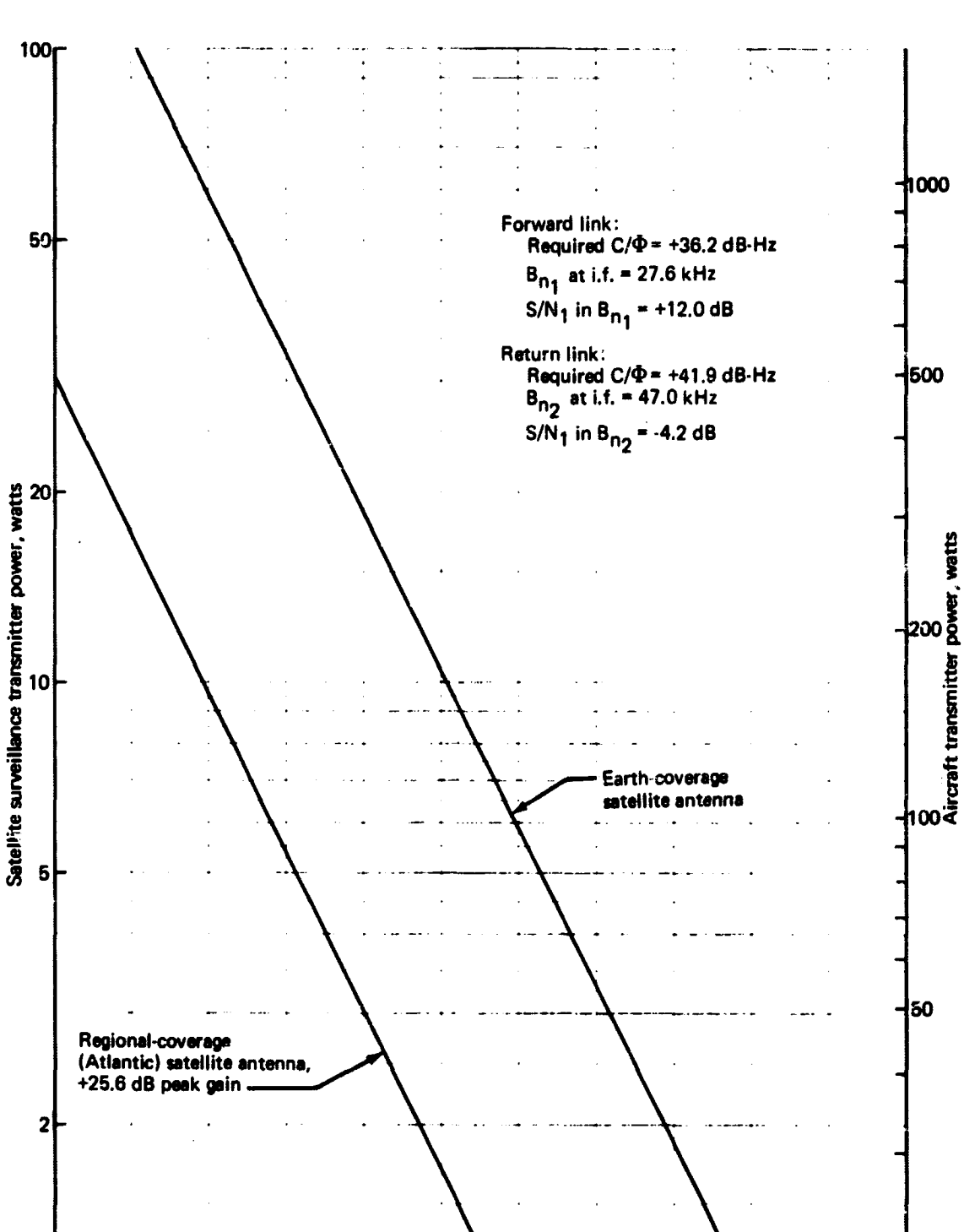

FIGURE 8.– TONE SURVEILLANCE LINK PERFORMANCE

the airplane is 1.9 dB. If the antenna were mounted 30° from the top of the airplane, the necessary fade margin allowance would be 4.2 dB. While the antenna gain has increased 4.5 dB, the fade margin has increased 2.3 dB. Thus, the net system improvement is only 2.2 dB.

It should be emphasized that the effects of the wings and tail are not present because the experimental patterns were taken on a model cylinder. A complete evaluation of a recommended system would include patterns taken on a model of the aircraft.

Because of the interrelation of ellipticity and gain at the angles of interest, both must be considered in defining a requirement for the antenna system. The differences in gain and ellipticity ratio for the angles corresponding to the direct- and reflected-ray paths are important criteria. The antenna requirements to provide a given maximum fade margin for elevation angles of incidence of 10° and 20° above the horizon can be found from figs. 9 and 10 for a 99% time availability of communication. These curves show that for a given antenna discrimination factor, the multipath fade-margin requirement is greater for a 20° elevation angle than that for 10°. This fact is substantiated by the analysis described in Sec. 6.2, vol. III. It should be noted, however, that for low elevation angles ($< 5°$), large fade margins are required because of the magnitude of the multipath and the inability of the antenna to provide adequate discrimination.

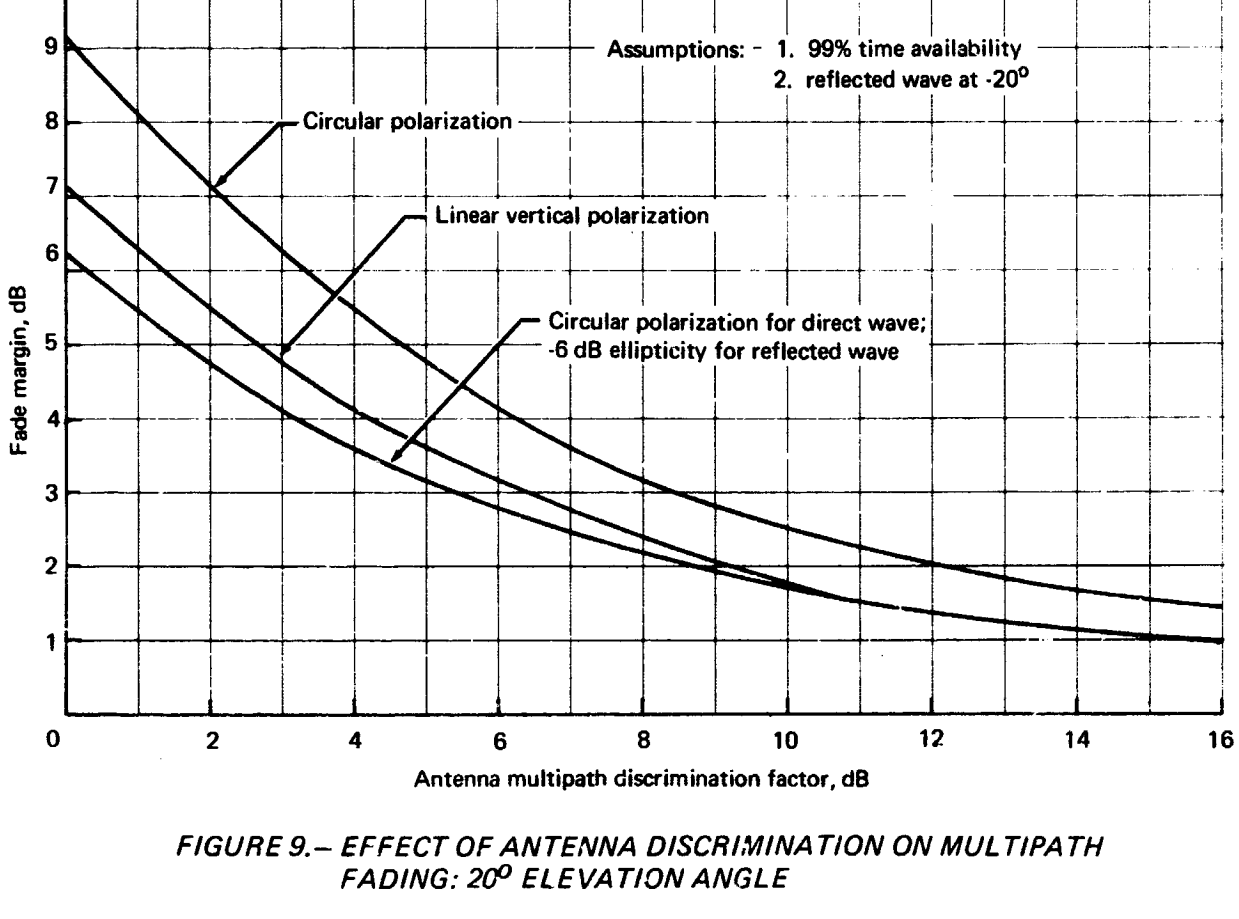

FIGURE 9.– EFFECT OF ANTENNA DISCRIMINATION ON MULTIPATH FADING: 20° ELEVATION ANGLE

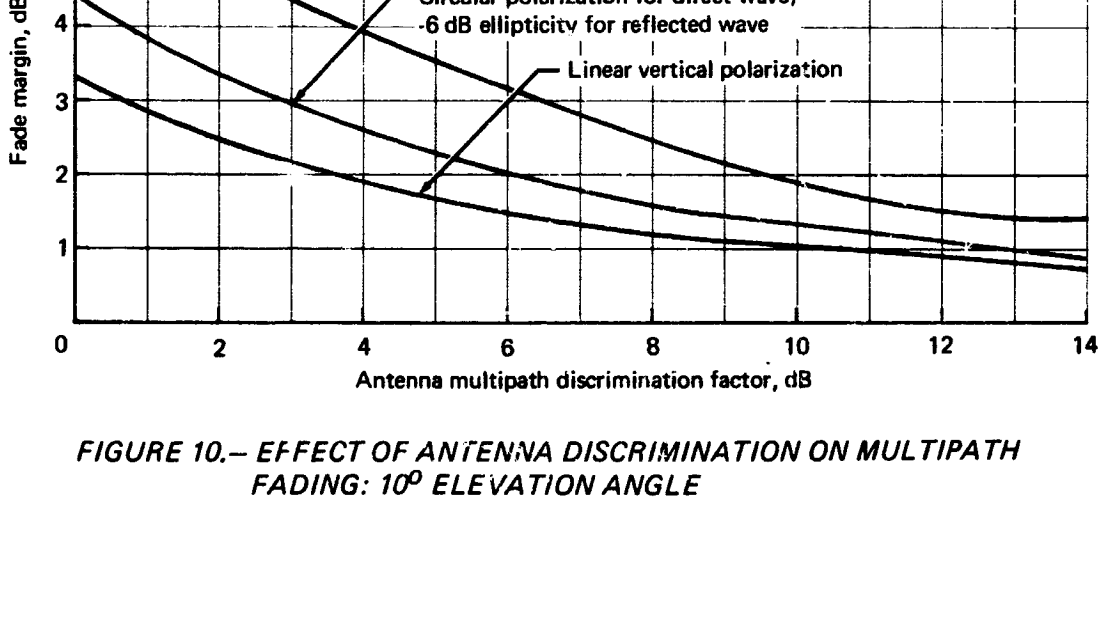

FIGURE 10.– EFFECT OF ANTENNA DISCRIMINATION ON MULTIPATH FADING: 10° ELEVATION ANGLE

3.0 LOW-GAIN ANTENNAS

It was assumed at the beginning of the program that the antenna gain requirements for the experimental terminal might fall anywhere between zero dB and 20 dB, depending on the results of the detailed systems analysis studies. Also, there was some thought given to using separate antennas for the surveillance and communications functions, because the coverage and gain requirements were believed to be quite different, based on the rather limited preliminary link analyses that had been performed. There was sufficient indication of the potential need for a low-gain, upper-hemispherical-coverage, circularly polarized antenna to initiate a laboratory development program. This program resulted in adaptation of an existing Boeing-designed, dual-mode cavity-backed four-arm, planar, log-spiral antenna (ref. 3) and an experimental demonstration of the feasibility of the orthogonal TE_{11}-mode cavity antenna.

The orthogonal-mode cavity was selected for the experimental study because of the expected good low-angle coverage associated with its small aperture and because of its small size and relative simplicity. These predicted advantages were confirmed in the laboratory.

The planar, log spiral antenna has good coverage but shows no advantage over the orthogonal-mode antenna and does, of course, have the disadvantage of a relatively complex feed and mode-switching network.

During the antenna state-of-the-art survey, discussions were held with personnel at American Electronics Laboratory (AEL) and Motorola about their efforts in low-gain antenna development. AEL is developing a circularly polarized, crossed-slot antenna for a satellite communications application (ref. 4). The expected performance would be similar to that of the orthogonal-mode antenna.

Motorola (ref. 5) is currently studying the properties of dielectric-loaded, cavity-backed spiral antennas. It is also developing a cavity-backed, conical spiral antenna.

3.1 Radiation-Pattern Measurements

Radiation patterns of the orthogonal-mode and planar log-spiral antennas were taken at the pattern measurement facilities of the Commercial Airplane Division. The specific pattern range used has a two-axis model positioner/tower combination on a trailer, providing a variable length to 500 feet. Scientific-Atlanta pattern range instrumentation is used throughout. The range is equipped to provide polar or rectangular analog patterns in relative power, relative field voltage, or decibels. Eight-bit binary coded decimal data in decibels on 1-inch paper tape and/or on an IBM output typewriter are available. The instrumentation also includes an automatic integrator that is used to determine the radiation pattern directivity.

The antenna radiation pattern coordinate system used for all experimental work is shown in fig. 11. The two-axis model positioner provides the coordinate direction movements indicated by θ and ϕ on the coordinate system diagram. A polarization positioner provides the capability for changing the electric-field vector polarization from $E(\theta)$ to $E(\phi)$ or any intermediate angle. Continuous rotation of this positioner enables recording of polarization patterns from which the ellipticity ratio can be determined.

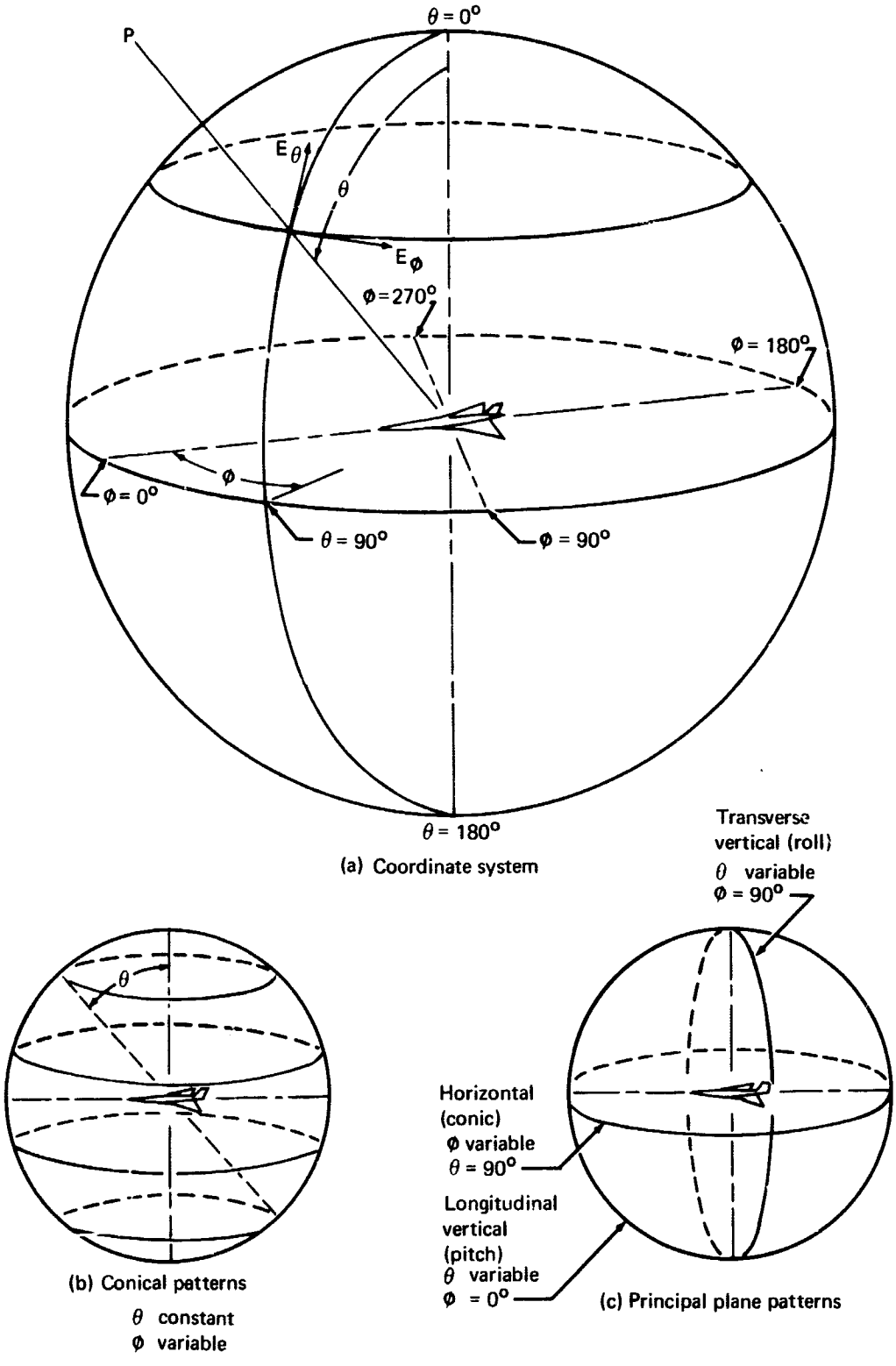

FIGURE 11.– ANTENNA RANGE COORDINATE SYSTEM

Because of the requirement for circular polarization on the airplane, it would have been desirable to have investigated the received field of the antennas with circularly polarized illuminators. However, since such illuminators were not available for the 9.6-GHz model frequency, all experimental radiation patterns were recorded for the two linear components, $E(\theta)$ and $E(\phi)$. To obtain the equivalent circularly polarized gain, the linear field components were combined using relationships developed by Kraus (ref. 6). This is possible when the phase relationships between the linear components $E(\theta)$ and $E(\phi)$ are known. This relationship is determined from the ellipticity ratio measurements described above. The Kraus model was programmed for a computer solution that resulted in a matrix-type printout from which the circularly polarized gain could be obtained, given the gain difference of the two linear components and their phase difference.

3.2 Orthogonal-Mode Cavity

The orthogonal-mode cavity antenna (fig. 12), consists of a right-circular cylindrical section about 0.7 wavelengths in diameter in which orthogonal TE_{11} circular waveguide modes are excited 90° out of time phase to provide circular polarization. The aperture size is reduced to slightly less than 0.5 wavelengths by an annular iris so that a broader pattern can be obtained. A 90°, 3-dB stripline hybrid mounted on the bottom of the cavity is used to provide the proper phase and power division for circular polarization. The preliminary, linearly polarized impedance model of the antenna is shown in fig. 12.

Power handling up to 1 kW average power is predicted for this antenna. There are L-band annular slot configurations on the market qualified to similar environments and even higher power levels for which the aperture voltage gradients at equivalent power inputs would not be significantly different. However, for power levels greater than 300 watts, the stripline hybrid must be replaced by a waveguide or coaxial hybrid.

Experimental radiation-pattern data have been obtained for a 1/6-scale model of this antenna (scale frequency 9.6 GHz) mounted on a cylinder 2 feet in diameter and 12 feet long. This diameter approximates that of a 1/6-scale fuselage section for SST-sized aircraft. Radiation patterns taken on airplane models will have perturbations due to the aerodynamic surfaces of the airplane. These will vary for each location. In general, for locations well forward on the fuselage of large commercial airplanes, the perturbations will be of secondary importance for elevation angles of $\theta < 80°$.

The principal-plane pitch ($\phi = 0°$, θ variable) and roll ($\phi = 90°$, θ variable) patterns for the predominant circular polarization are shown in fig. 13. The isotropic level was determined as outlined in Sec. 3.1. The maximum directivity D_{max} was measured to be 7.2 dB with respect to a circularly polarized reference.

There will be unavoidable ohmic losses in any radiating element design usable in an aircraft environment, especially the SST environment. These losses are attributed to a dielectric radome, high-temperature, foam-filled cavities, and matching, phasing, and power-dividing networks within the antenna. Based on past experience, these losses are not expected to exceed 1.0 dB.

When calculating the overall antenna radiating efficiency, the effects of impedance mismatch must be considered as well as ohmic losses. The mismatch loss for a 1.5 VSWR is 0.2 dB maximum. The total resultant antenna losses L for use in determinating system gain would then be a maximum of 1.2 dB.

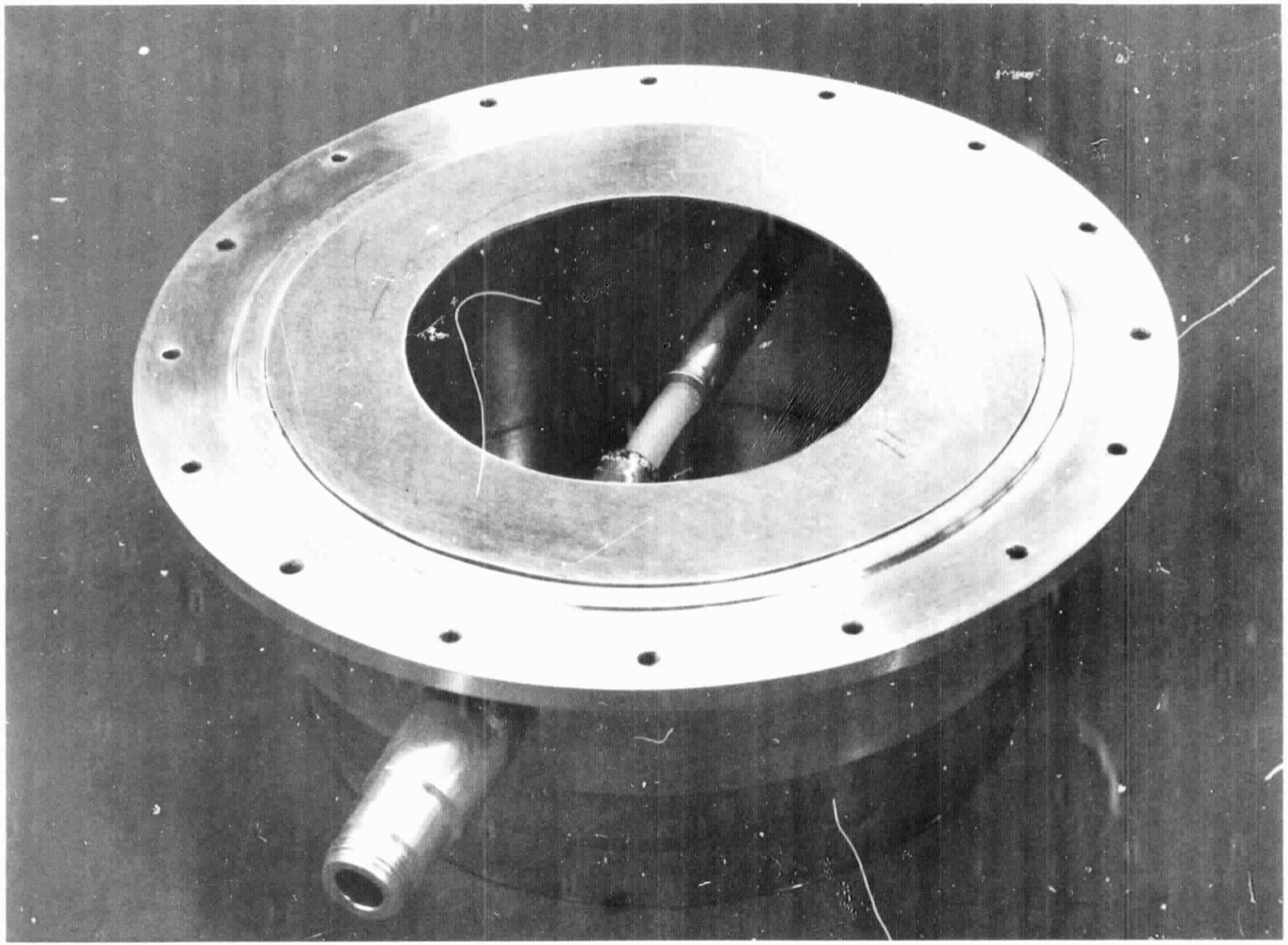

FIGURE 12.– ORTHOGONAL-MODE-CAVITY ANTENNA

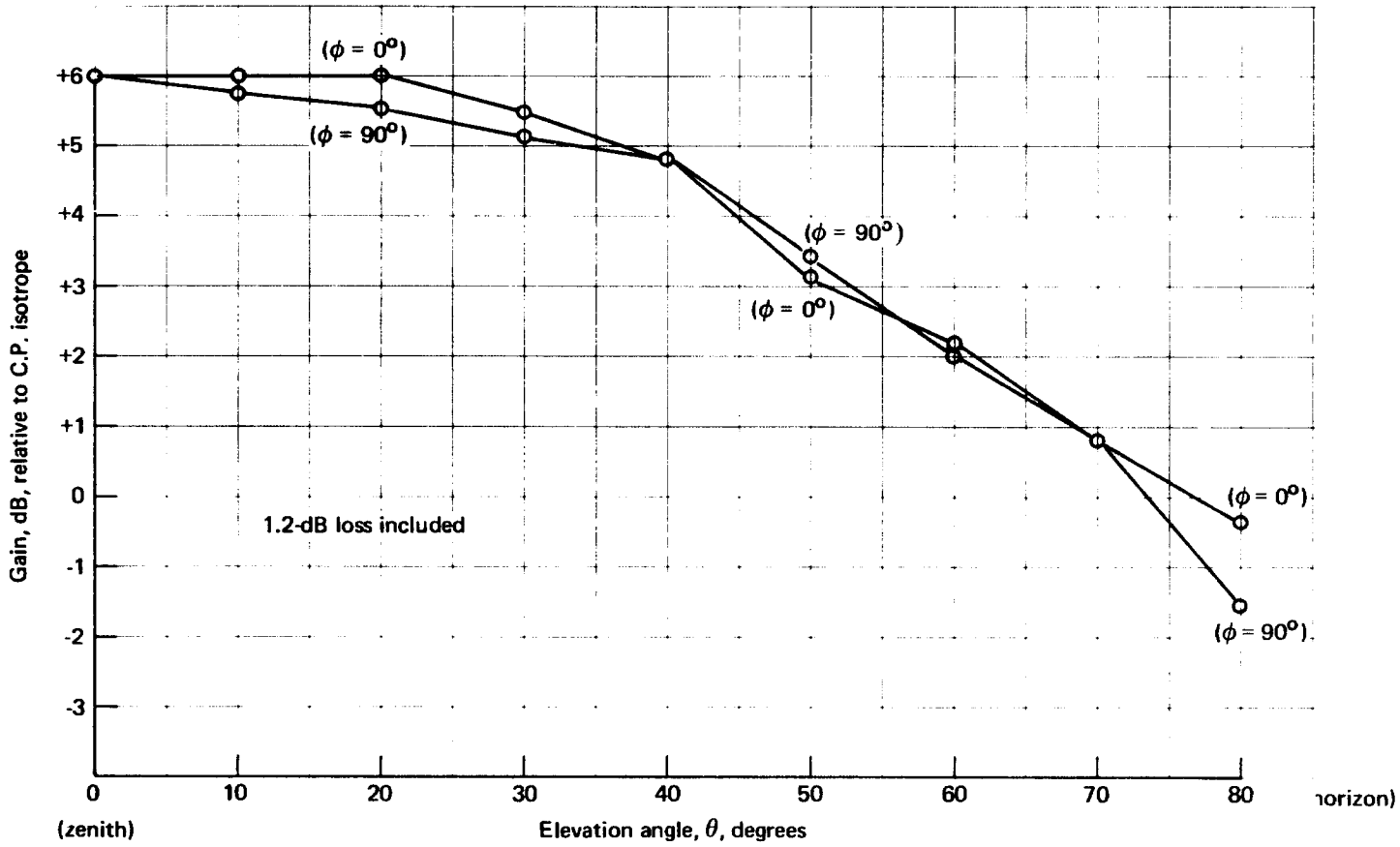

FIGURE 13.– PRINCIPAL PLANE PATTERNS FOR ORTHOGONAL-MODE-CAVITY ANTENNA

All radiation-pattern data presented herein include the effects of the predicted radiating-element efficiency; thus, the peak predicted antenna gain G_{max} is given by

$$G_{max} = D_{max} - L \tag{1}$$

where all quantities are in dB. Applying eq. (1), the maximum gain of the orthogonal-mode cavity is 6 dB.

Independent ellipticity measurements from $\theta = 0°$ to $\theta = 80°$ show the ellipticity of the orthogonal-mode antenna to be approximately equal to the difference in the $E(\theta)$ and $E(\phi)$ dB levels. The median ellipticity ratio for the conic ($\theta = 80°$) is about 12 dB. The experimental ellipticity as a function of ϕ for $\theta = 40°$, $60°$, and $80°$ is shown in fig. 14.

3.3 Four-Arm Log-Spiral Antenna

The four-arm log-spiral shown in fig. 15 consists of a planar dielectric sheet supporting four radiating elements. This assembly is mounted over a right-circular cylindrical cavity of about 0.9 wavelengths in diameter. The edges of one arm are defined in polar coordinates by the relationships

$$\rho_1 = e^{\alpha\theta} \tag{2}$$

and

$$\rho_2 = e^{\alpha(\theta-\delta)} \tag{3}$$

The other arms are defined by successive rotation of the above relationships in increments of $\theta = \pi/2$. The defining parameters are shown in fig. 15. The parameters ρ_o and ρ_m refer to the inner, or feed circle radius and the maximum, or terminating radius, respectively.

To provide upper-hemispherical radiation pattern coverage, it is necessary to mode switch. The theory of multimode excitation of log-spiral antennas has been presented by Dyson and Mayes (ref. 7). The sequential numbering of the feed terminals and the mode switching circuitry to provide mode 1 and mode 2 excitation is shown in fig. 16. Mode 1 excitation would be utilized to provide coverage for $0° < \theta < 35°$ and mode 2 would be utilized to provide coverage for $35° < \theta < 80°$. Experimental results obtained at Boeing (ref. 3) on an L-band test antenna are shown on a composite gain curve (in dB relative to isotropic) for modes 1 and 2 versus θ (vertical angle) in fig. 17. The gain curves shown in fig. 17 include a predicted efficiency value of 64% (-2 dB).

In the past, the log-spiral and other spiral antennas have been used primarily in receiving and low-power transmitting applications. This has been due to inherent limitations in dissipating heat due to power losses in the elements. However, recent advances in materials technology have resulted in the development of low-loss dielectric materials with relatively high thermal conductivity that can be utilized as the support structure for spiral elements. This permits the heat generated to be conducted to the surrounding cavity more readily. For example, Transco (ref. 8) has produced a UHF (240 to 500 MHz) spiral antenna rated at 2000 watts average power input. Motorola (ref. 5) is under contract to produce a 200- to 300-MHz, cavity-backed, log-periodic, two-mode, spiral antenna with the capability of 1 kW average power.

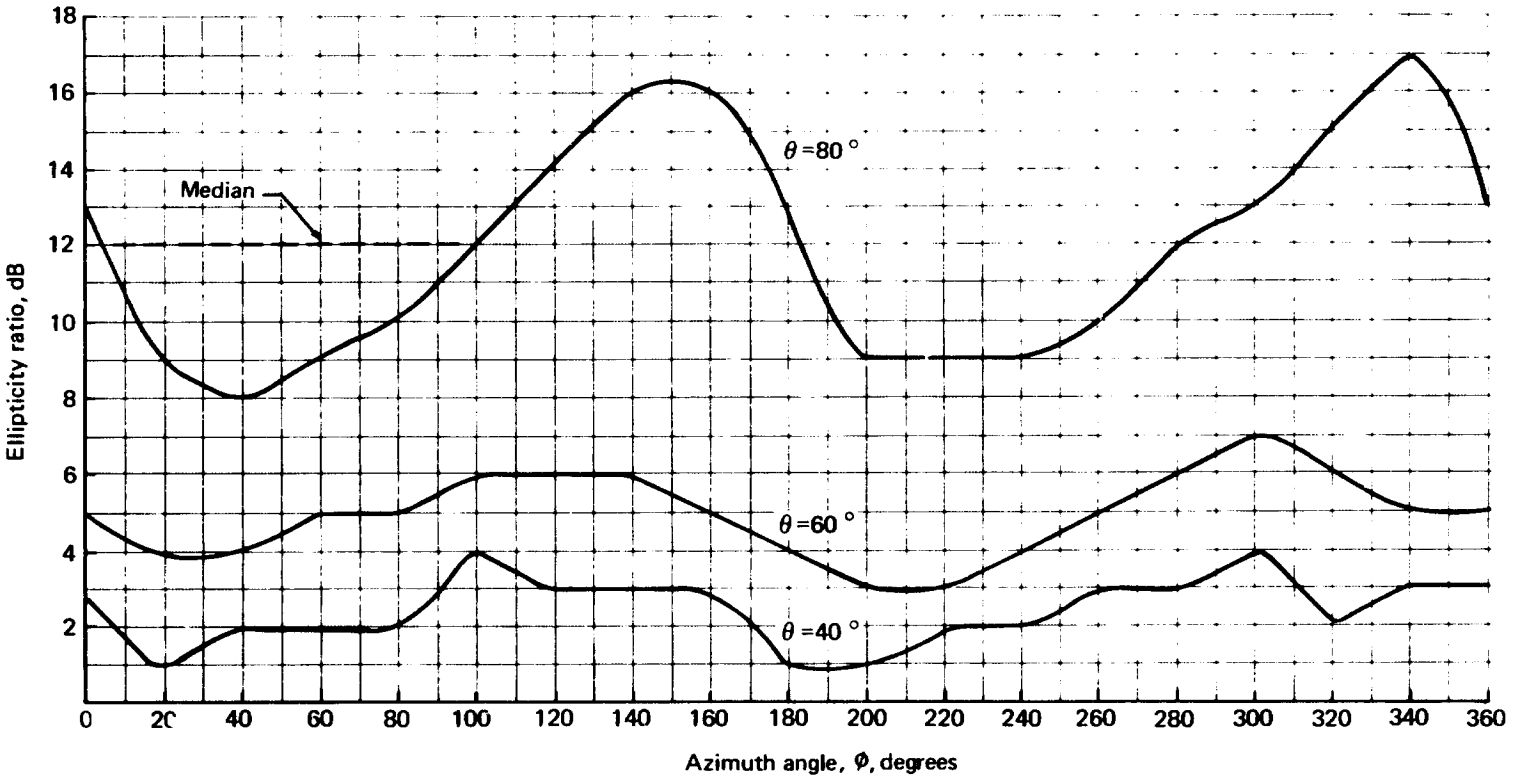

FIGURE 14.– ELLIPTICITY OF ORTHOGONAL-MODE-CAVITY ANTENNA

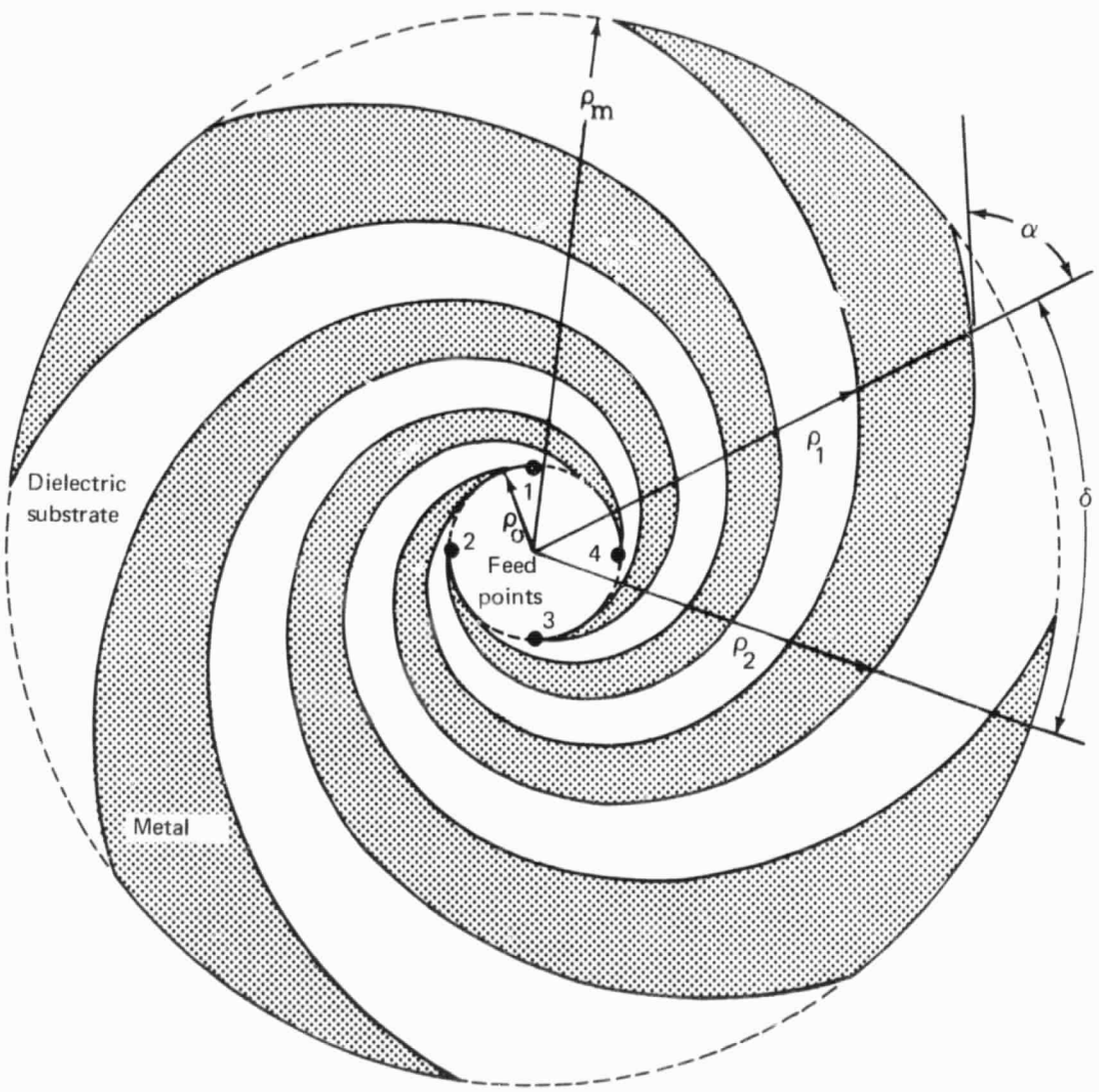

FIGURE 15.– SKETCH OF FOUR-ARM PLANAR LOG-SPIRAL

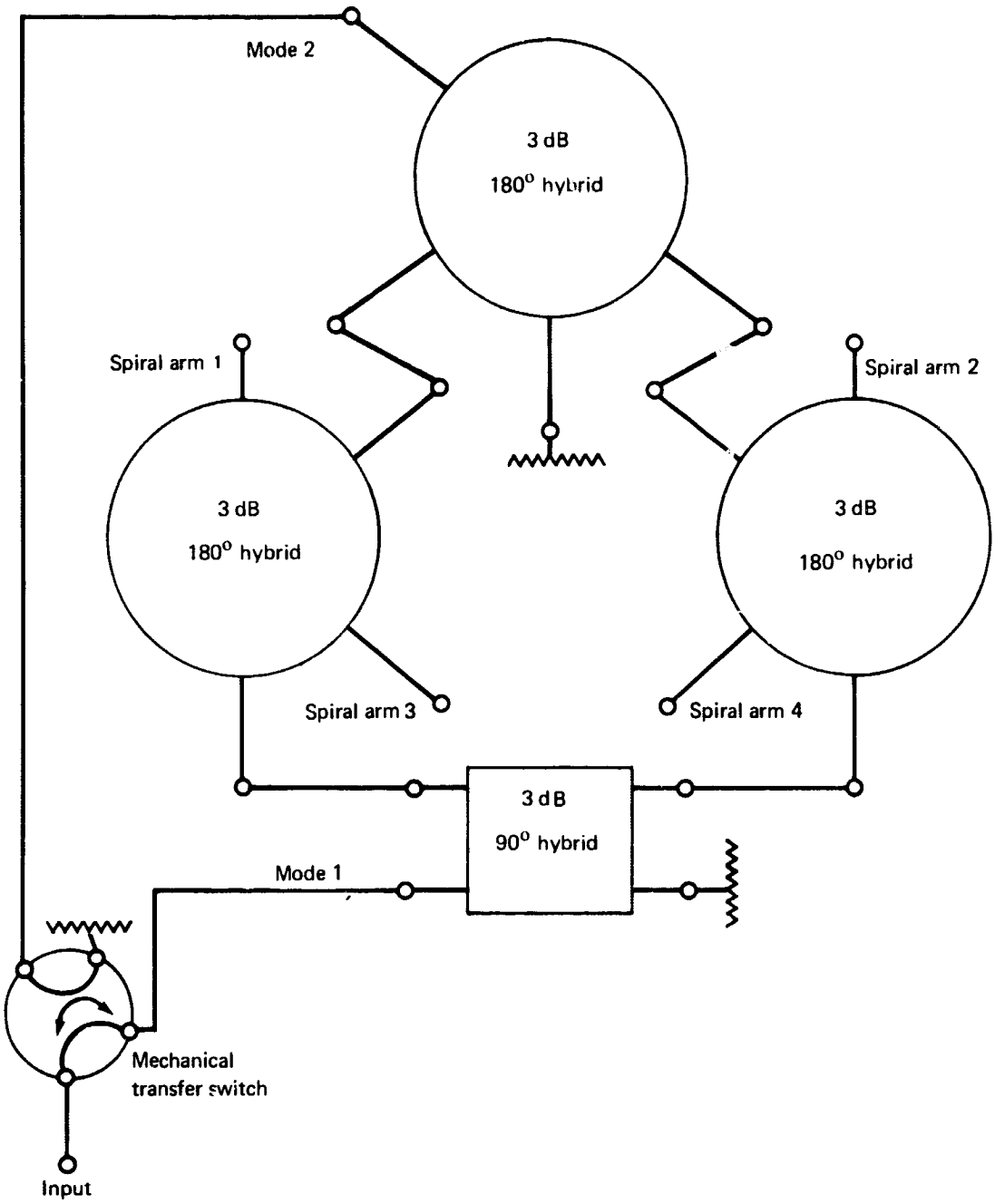

FIGURE 16.– FOUR-ARM SPIRAL MODE SWITCH

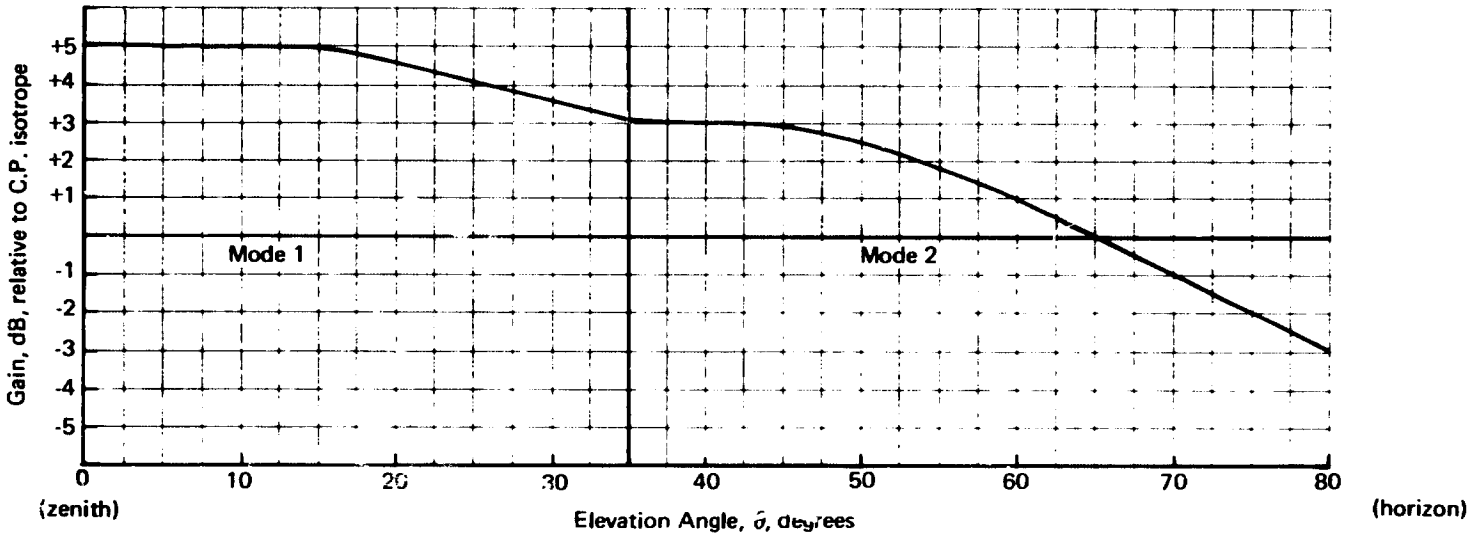

FIGURE 17.– FOUR-ARM LOG-SPIRAL ANTENNA GAIN

4.0 MECHANICALLY STEERED ANTENNAS

A mechanically steered antenna is one in which coverage is achieved by the physical movement of the antenna structure by an electromechanical drive system. The antenna beam is generally narrow in one or both planes; hence, relatively high gain is possible. The parabolic-dish weather radar antenna used on commercial airliners is a typical example. A half-power beamwidth of 3° to 4° in both planes and gains in excess of 30 dB are common for an X-band system.

The apparent advantages of mechanically steered antennas are not without penalty. To achieve high gain, a large aperture is required. This implies a narrow beam, which must be steerable throughout the solid angle established by the antenna pointing profile. The large aperture combined with typical antenna pointing profiles requires a large swept volume to accommodate the physical excursions of the antenna. This is, in general, incompatible with the structural and aerodynamic requirements of a commercial airplane. The outstanding exception is the weather radar antenna where aerodynamic, structural, and antenna pointing requirements are harmonious.

Use of mechanically steered antennas appeared to be a promising means of achieving gains at the higher end of the zero- to 20-dB range initially considered. Therefore, a portion of the antenna study effort was directed toward a review of mechanically-steered-antenna types and design techniques. Additionally, a laboratory effort was performed to establish the feasibility of a steerable, flush-mounted geodesic Luneberg Lens antenna.

4.1 Parabolic Dish

The directivity (D) of a parabolic-dish antenna can be approximated by (ref.9)

$$D = 6.4\, d_\lambda^2 \tag{4}$$

where d_λ is the diameter of the dish in wavelengths. If the dish is too small, feed blockage and spillover loss become appreciable. The minimum practical size of a dish antenna is about 4 wavelengths, which provides a directivity of about 20 dB. For 1.54 GHz, this represents an antenna 30.6 inches in diameter.

4.2 Parabolic Cylinder

The parabolic-cylinder antenna (ref. 9) is useful where there are space limitations in one direction. The feed system can be either a line source or a point source. A waveguide slot array is often used as a feed.

Feed blocking is a more serious problem with the parabolic cylinder than with the parabolic dish because of the increased feed size with respect to the dish. The realizable directivity can be approximated by

$$D = 8.2\, d_x d_y \tag{5}$$

where d_x is the length of the cylinder in wavelengths and d_y is the height of the parabolic section in wavelengths. A 10-inch-high, 40-inch-long antenna would have a directivity of approximately 17.5 dB at 1.54 GHz.

4.3 Axial-Mode Helix

Boeing has examined the problems of the helix antenna and of arrays of helical antennas in detail (ref. 10). It was concluded by measurements that the gain of a helix antenna can be described by

$$G = 8C_\lambda^2 d_\lambda \tag{6}$$

where C_λ is the circumference of the antenna in wavelengths and d_λ is the length of the helix in wavelengths.

The 3-dB beam width is given by

$$\text{HPBW} = \frac{52}{C_\lambda \sqrt{d_\lambda}} \tag{7}$$

Good impedance properties and circular polarization can be obtained when C_λ is from 0.8 to 1.25 wavelengths and when a ground plane 0.8 to 1 wavelength in diameter is used at the feed point. Measurements of a two-element helical array indicated a 3-dB increase in gain over that obtained from the single element for an element spacing of 1 wavelength. A 15-inch-long helix will provide a gain of about 13.5 dB. An array of two elements spaced 7.6 inches apart will provide a gain of approximately 16.5 dB.

4.4 Motorola End-Fire Array

Motorola has developed (ref. 5) a flush-mounted, linearly polarized, mechanically scanned antenna of end-fire elements. Each element of the array is a waveguide-fed dielectric-rod end-fire surface-wave antenna. The length of the element is about 4 wavelengths, or 32 inches at L-band. Motorola observed that mutual coupling between the elements can be controlled by proper element design and that a 20- to 21-dB gain is possible with a four-element array. The depth of the antenna is determined by the necessary vertical scan requirements. Horizontal scan can be accomplished by rotating the entire assembly; vertical scan is accomplished by rotation of the elements within the structure.

4.5 Unit-Index Geodesic Lens Antenna

The flush-mounted, unit-index geodesic Luneberg Lens antenna offers the possibility of gains in the 10- to 20-dB range with coverage throughout the upper hemisphere by electromechanical movement of the feed. The potential of this configuration appeared attractive enough to warrant a laboratory study effort. A feasibility test model was constructed and radiation patterns taken to demonstrate the approach. A conventional spherical dielectric Luneberg Lens has the capability of collimating the radiation from a source placed on its surface. This is accomplished by a prescribed radial variation of the index of refraction of the sphere. The radiation pattern of the collimated beam is narrow and symmetrical, similar to that produced by a parabolic-dish antenna of like diameter. The collimating action of the lens and its representative radiation patterns are shown on the left-hand side of fig. 18.

The two-dimensional Luneberg Lens antenna can be visualized as a pancake-shaped central slice taken from a spherical Luneberg Lens. If the two planar surfaces are covered with conductive sheets, a source placed on the dielectric edge of the slice will generate a

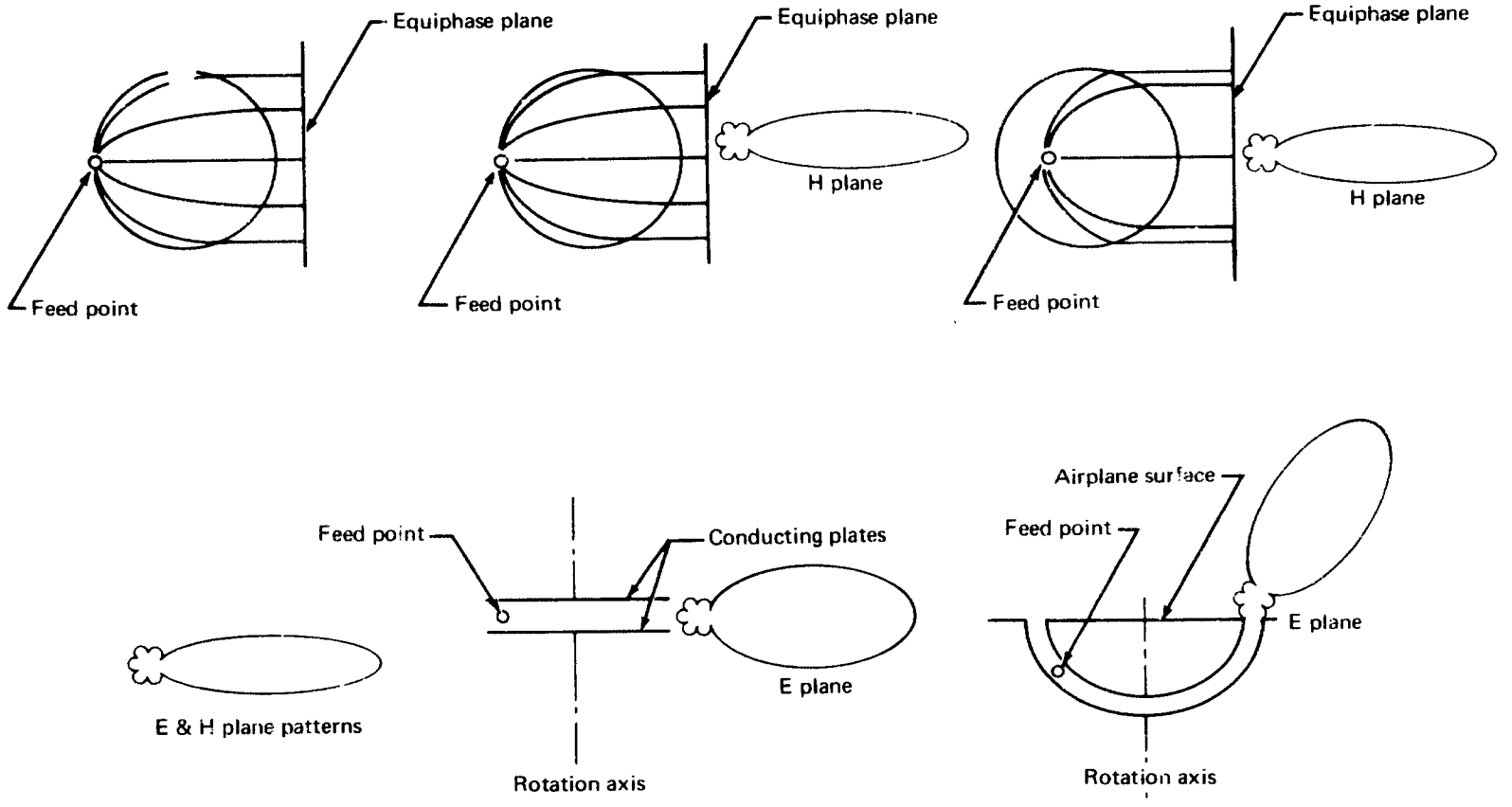

(a) Conventional Luneberg Lens (b) Two-dimensional Luneberg Lens (c) Geodesic Luneberg Lens

FIGURE 18.– EVOLUTION OF UNIT-INDEX LUNEBERG LENS

collimated beam emanating from the lens edge directly opposite the source. The radiation pattern in the plane of the slice is the same as that of a spherical lens. In the orthogonal plane, however, the pattern is broad, typical of that of an open-ended waveguide with a vertical aperture equal to the thickness of the lens. The two-dimensional lens and its representative patterns are shown in the center of fig. 18.

The unit-index geodesic Luneberg Lens is derived from the planar, two-dimensional lens by eliminating the dielectric material between the conducting sheets (hence the term "unit index") and by "deforming" the plates in a manner that is rigorously prescribed mathematically (ref. 11). The unit-index geodesic lens and its representative patterns are shown on the right-hand side of fig. 18.

The feed source need not be at the rim, as with the two-dimensional lens. In fact, an important property of the unit-index geodesic lens is that the angle of the beam peak in the plane perpendicular to the lens rim can be varied by changing the feed-point radius. This is shown in fig. 19 for several feed radii. Although the lens is strictly in focus for only one radial feed point and the vertical beam angle β associated with it, approximate focus can be maintained at other feed positions. There is a specific class of lens design wherein the defocusing effect is small for a wide range of feed movement and β's (ref. 11). Hence, it is possible to scan a major portion of a hemisphere by a combination of radial-feed movements to provide vertical beam steering and azimuth feed movement for azimuth steering.

To demonstrate the capability of this type of antenna to provide the necessary gain and coverage, a prototype was fabricated using the lens contour shown in fig. 20. This contour results in a theoretical beam elevation position of 45° with respect to the plane of the lens rim, which would be contained in the surface of the aircraft. This beam position results when fed at the focal point indicated as feed point 2 in fig. 20. The feed positions indicated as feed point 1 and feed point 3 were chosen to provide approximate focus at 15° and 75° elevation positions, respectively. With a nominal elevation beamwidth of 30°, this would provide beam crossovers about 3 dB below the peak gain.

The prototype antenna was about 24 inches in diameter and 9 inches in depth with a 1-inch plate separation. A test frequency of 1700 MHz was utilized on the antenna radiation pattern range. Elevation and azimuth patterns taken through the beam maximum were recorded for feed position 2 and are shown in figs. 21 and 22, respectively.

The peak gain of the antenna was measured to be 10.3 dB by the substitution method using a 15-dB standard-gain horn. The isotropic level shown in figs. 21 and 22 was established from the gain measurements.

The gain predicted for the lens was 15 dB; however, this was not achieved because of unexpected problems in the design of the feed and apparent phase errors in the model, which resulted in a defocused, split-elevation beam. Radiation patterns were not attempted at feed positions 1 and 3 because of the aforementioned problems.

Because of the limited success with the laboratory model of the geodesic lens antenna, further development would be required before it could be considered a serious candidate.

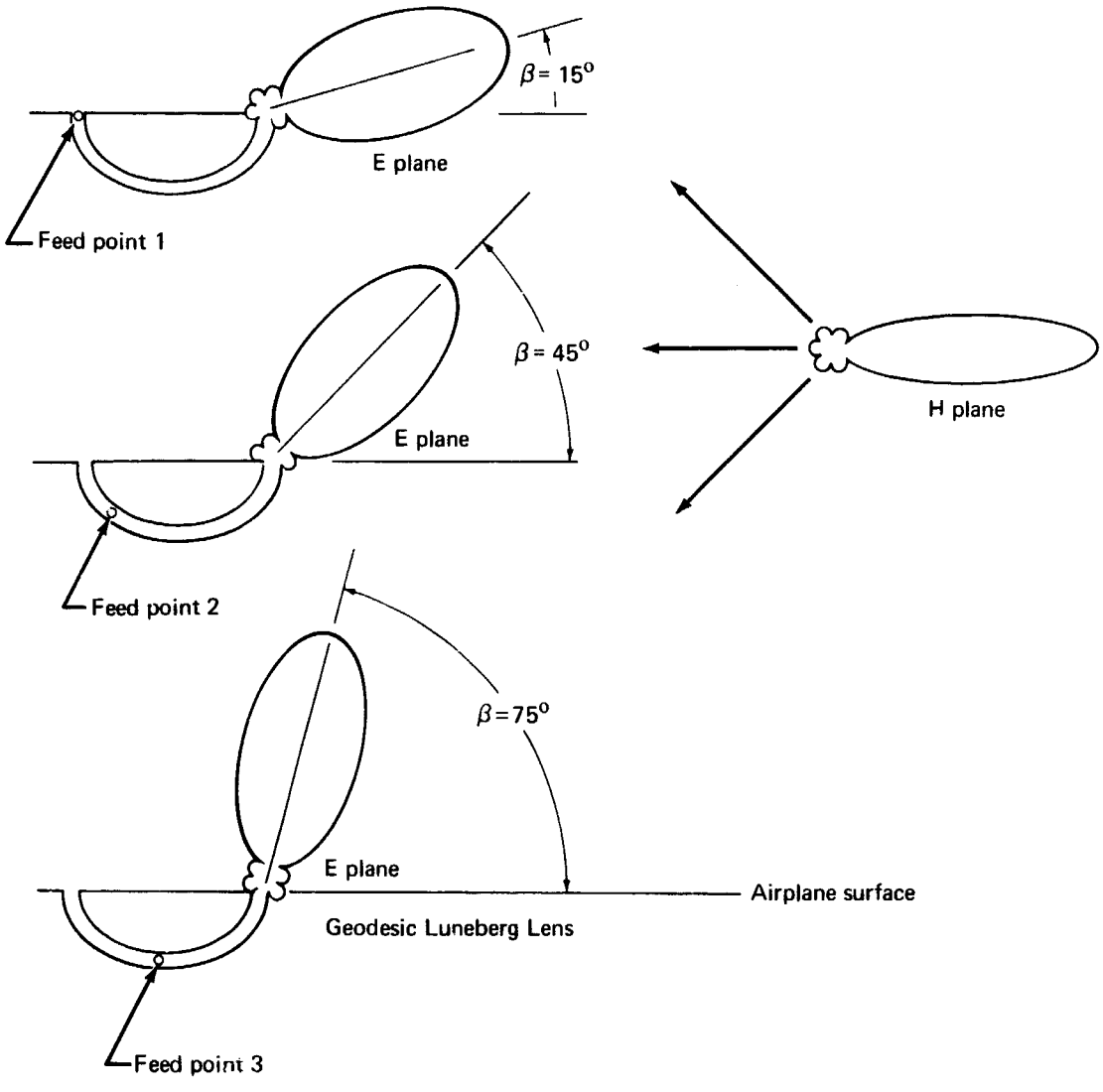

FIGURE 19.– GEODESIC-LENS BEAM POSITIONING BY FEED SWITCHING

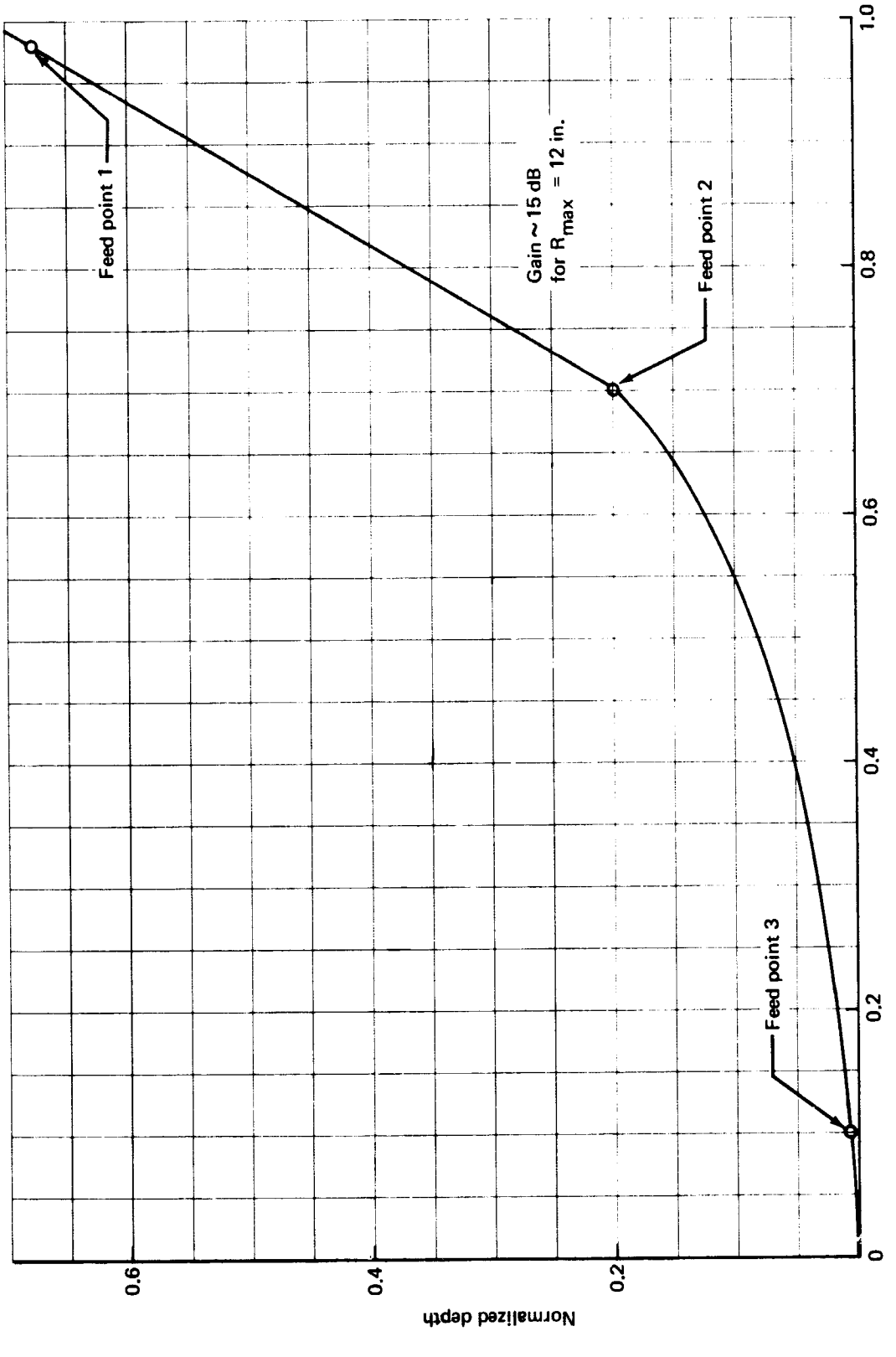

FIGURE 20.— GEODESIC UNIT-INDEX LENS CONTOUR

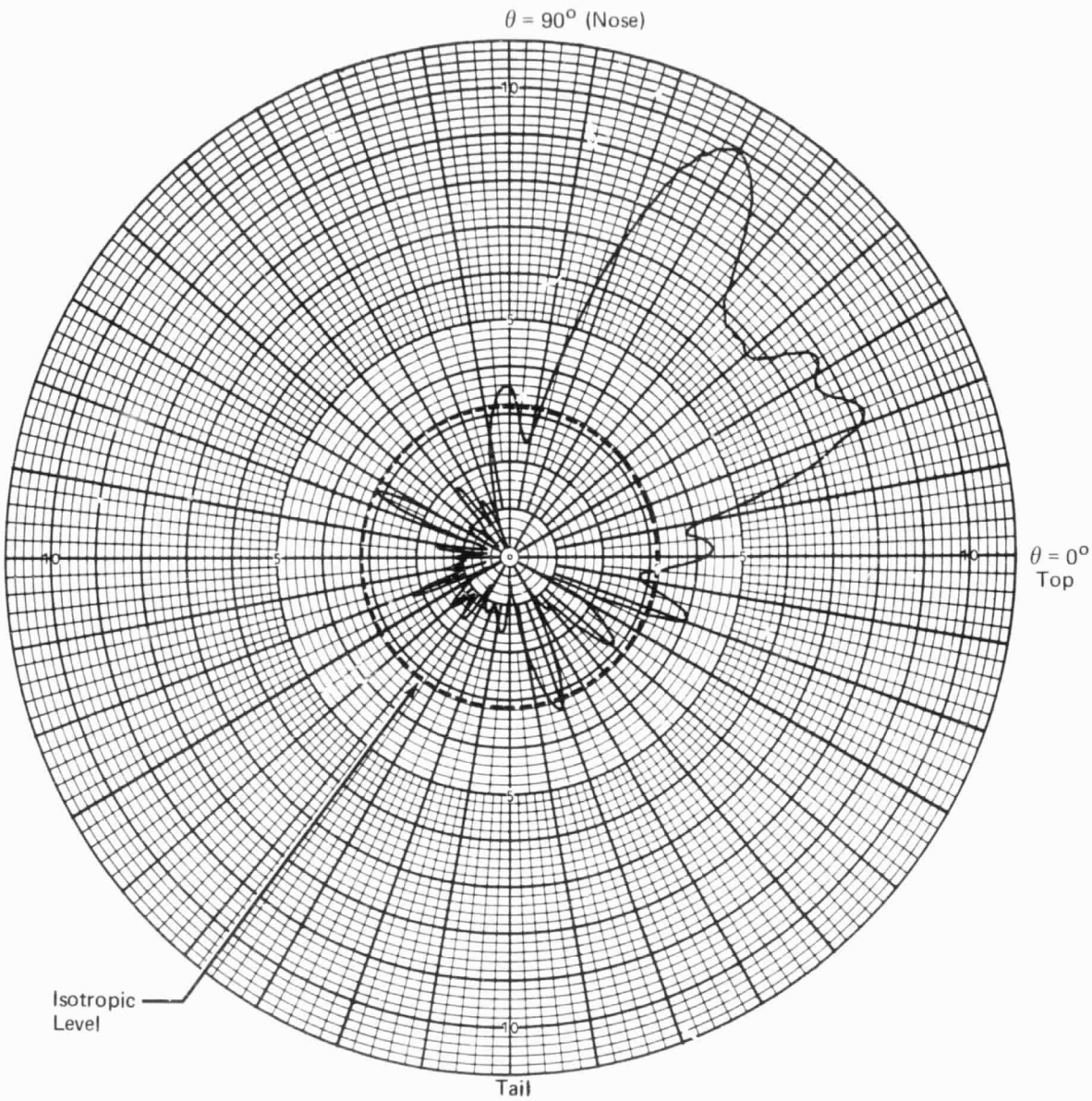

E_θ polarization
θ variable
ϕ = 0°
f = 1.7 GHz

FIGURE 21.– ELEVATION PATTERN WITH GEODESIC LUNEBERG LENS

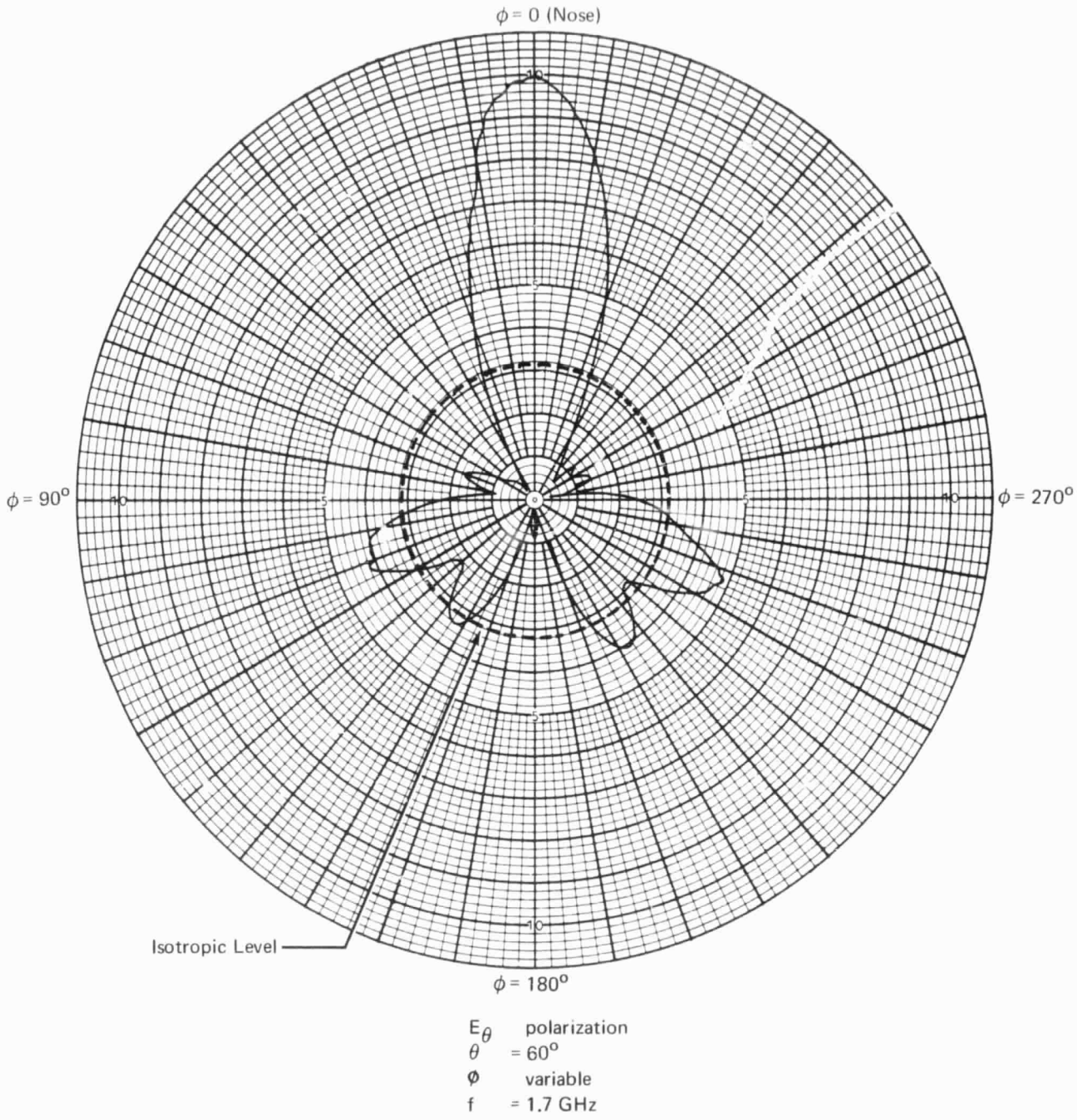

FIGURE 22.– AZIMUTH PATTERN FOR GEODESIC LUNEBERG LENS

5.0 ELECTRONICALLY STEERED ANTENNAS

Electronically steered antennas can be flush mounted and offer the potential of providing high gain and inertialess beam steering. These features, however, are accompanied by increased complexity and a natural decrease in gain as the beam is scanned away from broadside to the array. This section considers the basic design factors, performance capabilities, and limitations of phased arrays.

5.1 General Phased-Array Theory

The electrical performance of a phased-array antenna is determined by the array geometry, the array elements, and the method of excitation of the array. The main beam width is determined by the size of the array. The side-lobe structure, polarization, gain, and impedance characteristics, as well as the change of characteristics with scan are affected by the element spacing within the array, the number of elements, the type and size of elements, the means of excitation of the elements, and the mutual coupling effects between the elements. Element spacing of about 0.5 wavelength is necessary for scanning without grating lobes. With this order of spacing, there is considerable mutual coupling between array elements. Mutual coupling can provide serious degradation of the ellipticity for a linear array with as few as seven elements. The resulting impedance change with scan becomes more apparent in large arrays. The coupled energy represents a system loss that should be minimized.

5.1.1 Mutual coupling.– The usual concept of the far-field pattern of an array is one of pattern multiplication; that is, the total pattern is the product of an array factor determined by assuming isotropic elements and the element factor of an isolated element. This concept assumes no mutual coupling between elements. With closely spaced elements, this assumption is not valid, but the concept is still valid if the mutual coupling is considered in the definition of the element factor.

The array-element pattern of the mn^{th} element $f_{mn}(\theta,\phi)$ is defined as the pattern of the element per unit exciting current when the element is excited and all other array elements are terminated by their generator impedance (ref. 12). The total pattern is the superposition of all the element patterns. That is,

$$F(\theta,\phi) = \sum_m \sum_n f_{mn}(\theta,\phi) i_{mn} e^{j\psi_{mn}} e^{j2\pi(mD_x\cos\alpha_x + nD_y\cos\alpha_y)} \tag{8}$$

where $i_{mn}e^{j\psi_{mn}}$ is the complex current driving the mn^{th} element. Angles α_y and α_x are direction angles between R and the x and y axes, respectively. The array coordinate system is shown in fig. 23.

The directivity and gain of an antenna array is defined as

$$D(\theta,\phi) = \frac{4\pi}{P_R} \left| F(\theta,\phi) \right|^2 \tag{9}$$

$$G(\theta,\phi) = \frac{4\pi}{P_I} \left| F(\theta,\phi) \right|^2 \tag{10}$$

where P_R is the total radiated power of the array and P_I is the total incident power to the array.

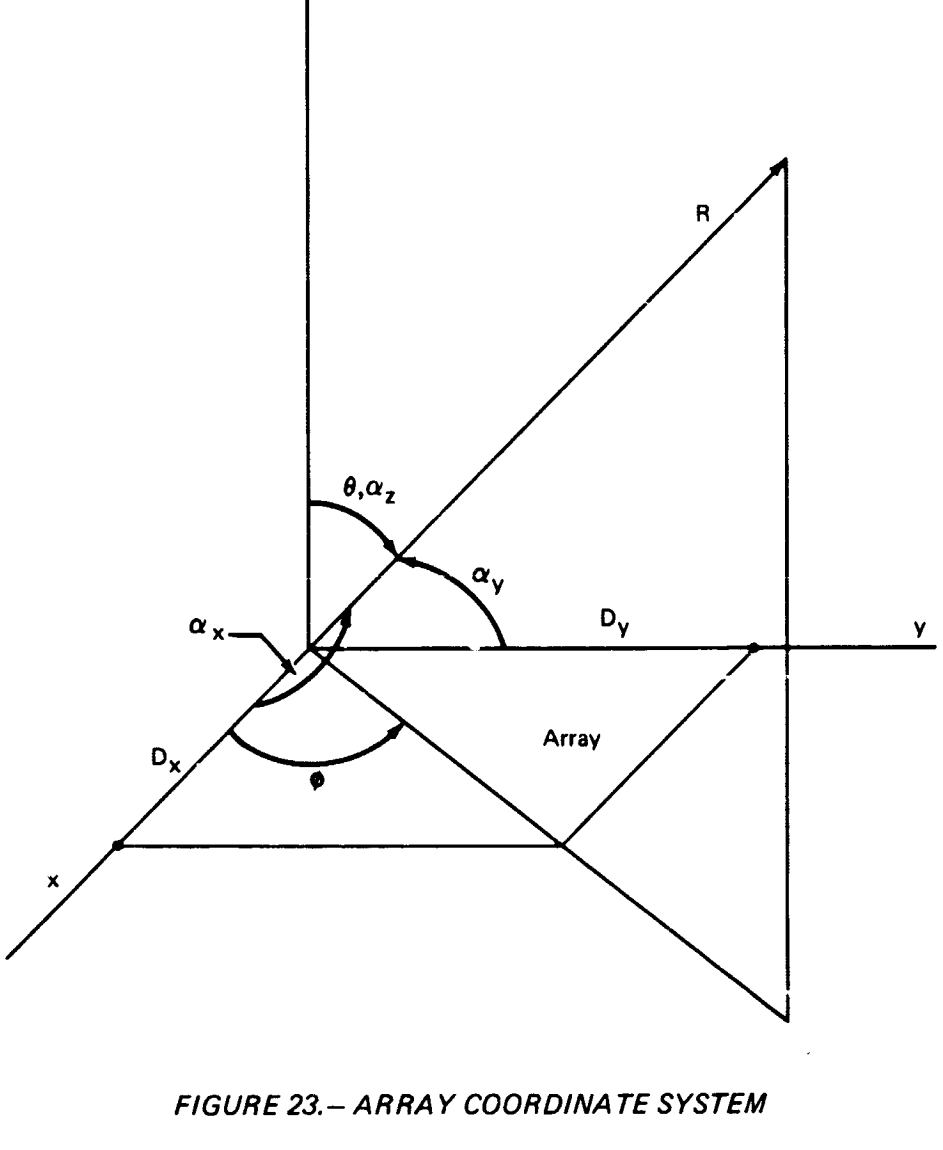

FIGURE 23.– ARRAY COORDINATE SYSTEM

If there is no dissipation in the antenna, the difference between the directivity and gain is due to the reflected energy. This is described by the reflection coefficient $\Gamma(\theta,\phi)$, which changes with pointing angle due to the mutual coupling. That is,

$$G(\theta,\phi) = D(\theta,\phi)\,(1 - |\Gamma(\theta,\phi)|^2) \tag{11}$$

The element gain function $g_{mn}(\theta,\phi)$ can be defined as

$$g_{mn}(\theta,\phi) = \frac{4\pi}{P_{I_{mn}}} |F_{mn}(\theta,\phi)|^2 \tag{12}$$

Where $P_{I_{mn}}$ is the total power incident to element mn. F_{mn} is the mn^{th} term of the sum of eq. (8). Using this definition, it can be shown that the gain for a large array, where the element gain function can be assumed to be the same for all elements, is

$$G(\theta_o,\phi_o) = g(\theta_o,\phi_o)N\eta \tag{13}$$

where N is the total number of elements in the array, η is the amplitude taper efficiency factor (1.0 for uniform excitation), and (θ_o,ϕ_o) is the direction of the principal beam maximum.

Considering the antenna as a single large aperture, the maximum directivity is proportional to the projected area of the aperture normal to the direction of the beam maximum. For an array of N equally spaced elements, with spacings D_x and D_y wavelengths, the total area is ND_xD_y. Thus, the directivity of an antenna in the direction of the principal beam maximum is

$$D(\theta_o,\phi_o) = 4\pi\eta N D_x D_y \cos\theta_o \tag{14}$$

Again, assuming lossless elements, the gain of the antenna differs from the directivity only because of the reflected energy. That is,

$$G(\theta_o,\phi_o) = 4\pi\,\eta\,ND_xD_y\cos\theta_o\,(1 - |\Gamma(\theta_o,\phi_o)|^2) \tag{15}$$

Comparing eqs. (13) and (15),

$$g(\theta_o,\phi_o) = 4\pi D_x D_y \cos\theta_o\,(1 - |\Gamma(\theta_o,\phi_o)|^2) \tag{16}$$

Thus, from eqs. (8) and (12),

$$f(\theta_o,\phi_o) \sim \cos^{1/2}\theta_o\,(1 - |\Gamma(\theta_o,\phi_o)|^2)^{1/2} \tag{17}$$

Note that two conditions of operation of the array are represented in eqs. (16) and (17). The element gain function is determined by exciting one element of the array. The reflection coefficient is determined by exciting all of the elements of the array such that the beam maximum is in the direction (θ_o,ϕ_o).

For the antenna to operate as a single large aperture, eq. (16) must hold regardless of the type of element. The difference in the isolated element pattern and the array element pattern must be compensated by mutual coupling. Thus, to minimize mutual coupling, the element pattern of the isolated elements should approach the $\cos^{1/2}\theta$ array element pattern.

There can be more than one angle where all the terms of the sum in eq. (8) add in phase. Beams at other than the principal maximum are called grating lobes. Grating lobes are eliminated if the element spacing satisfies the following equation:

$$D_m < \frac{1}{1 + |\sin \theta_m|} \tag{18}$$

where D_m is the maximum spacing between elements in wavelengths in the plane in which θ_m is measured. Thus, for scanning to ±60°, the spacing must be less than 0.54 wavelength.

Grating lobes can also be eliminated by providing a null in the array element pattern in the direction of the grating lobe.

5.1.2 Effect of mutual coupling on circular polarization. – Mutual coupling of elements can cause a serious deterioration of the ellipticity of a phased-array antenna. This is because the coupling to adjacent radiators from an antenna that radiates left-hand circular polarization appears at the feed terminal that would normally radiate right-hand circular polarization. Reflection of this received signal will be essentially right-hand circular. Thus, mutually coupled energy that is allowed to reradiate will seriously degrade the ellipticity. Parad and Kruetal (ref. 13) showed the severity of the problem by measuring patterns of a circular coaxial element imbedded in an array. A quarter-wave dielectric plate properly placed in the element was used to provide circular polarization. The ellipticity of the element changed from essentially zero dB on axis for the single element mounted on a ground plane to 8 dB with the element mounted in the center of a seven-element array with the other elements terminated in their characteristic impedance. The problem can be solved by providing a proper termination at the orthogonal port so that coupled energy is not reradiated.

5.1.3 Array size. – Curves based on eq. (14) (antenna gain as a function of the number of elements) are shown in fig. 24 for an array capable of scanning to ±60° without grating lobes. The elements are assumed to be on a rectangular grid with an element spacing of 0.54 wavelength. Three curves are shown. The first shows the theoretical maximum gain obtainable. The second shows the theoretical maximum gain for the antenna scanned to 56°. The third curve includes a 3-dB loss factor (50% efficiency) for scanning to 37° to include the effects of amplitude taper, mutual coupling, and dissipative loss in the array.

Tai (ref. 14) has derived the optimum directivity of uniformly spaced arrays of dipoles without considering mutual coupling. Applying this information to an array above a ground plane so that all of the radiation is in one hemisphere only, the maximum directivity of an eight-element broadside array of crossed dipoles phased for circular polarization and spaced 0.54 wavelength apart is 23.5 or 13.8 dB. For collinear dipoles, the maximum directivity is 12.6 dB; for parallel dipoles, 15 dB.

The curves of fig. 24 are based on eq. (14) for more than 10 elements and Tai's curves for a crossed dipole for less than 10 elements.

These curves can only serve as a guide to the necessary size of an array, especially for small arrays. The type of element and feed system will determine the actual performance with scanning. Thus, the actual gain, impedance, and polarization characteristics of a candidate system must be measured.

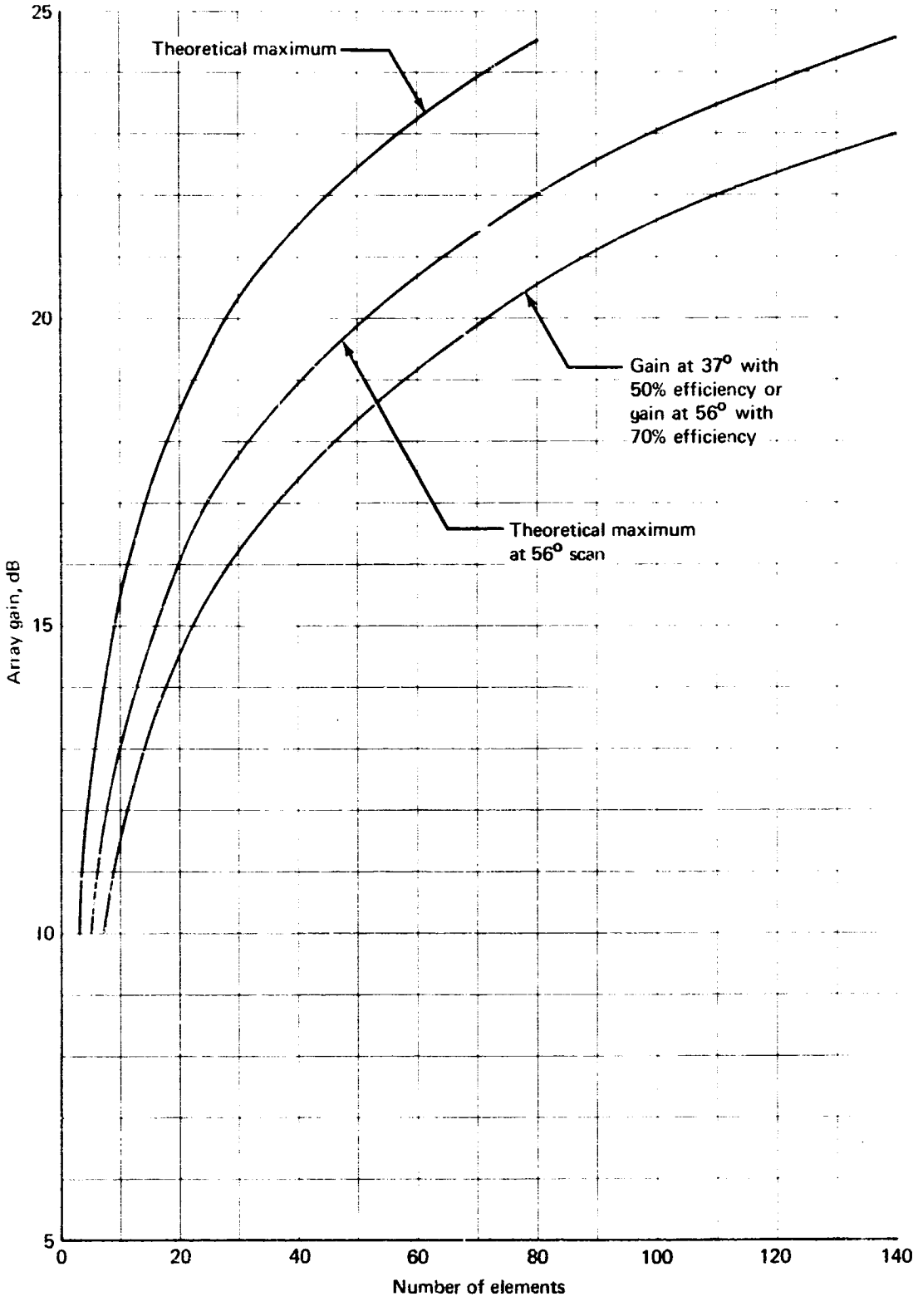

FIGURE 24.– ARRAY GAIN

5.2 Array Element Considerations

The relative spacing of elements of a phased array must be less than 0.54 wavelength for scanning to ± 60° without grating lobes. The ideal element pattern is $\cos^{1/2}\theta$. The element should be circularly polarized with the ability to operate throughout the 1.54- to 1.66-GHz frequency range. If a linear array is needed, the 0.54-wavelength spacing requirement and pattern requirement will hold in one plane only. However, the dimension of the element aperture perpendicular to the line of the array must be kept small so that the pattern in the orthogonal plane will be as broad as possible.

For the SST application, an array must be flush mounted or be mounted behind a conformal radome. The airplane surface temperature will be near 450° F during flight. Thus, the SST represents the most severe requirements on the antenna system of any commercial airplane.

Cavity-backed crossed slots, cavity-backed spirals, and circular waveguide elements are examples of flush-mounted circularly polarized elements for a phased-array antenna. Crossed dipoles mounted a quarter wave above a ground plane and fed in the proper phase for circular polarization approach the pattern of an ideal element and are desirable for applications where flush mounting is not necessary.

5.2.1 Flush-mounted array elements. Two-dimensional arrays constrain the outside dimensions of an element to 0.54 wavelength in two planes for rectangular spacing and scanning to ± 60° in both principal planes. A circular waveguide element will be used to discuss typical problems of size restrictions of elements.

The dominant mode in a circular waveguide is the TE_{11} mode. The cutoff frequency of the TE_{11} mode is

$$f_{c_{11}} = \frac{0.293c}{a\sqrt{\mu\epsilon}} \tag{19}$$

where $2a$ is the diameter of the guide, μ is the relative permeability, ϵ is the relative permittivity, and $c = \lambda_0 f$ is the velocity of light wave in free space.

For $2a/\lambda_0 = 0.52$ and an air-filled guide, eq. (19) indicates that the operating frequency f is $0.88\, f_{c_{11}}$. Thus, the guide is below cutoff. It is desirable to operate the guide at frequencies at least 20% above cutoff. This can be accomplished by loading the guide with a uniform dielectric with a relative permittivity of 2. For this case, $f = 1.25\, f_{c_{11}}$.

The ratios of the TM_{01} and the TE_{21} cutoff frequencies to the TE_{11} cutoff frequency are 1.31 and 1.66, respectively. Thus, to restrict the guide to one mode and also be 20% above cutoff, the frequency of a circular uniformly loaded guide is limited to the range from $1.2\, f_{c_{11}}$ to $1.3\, f_{c_{11}}$, or an 8% bandwidth.

This bandwidth can be increased by loading with a sleeve of dielectric (ref. 15) so the the cutoff-frequency ratio of the TM_{01} mode becomes 1.4. By loading with periodic disks of dielectric (ref. 16), the cutoff frequency of the TM_{01} mode can be increased higher than that of the TE_{21} mode.

For the L-band system of 1.54 to 1.66 MHz, the 8% bandwidth for the uniform loading would be marginally acceptable. The increase of bandwidth available using a sleeve dielectric would provide the necessary margin to eliminate any potential problems because of changes due to temperature. An example of a typical circular waveguide element with a sleeve dielectric is shown in fig. 25.

The patterns and performance of this antenna are similar to that of the orthogonal-mode circular cavity described in Sec. 3.1, wherein the diameter of the cavity was made larger so that no dielectric loading was necessary.

The cavity-backed, two-arm, conical spirals and the dielectric-loaded, two-arm, cavity-backed planar spirals currently being studied by Motorola (ref. 5), and the cavity-backed, crossed slots being developed by AEL (ref. 4) are other types of flush-mounted elements being developed for use in phased arrays.

The optimum element for a linear array will provide the widest coverage in the plane normal to the array and the minimum mutual coupling between elements. Measurements of coupling as a function of the scan and patterns of an array of the sleeve-loaded, orthogonal-mode cavities are recommended for phase II of this program to provide a basis for array specifications.

5.2.2 Nonflush elements.– A properly fed dipole turnstile mounted approximately 0.25 wavelength above a ground plane approaches the ideal circularly polarized element pattern described in Sec. 5.1. The curved dipole turnstile developed by Wong (ref. 30) may also be applicable for a linear array. Experimental measurements of mutual coupling would be necessary to determine if the coupling of the curved dipoles is excessive.

Dipole turnstile elements covered with a radome would protrude about 4 inches from the aircraft surface. Thus, this type of array would be applicable to subsonic aircraft. This type of element would also be applicable to an array mounted behind a conformal radome that could be mechanically steered in one plane.

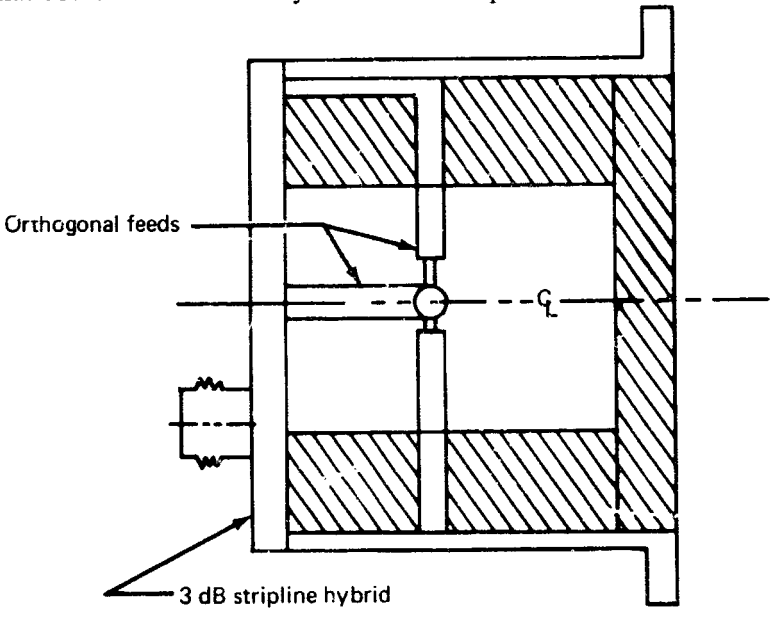

FIGURE 25.–SLEEVE-DIELECTRIC-LOADED ORTHOGONAL-MODE-CAVITY ELEMENT

5.3 Beam Steering Methods

There are three basic methods of beam steering. One is to provide computer-controlled phase shifters in series with each element of the array. The second is to switch between fixed multiple beams formed by a passive feed matrix. The third is to accomplish beam steering by using a pilot tone from the other end of the communications link.

The two basic types of phase shifters used in series with an element are diode and ferrite phase shifters. In general, losses, power requirements, and the weight of ferrite phase shifters limit their application to S-band or above. Thus, only diode phase shifters will be discussed in this section.

5.3.1 Diode phase shifters.– The hybrid forms the basis of two types of diode phase shifters. The initial development of a digital phase shifter utilized the hybrid with diodes for the basic function of providing a short or open. The hybrid has the property that a short at arms 2 and 3 causes the entire output to occur at port 4. Thus, the shorted condition is a reference phase condition. When the diode is opened, the signal travels a distance equal to twice the length of the stubs, thereby providing a phase delay at the output. The diode capacitance is compensated by adjustment of the length of line. A four-bit phase shifter including four hybrids connected in series with relative phase delays of 22.5°, 45°, 90°, and 180° is shown in fig. 26.

An analog phase shifter can be designed using a hybrid. In this case, a matched pair of varactor diodes are used. The varactor is capable of providing a variable capacitance, resulting in a continuous change in phase. A lumped constant equivalent of the hybrid has been developed so that the technique can be used for phase shifters at frequencies from a few megahertz through UHF (ref. 17). At the L-band frequency range, a limit of 90° phase shift per hybrid is typical.

An example of an eight-element series feed with analog hybrid phase shifters (ref. 18) is shown in fig. 27. The proper couplers to provide uniform distribution assuming lossless transmission lines are included. Beam steering is accomplished by providing the same dc control voltage to each diode. The type of system is limited to small arrays because of the value of couplers and the cumulative phase errors that are inherent in a series feed.

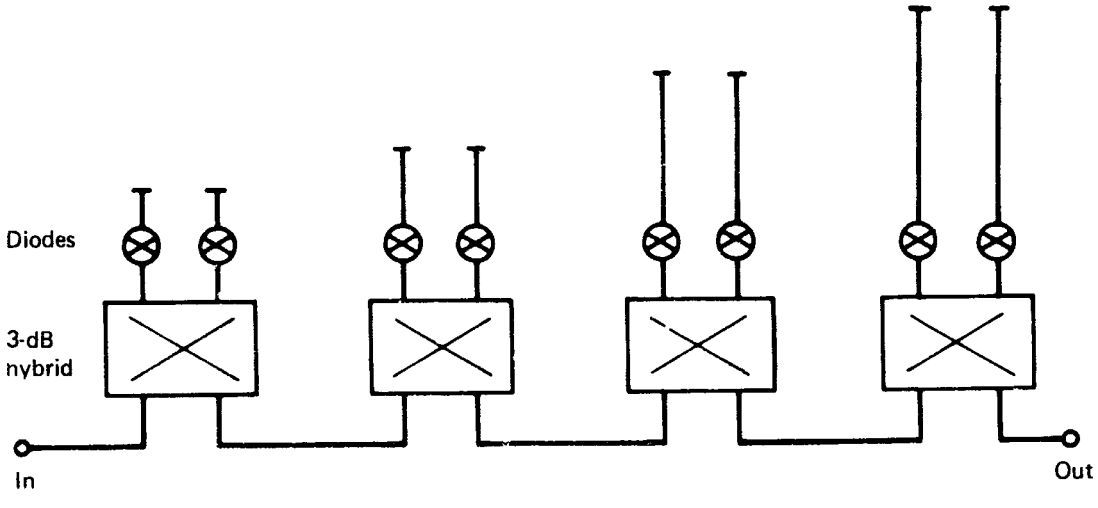

FIGURE 26.-- DIODE HYBRID FOUR-BIT PHASE SHIFTER

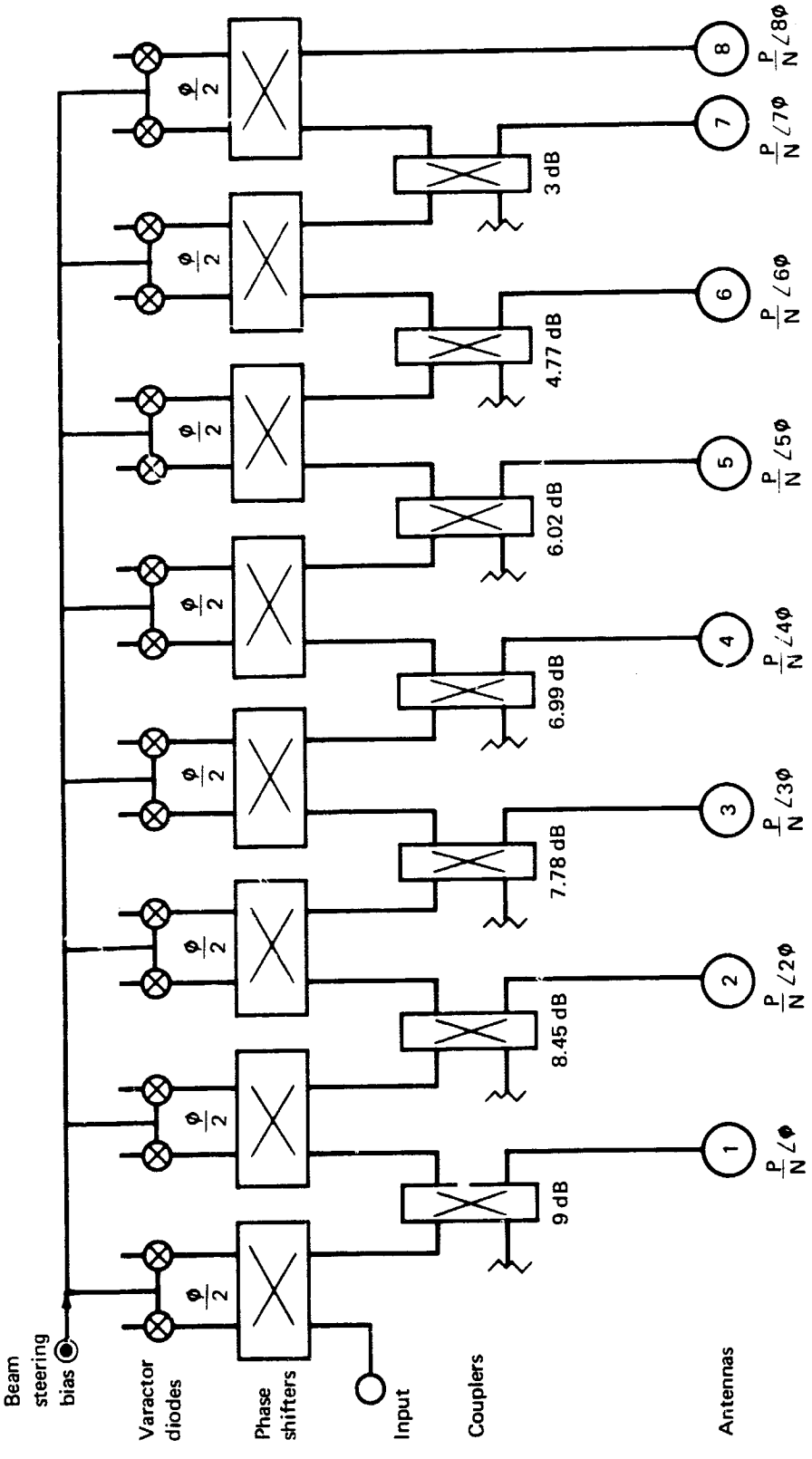

FIGURE 27.– ANTENNA-ARRAY SERIES FEED

5.3.2 Multiple, simultaneous, fixed-beam-array feed system.– A two-dimensional Butler matrix (ref. 19) will connect an N-by-M array of NM elements and provide NM independent simultaneous beams with NM input ports. Each beam will have the full gain of the aperture. The 3-dB hybrid is the basic element of the matrix. The number of elements must be 2 raised to an integral power. An eight-element matrix is shown in fig. 28. Tracing a signal from an input port to the elements will yield a linear phase taper that is different for each beam port.

The outputs of the matrix can be switched by diodes having the capability of handling up to 200 watts cw power (ref. 20). The matrix, which is completely passive, can be manufactured in stripline. The only loss in the feed is ohmic copper loss, which can be limited to 0.3 dB for an eight-element matrix. A ceramic that would allow operation to 500° F can be used for the dielectric.

Some basic properties of the array, derived from the basic far-field expression of linear array of N equally spaced isotropic elements with equal illumination, are summarized as follows. The far-field voltage expression of the array is

$$F = \frac{1}{N} \frac{\sin \frac{N\psi}{2}}{\sin \frac{\psi}{2}} \tag{20}$$

where

ψ = $2\pi D_\lambda \sin\theta - \delta$
D_λ = the spacing between elements in wavelengths
δ = the element-to-element relative phase

Beam maxima occur where ψ becomes zero. Another lossless beam is possible if the maximum of the beam occurs where the first beam has a null. It can be shown that the total number of beams that can be formed by a lossless feed is equal to the number of elements.

The angles of the main beam peaks are given by

$$P_K = \sin^{-1}\left[\frac{K - 1/2}{ND_\lambda}\right] \tag{21}$$

where the subscript K denotes the K^{th} beam (K = 1, 2, . . . N). The relative phase for the K^{th} beam δ_K between elements is given by

$$\delta_K = \frac{(2K - 1)}{N} \tag{22}$$

The angular coverage between the peak of the far-left beam and the peak of the far-right beam is given by

$$\alpha_t = 2 \sin^{-1}\left[1 - \frac{1}{N}\right] \tag{23}$$

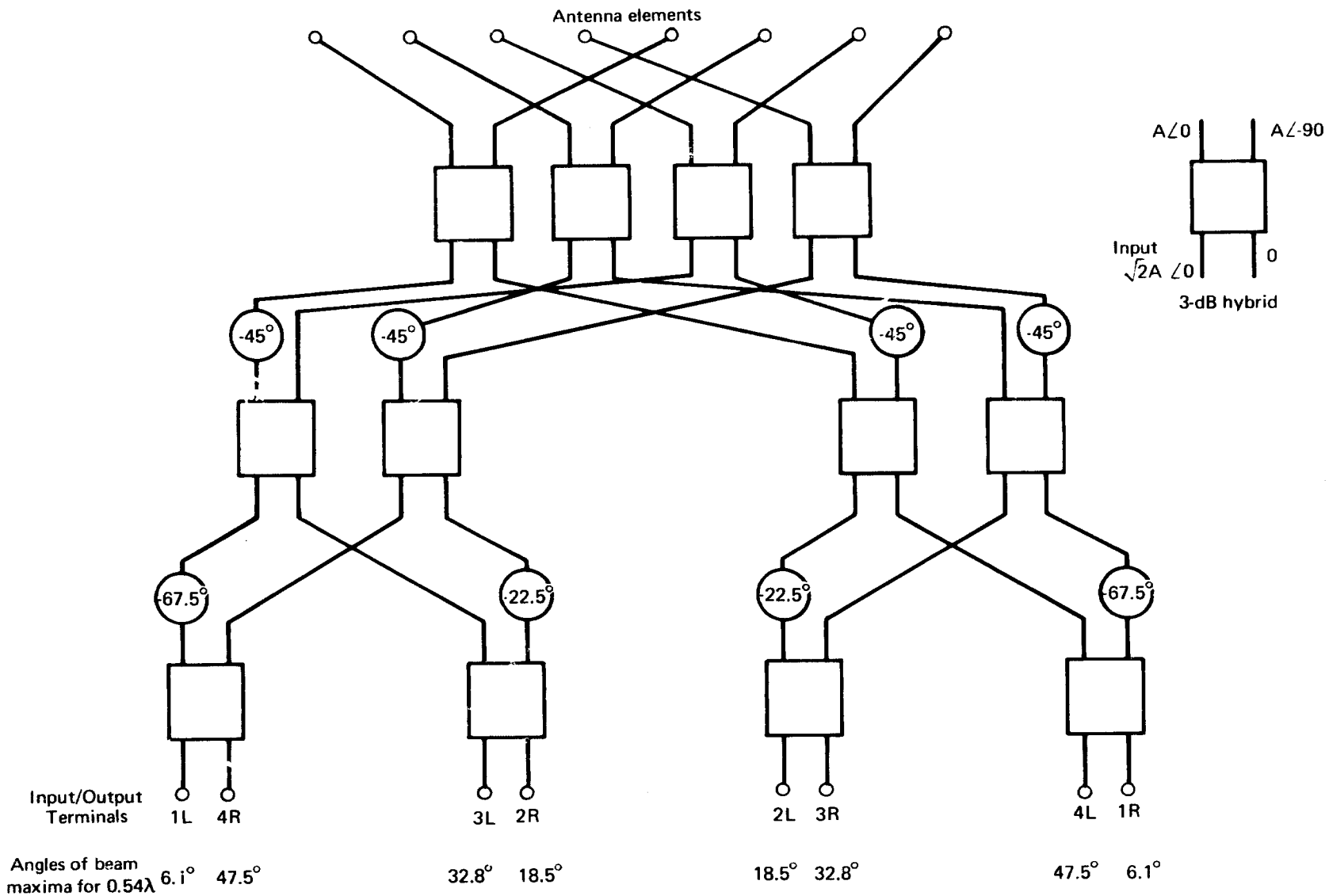

FIGURE 28.– BUTLER-MATRIX FEED SYSTEM

The angular beam crossover points between the K^{th} and the $(K + 1)^{th}$ beam is

$$\alpha_C = \sin^{-1} \frac{K}{ND} \tag{24}$$

The crossover level is

$$F_C = \frac{1}{N} \left(\frac{1}{\sin \frac{\pi}{2N}} \right) \tag{25}$$

For arrays of 10 elements or more, eq.(25) approaches $2/\pi$, a power crossover level of -3.92 dB down from peak, and is independent of the beam position, element spacing, or wavelength.

The gain of a Butler-matrix-fed array varies with pointing angle as the beams are fixed in space with approximately -4-dB crossover points. As an example, consider an eight-element array of the dielectric-loaded circular waveguides discussed in Sec. 5.2.1. The pattern perpendicular to the centerline of the array will be similar to the patterns shown in Sec. 3.2 for the orthogonal-mode-cavity antenna. The maximum directivity of the array, from the curve of fig. 24, is 13.8 dB for an eight-element array.

Assuming a 1.5-dB loss in the elements and feed, the maximum gain possible is 12.3 dB. The positions of the beam maxima were calculated using eq. (21). The gain of each beam is reduced by the cosine of the pointing angle. Using these facts and the pattern of the dual-mode cavity, the relative gains at the beam peaks and the beam crossover points were calculated and tabulated in table 2.

TABLE 2.– GAIN PERFORMANCE OF EIGHT-ELEMENT BUTLER ARRAY

Elevation angle	Azimuth angle				
	±0°	±30°	±45°	±60°	±70°
± 6.1°	12.3	11.1	10.3	9.3	8.6
±12.3°	8.3	7.1	6.3	5.3	4.6
±18.5°	12.1	10.9	10.1	9.1	8.4
±25.6°	8.1	6.9	6.1	5.1	4.4
±32.8°	11.5	10.3	9.5	8.5	7.8
±40.1°	7.5	6.3	5.5	4.5	3.3
±47.5°	10.6	9.4	8.6	7.6	6.9
±55.0°	6.6	5.4	4.6	3.6	2.9

Array spacing: 0.54 λ
Assumed loss: 1.5 dB

Patterns of an eight-element array of circularly polarized crossed dipoles fed by a Butler matrix that were obtained during a previous study at Boeing are shown in fig. 29. The array was mounted on a ground plane with an element spacing of 0.57 wavelength. The patterns were measured at 3 GHz. The relative gain varies from one pattern to the next so that a comparison of array gain for each beam is not possible. The patterns do, however, demonstrate the scanning capability of the Butler-fed array. At the present time, the Butler matrix is the simplest state-of-the-art means of providing beam steering, even though it has the limitation of fixed beams.

One possibility of increasing the gain at the crossover points of the beams without increasing the number of antenna elements is to combine electrically the outputs of two fixed beams so that the sum is present in the output. This technique has been studied by Ross and Schwartzman (ref. 21). Before such a system is used, the relative cost of the electronics must be determined with respect to the cost of realizing 3 dB more gain at the crossover points by doubling the number of elements. The other part of the tradeoff is the relative cost of the eight-element Butler-matrix summing network system and a steerable-beam array with a beam-steering technique similar to those described in Sec. 5.3.1 or Sec. 5.3.3 that will provide the same gain.

5.3.3 Pilot tone techniques.– Beam forming at an i.f. frequency provides the ability for automatic beam tracking, greater manufacturing tolerances, and a reduction in the number of active elements needed for beam steering. At the present time, many companies are working on proprietary programs to develop this type of beam steering.

Automatic beam steering (that is, self-phasing with the use of a pilot reference signal) (refs. 22 and 23) appears attractive for application to satellite communications because the surveillance signal can provide the pilot signal.

One basic method of self-phasing is shown in fig. 30. One element is used as the reference. The phase of the signal at all other elements of the array will vary according to the angle of arrival of the beam. The internal line lengths can be adjusted so that the signal at the phase comparator is $\cos(\omega t)$ for the reference and $\sin(\omega t + \varphi_n)$ for the nth element. An error voltage proportional to φ_n can then be used to adjust the phase of the voltage-controlled oscillator until angle φ_n is zero.

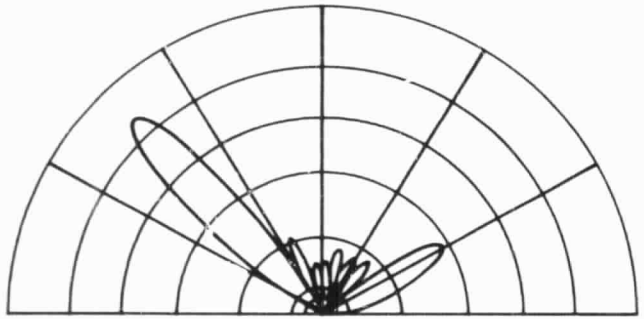

Beam 4, left: $\theta = 43°$
HPBW = 13°

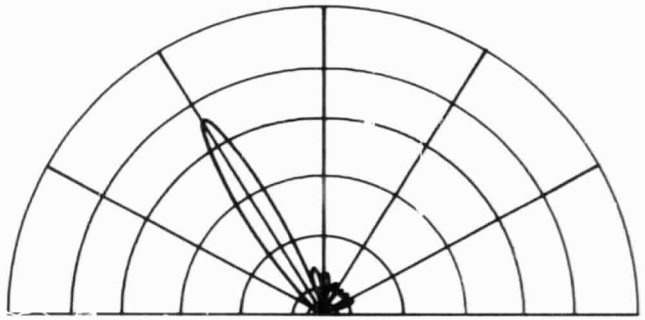

Beam 3, left : $\theta = 30°$
HPBW = 11°

Crossed dipoles, Spacing: 0.57λ, Scale frequency: 3 GHz

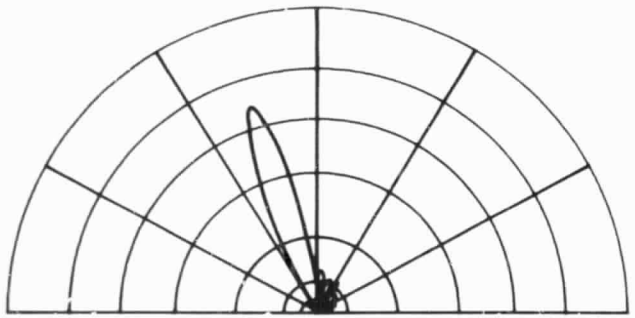

Beam 2, left: $\theta = 17°$
HPBW = 10°

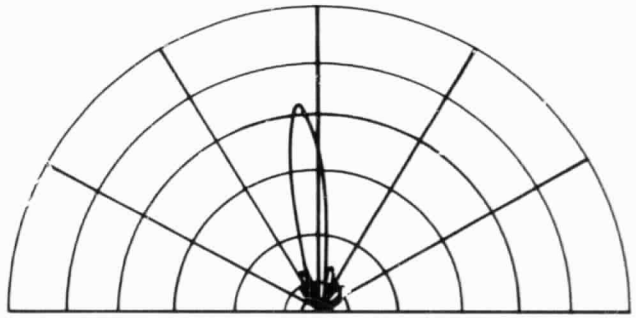

Beam 1, left: $\theta = 5°$
HPBW = 10°

FIGURE 29.– EIGHT-ELEMENT BUTLER-MATRIX ARRAY PATTERNS

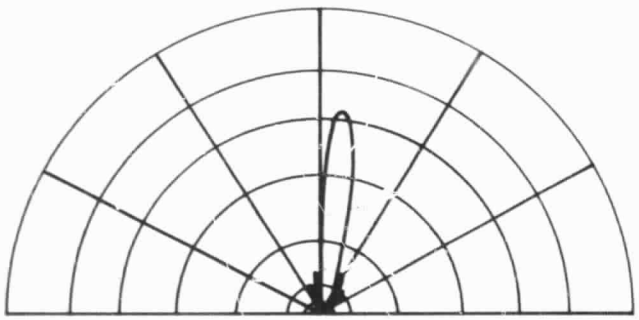

Beam 1, right: θ = 6°
HPBW = 10°

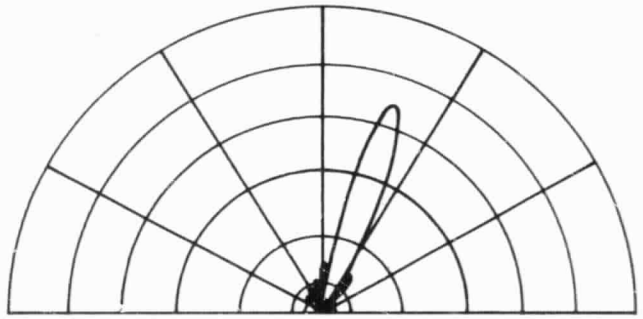

Beam 2, right: θ = 18°
HPBW = 10°

Crossed dipoles, Spacing: 0.57λ, Scale frequency: 3 GHz

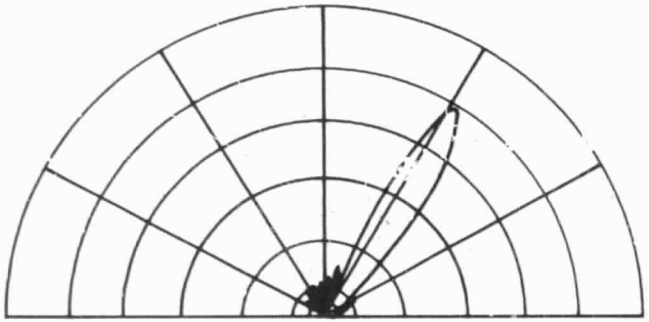

Beam 3, right: θ = 31°
HPBW = 11°

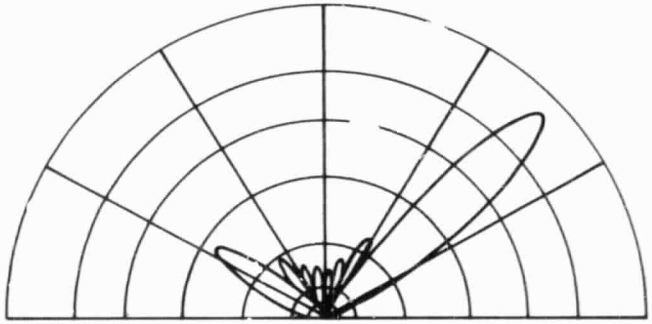

Beam 4, right: θ = 46°
HPBW = 13°

FIGURE 29.– Concluded

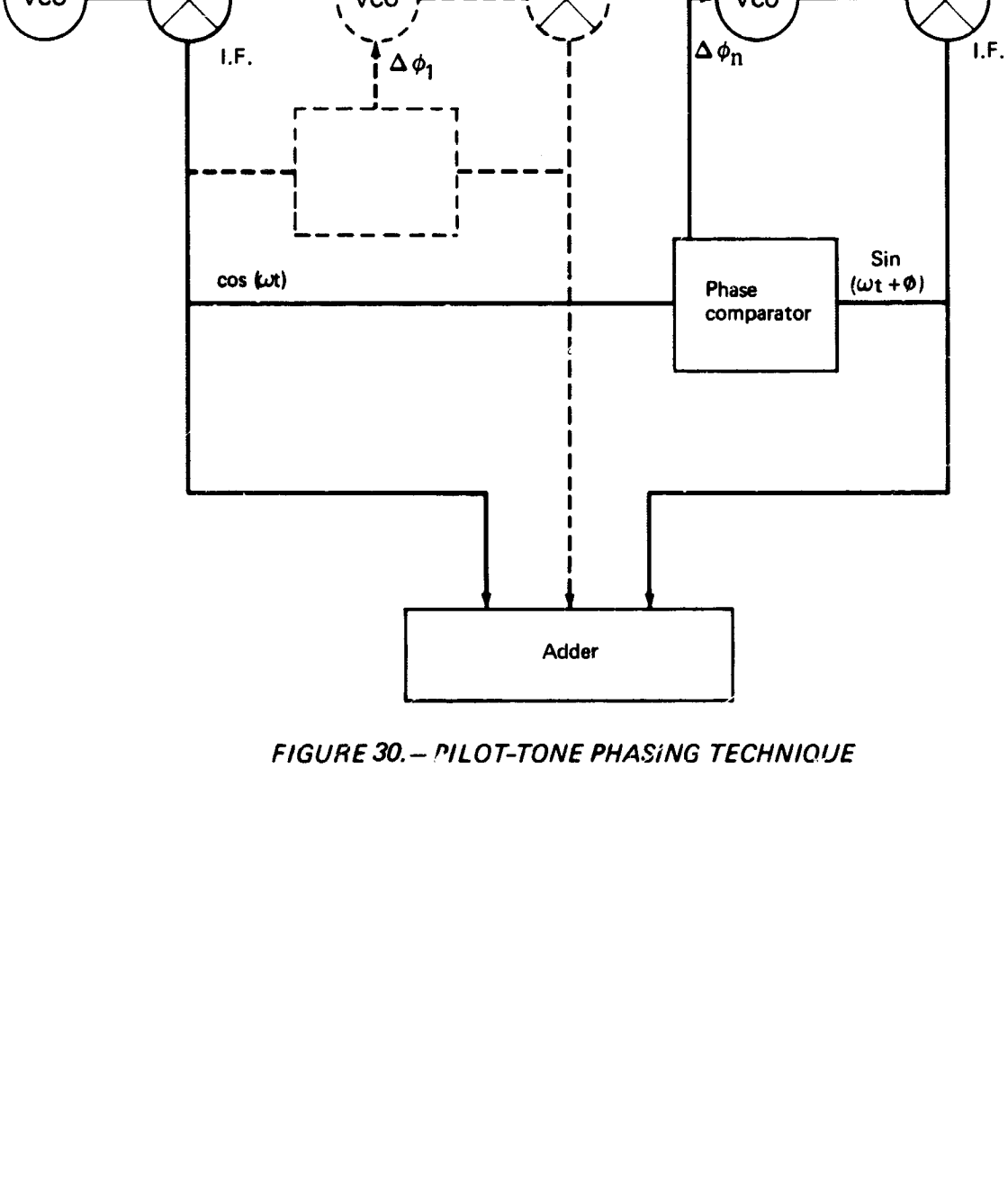

FIGURE 30.– PILOT-TONE PHASING TECHNIQUE

One means of providing the error signal is with the use of a square-law detector. The product of the two signals in the output is

$$\cos\omega t \sin(\omega t + \phi_n) = \frac{1}{2}\sin\phi_n + \frac{1}{2}\sin(2\omega t + \phi_n) \qquad (26)$$

The dc term represents an error voltage proportional to the sine of the phase difference that can be used to control the VCO. As the error approaches zero, the $\sin\phi_n$ approaches ϕ_n.

Beam steering for the transmitter can be accomplished by the principle of phase conjugacy. If the relative phase of the received pilot signal between the reference and the nth element is $-\phi_n$ degrees, the proper phase relation to transmit in the direction of the incoming signal is ϕ_n degrees. The original mixer will provide two sidebands: $\omega_c + \omega_{cf}$ and $\omega_c - \omega_{cf}$. If the phase of the lower sideband is $-\phi_n$, the phase of the upper sideband is ϕ_n. Thus, the required phase information for the transmitting mode can also be derived from the pilot signal.

The Ryan Corporation (ref. 24) has a patent application pending for a means of phase shifting that they are using in an integrated antenna system. Block diagrams of their integrated antenna-transmitter and antenna-receiver are shown in fig. 31. Ryan indicated that their system is capable of self-tracking.

IBM Federal Systems Division is developing a communications system with simultaneous multiple-beam capability using a "singing" array technique (ref. 25). The basic difference between the "singing" array system of IBM and the array repeater described by Cutler, Kompfner, and Tillotson (ref. 23) is that the magnitude of the pilot tone is built up by an oscillatory phenomenon between the two ends of the link. That is, the transmitting array is turned on with the transmitter in each element of the array incoherent with any other. Some energy is transmitted in the direction of the receive array. That signal arrives

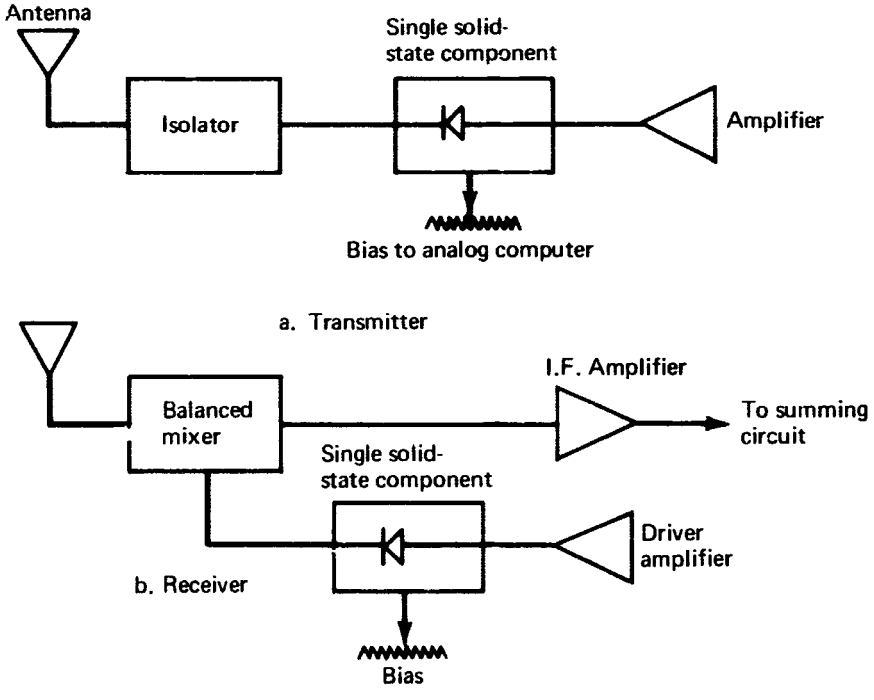

FIGURE 31.– RYAN INTEGRATED ANTENNA BLOCK DIAGRAM

at the receiving array with a phase coherence across the array. The signal is amplified, added to the signals of random phase at the second-array transmitters, and sent back to the first array. The process is repeated until a large signal is built up. This pilot tone is mixed with a modulated subcarrier that is about 10% different in frequency.

The signal that is built up will include many frequency components, because there is a time lag in the feedback loop. A bandpass filter and a limiter reduce the number of frequency components that build up so that the desired pilot tone predominates. A retrodirective array can be at either or both ends of the link. Simultaneous beams in different directions can be formed using different frequency channels for each beam.

5.4 Modular Arrays

There has been an industry-wide research and development effort to design integrated phased-array elements. Each element contains the antenna, transmit-receive switch, solid-state transmitter, receiver, mixer, and a phase-shifting mechanism. Texas Instruments' MERA (Molecular Electronics Radar Array) (ref. 26) development and RCA's Blue Chip (ref. 27) programs were among the first. Ryan (ref. 24), Dalmo Victor (ref. 28), Motorola (ref. 5), AEL (ref. 4), Sanders Associates (ref. 20), and IBM Federal System Division (ref. 25) were visited during the state-of-the-art survey and indicated that they were working on integrated-circuit phased arrays, but that the details were company proprietary. Integrated-circuit techniques make possible low per-unit cost for large production runs. It was the general consensus among company personnel visited during the survey trip that modular arrays would be cost competitive with mechanical-scanning antennas on a production basis for 1975.

Single-transistor, solid-state L-band transmitters are currently available with a 5- to 7-watt cw power output. By 1970, 10 to 20 watts of cw power output per transistor is expected. Noise figures of 4.5 dB for transistor preamplifiers are within today's technology.

One advantage of the modular array is graceful degradation rather than failure. For example, the failure of one transmitter in an eight-element array will degrade the output power by only 0.6 dB; one transmitter in a sixteen-element array, 0.3 dB.

A major problem in designing a modular antenna for the SST is that cooling would have to be provided at the antenna; the active components have an upper operating temperature limit of about 150°F, whereas the array surface will experience temperatures near 450°F. An example of one type of element that can be used with high surface temperatures is the disk-loaded circular waveguide shown in fig. 32. The complete receiver-transmitter microstrip circuitry can be contained in a one- or two-layer printed circuit module at the bottom of the element. The dielectric disks can be constructed of a ceramic material (alumina, for example) having excellent resistance to heat and good thermal conducting properties. The spaces between the disks might be filled with low-density, high-temperature foam disks (ref. 29), which have excellent insulation properties. Thus, cooling the metal waveguide will provide protection for the circuit elements.

The Boeing Company has been developing an experimental solid-state module to gain an understanding of the problems in applying modular antenna techniques. A block diagram of the module is shown in fig. 33. The module circuits were designed on a series of twelve disks to make possible independent testing of each circuit. The operating frequency of the element is 3 GHz, and the element uses a four-bit diode digital phase shifter operating at 800 MHz. New construction techniques resulted in a loss of less than 1.0 dB for all phase positions. A miniature 50-ohm transmission line is used for interconnections between the substrates. Alumina (Al_2O_3) is used for the substrate of the microstrip circuit. The antenna on the prototype module is a printed dipole, but other configurations such as the circular waveguide radiator of fig. 31 could also be used. The complete S-band package with materials suitable for subsonic aircraft weighs 0.3 pound. A projected production module would be configured to minimize the interconnections between substrates and have a weight of 0.2 pound.

The dimensions of an element designed for 1.5 GHz would be twice the dimensions of the experimental module. Assuming the same wall thickness of the metal cylinder for both elements, the weight of the L-band production element would be approximately 0.4 pound.

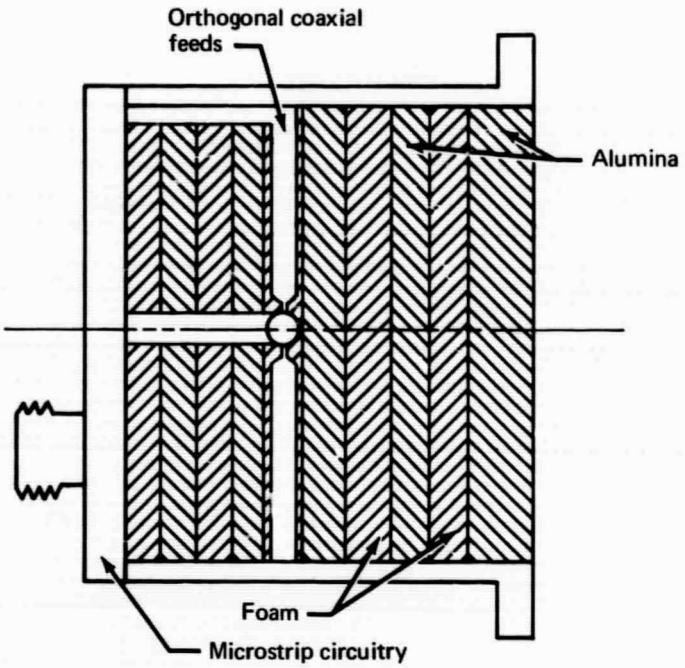

FIGURE 32.– ORTHOGONAL-MODE-CAVITY MODULAR ELEMENT

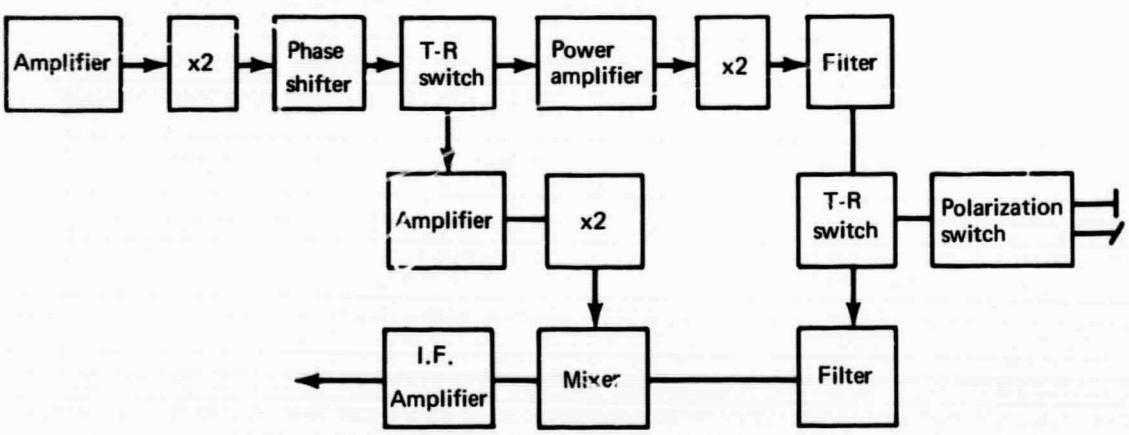

FIGURE 33.– BOEING MODULE BLOCK DIAGRAM

5.5 The Dioscures Antenna

A Request for Proposal for a detailed design study of a dual-beam antenna has been issued by the French government to their industry for the development of an airborne L-band antenna for the Dioscures satellite communications system. The antenna is to be two adjacent 3 x 4 element arrays fed by a multiple-beam matrix similar to a Butler matrix but designed to work with other than 2^n elements in a row. The electrical design goals for the antenna are shown in table 3. If these design goals can be met, this antenna is applicable for use in the experimental terminal with a low-power satellite.

TABLE 3.– DESIGN GOALS OF DIOSCURES ANTENNA GAIN FOR ELEVATION ANGLES OF +5° TO 90°

Frequency, MHz	Azimuth angle	
	±40°	+75° to -65°
1550	13.5 dB	12.0 dB
1650	14.0 dB	12.5 dB

Multipath discrimination factor: 12 dB minimum
Axial ratio: 4 dB maximum
Temperature limits: -40° C to +130° C
Overall dimensions: 60 x 60 x 20 cm
Weight: 20 kg maximum
Transmitter power: 50 watts maximum

6.0 EXPERIMENTAL-TERMINAL ANTENNA SYSTEM LOCATIONS ON THE SST

The general guidelines for evaluating prospective locations for the SST terminal antenna system are as follows:

(1) The antenna system must not change the outer contour of the SST.

(2) The antenna system must not cause structural changes that result in excessive weight penalties.

(3) The antenna system must operate reliably in the physical and electrical environment of the SST.

(4) The antenna system must be compatible with the other electronic and mechanical systems aboard the SST.

To minimize the weight and structural penalties to be incurred due to the antenna system installation, low-stress unpressurized areas should be utilized if possible. Such areas are available in a typical SST configuration in the wing-strake region, weather-radar radome area, and the tail cone (aft fuselage section). Also to be considered in the choice of any antenna system location are the lengths of the transmission line and control cabling. These items have direct affects on weight and cost for a given performance.

The following sections provide an analysis of candidate locations for the various classes of antennas considered for an experimental terminal on the B-2707-200 SST configuration. Locations for nonsteerable low-gain antennas, mechanically steerable antennas, and electronically steerable arrays are shown in fig. 34. They are numbered for ease of discussion.

6.1 Locations for Nonsteerable Low-Gain Antennas

Locations 1 and 2 in fig. 34 represent possible locations for single low-gain antennas that are located well forward on the fuselage. This location minimizes transmission line and cable runs and minimizes radiation-pattern interference from the aerodynamic surfaces.

Locations 3 and 4 represent positions for a switched two-antenna system that can provide an increased gain near the horizon. All four of these locations have depth restrictions that limit possible antennas to the simple types described in Sec. 3.0 that are 3 to 4 inches in depth. It may also be feasible to provide a left-right-coverage system by locating one antenna on the upper surface of each wing (locations 7 and 8). The desirability of such a location would be determined by the configuration of the aerodynamic surfaces of the aircraft and the tradeoffs of radiation pattern improvement versus the cost due to the weight and performance penalties imposed by the requirement for longer transmission lines.

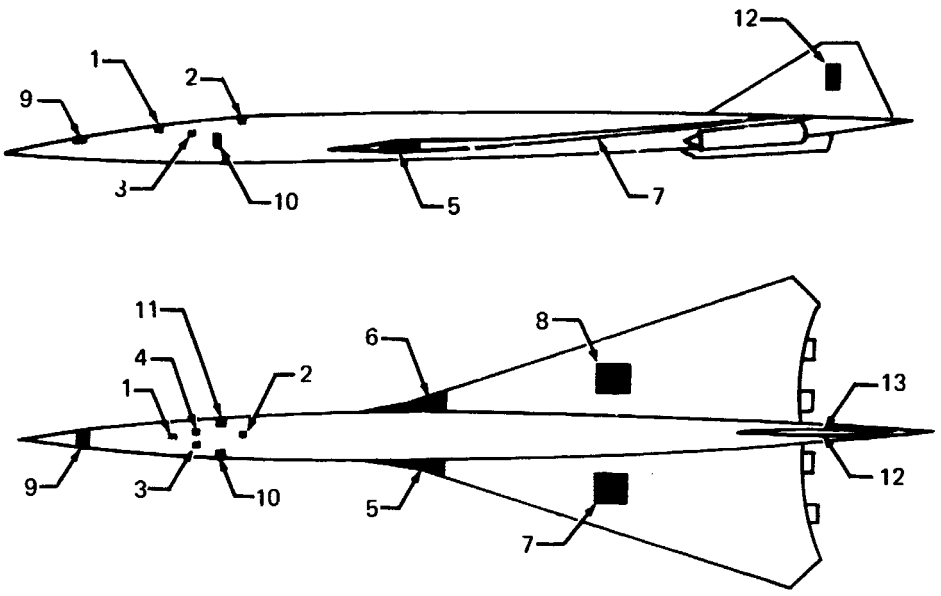

FIGURE 34. – B-2707-200 POTENTIAL ANTENNA LOCATIONS

6.2 Locations for Mechanically Steerable Antenna Systems

The depth requirements for mechanically steerable antenna systems preclude fuselage mounting. The general areas available for such installations are shown in locations 5 through 9 in fig. 34.

Locations 5 and 6 would be suitable for providing coverage in the left-forward and right-forward quarters of the upper hemisphere, respectively, by an antenna mounted behind a radome on each side of the airplane, except for a segment resulting from the fuselage shadowing. Although the amount of shadowing would be gain- and pattern-shape dependent, the null regions should be limited to 10° to 15° on either side of $\phi = 0°$ (nose on). Locations 7 and 8 would be suitable for providing coverage over the left and right halves of the upper hemisphere, respectively, using flush-mounted antennas similar to those described in Secs. 4.3 and 4.4 These locations would give fuselage shadowing of less than 10° on either side of $\phi = 0°$ at low elevation angles with decreased shadowing at higher elevation angles. Location 9 at the rear of the weather radar radome area could provide coverage of most of the forward half of the upper hemisphere at a medium-gain level (10 to 12 dB); however, sufficient swept volume would not be available for a high-gain antenna.

6.3 Locations for Phased Arrays

Locations 10 through 13 are possible areas for the installation of phased arrays. Locations 12 and 13 have the advantage of being in an unpressurized area, but they would require long transmission-line runs and any possibility of cooling would be precluded due to the remote location. Locations 10 and 11 are symbolic of side-fuselage mounting in a pressurized area. The available depth in these areas is limited to 3 to 6 inches. An ideal location for the experimental terminal to minimize the necessary vertical scan would be to

place the center of the arrays 25° above the broadside direction. For an operational system with complete upper hemispherical coverage using phased arrays, the arrays should be placed at 45°.

There will be service doors in the general area of locations 10 and 11. These doors would provide a simple means of installing a phased array as large as 6 x 10 elements, because the mounting of the array in a service door could be accomplished away from the airplane. The array would point broadside toward the horizon, thus requiring scanning to 41°. This additional vertical scanning with respect to the optimum location causes an additional 0.6-dB pointing loss.

7.0 EXPERIMENTAL-TERMINAL ANTENNA SYSTEM CONFIGURATIONS

From the user standpoint, the aircraft-terminal antenna system for an operational satellite communications/surveillance system should be simple, reliable, and inexpensive. The satellite terminal should be more complex and sophisticated. The experimental terminal should be designed so that it is possible to demonstrate a growth capability into an operational terminal.

The choice of aircraft antenna system for the experimental system will depend on the satellite available. Since the satellite is not known, antenna systems with high, medium, and low gains are described in this section. The surveillance function of the satellite communications system can be accomplished with less antenna gain than that of the voice communications function. The surveillance system has the additional requirement of pointing at more than one satellite simultaneously. Therefore, the antenna systems for surveillance will be discussed separately.

Phased arrays will be discussed in terms of an element spacing of 0.54 wavelength and a dielectric-loaded circular waveguide element. However, the final choice of an element type for a phased-array application will be left to phase II of the program. The number of elements needed to provide a specific array gain in each case was determined from the curves of fig. 24. The specified size of each array includes 1 inch on each side of the array for mounting hardware. The depth of the antenna element for any of the basic array types described in Sec. 5.2.1 should be not greater than 3 inches. Thus, a maximum depth including feed matrix and mounting hardware of 4 inches is a practical design goal.

The principal-plane, 3-dB beamwidths of two-dimensional arrays at the maximum gain point can be approximated by

$$\text{HPBW} = \frac{58}{d_\lambda} \quad \text{(degrees)} \tag{27}$$

where d_λ is the length of the array in the principal plane in wavelengths. For linear arrays, the pattern in the plane orthogonal to the line of the array is assumed to be that of the dual-mode cavity discussed in Sec. 3.0.

The pointing angle θ of the array with respect to the antenna normal was calculated by the following equation :

$$\tan\theta = (\tan^2\theta_v + \tan^2\theta_h)^{1/2} \tag{28}$$

where θ_v is the vertical angle with respect to the antenna normal and θ_h is the horizontal angle with respect to the antenna normal.

7.1 Low-Gain Antennas

A single orthogonal-mode cavity located on top of the fuselage at position 1 or 2 of fig. 34 will provide upper-hemispherical coverage to within 10° of the horizon with a minimum gain of about -1 dB. Experimental patterns for this antenna mounted on a cylinder, which simulates the forward fuselage, are shown in fig. 13. The gain 10° above the horizon for a top-mounted antenna is between -0.5 and -1.5 dB for an assumed 1.2-dB loss.

The presence of aerodynamic surfaces will cause interference in some directions. If model measurements indicate inadequate coverage at the required minimum-gain level in a given direction for a particular installation at position 1, a second antenna can be installed at position 2.

An orthogonal-mode cavity mounted so that the antenna normal points 60° above the horizon provides 3-dB gain 9° above the horizon. However, this antenna provides insufficient multipath protection. It was shown in Sec. 2.4 that an additional 2.3-dB fade margin must be added to the link gain budget. Thus, the equivalent gain of the antenna can be considered as 0.7 dB for the satellite communications application. Mounting the antenna so that the antenna normal points 25° above the horizon provides a 3-dB gain 9° above the horizon, but the fade margin requirements have increased by an additional 4 dB. Thus, in terms of the total link budget, the maximum equivalent gain of a low-gain antenna 9° above the horizon is approximately 1 dB.

7.2 Antennas With 3- to 6-dB Gain

The discussion in Sec. 7.1 indicated there is no location where a single antenna will provide a 3-dB gain and adequate multipath discrimination for a system fade margin of 2 dB. The required antenna discrimination to provide the 2-dB maximum fade margin is shown in figs. 9 and 10. Adequate discrimination can be realized by arraying antennas or by increasing the vertical dimensions of the antenna to decrease the elevation beamwidth. A minimum antenna depth can be realized by arraying two antennas.

Patterns of two-element and three-element arrays of orthogonal-mode cavities are shown in fig. 35. These patterns were calculated using the principle of pattern multiplication, whereby the pattern of fig. 13 was used as the element factor and the array factor is given by eq. (20). These patterns will provide the basic pattern shape. However, the final design should be based upon model antenna radiation pattern data obtained by laboratory measurements of a scaled antenna mounted on an airplane model. The maximum realizable gain for two elements is 1 to 3 dB greater than that of a single antenna element. For this discussion, a maximum gain will be assumed of 7.5 dB for the two-element array and 9.0 dB for the three-element array.

The pattern of the three-element array indicates that 6-dB discrimination at 10° above the horizon can be obtained when the beam maximum is pointed 12° above the horizon. Thus, an array of three elements or more will satisfy the system multipath discrimination requirements. The gain ±36° in azimuth will be about 1-dB less than the on-axis gain. Consider two examples of required antenna gain that might result from a typical link power budget. These examples are a required antenna gain of either +3 dB or +6 dB at 9° above the horizon. The elevation pattern of fig. 35 shows that to obtain +3-dB gain 9° above the horizon, a three-element array should be mounted so that the array normal points to 30° above the horizon. The antenna would provide a minimum of +3-dB gain from 9° to 51° in elevation and ±36° in azimuth. For the second example (an antenna gain of +6 dB at 9° above the horizon), the normal for the three-element array should be pointed to 22° above the horizon. The resulting coverage is from 9° to 35° in elevation and ±36° in azimuth. The resultant elevation coverage provided is less than the 26° elevation sector coverage required for a typical New York-to-London flight. Thus, if an antenna gain of 6 dB or greater was required for such a sector, then a need for beam steering would result.

To obtain 3-dB gain at 9° elevation and ±36° azimuth with the two-element array, assuming 7.5-dB maximum gain, the array should be mounted with the array normal 38° above the horizon. The resulting discrimination is 9.0 dB at an elevation angle of 10° and 18 dB at 20°. The resulting coverage is from 9° to 67° elevation and ± 36° azimuth.

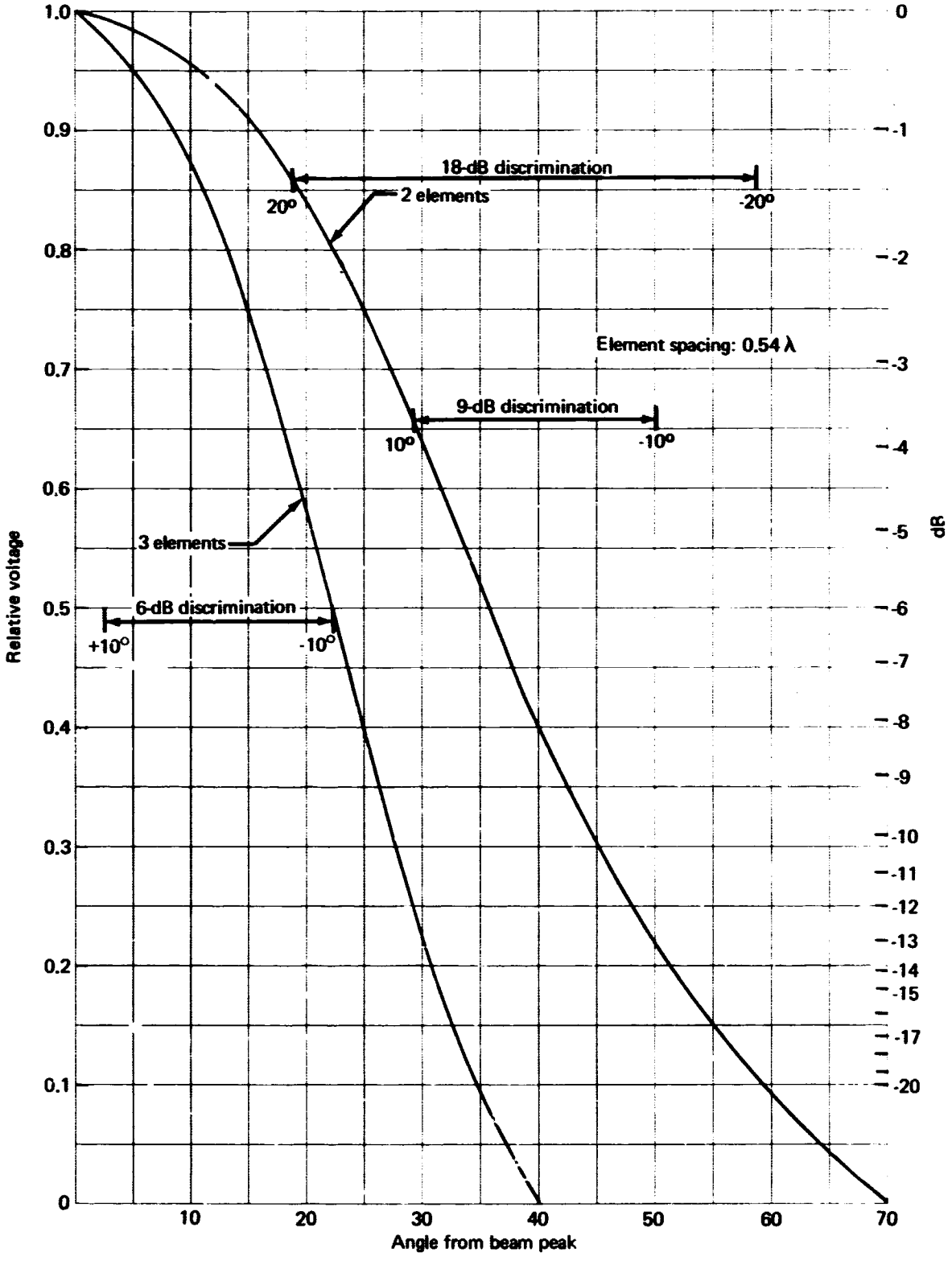

FIGURE 35.– ELEVATION PATTERNS OF TWO- AND THREE-ELEMENT ARRAYS

7.3 Antennas With 7- to 10-dB Gain

An 8-dB-gain antenna must have the multiple-beam or steerable-beam capability discussed in Sec. 7.2. The introduction of beam steering necessitates additional rf circuitry with a resulting increased loss from 0.3 dB to a maximum of 2 to 3 dB.

A four-element, 50%-efficient linear array mounted so that the array normal points 25° above the horizon will provide approximately 8-dB gain when the array points ±33° azimuth and 41° elevation. Beam steering can be accomplished by using the series feed described in Sec. 5.3.1. The loss due to the feed can be limited to about 2 dB. The principal-plane beamwidths of the array at the beam maximum are 104° and 27°. The array dimensions are 6 by 16.5 inches.

Mounting the array in a service door would require pointing the array normal toward the horizon, which results in an additional 1-dB pointing loss with respect to the optimum 25° pointing angle for scanning to 41° elevation. For this case, it may be necessary to use a six-element array. The principal-plane beamwidths of a six-element array are 104° and 17°. The array dimensions are 6 by 24 inches.

An eight-element array fed by a Butler matrix mounted so that the beam normal is pointed 25° above the horizon will meet a 7-dB gain requirement. The gain of the array for 0.54λ element spacing is shown in table 2. By increasing the array spacing to 0.57λ, the array gain can be increased by 0.2 dB. The vertical scanning requirements can be accomplished using the first two beams on each side of the normal.

Installation of the antenna in a service door would require the use of three overlapping beams on one side of the normal. The matrix can be adjusted so that the first beam maximum points to 14° above the horizon with a resulting 9.3-dB gain at the 9° minimum required angle. The third beam maximum would then point to 41°. The resulting minimum gain at the crossover point between beams 2 and 3 and ±33° azimuth would be 6.8 dB. The gain at the beam minima can be increased by summing the outputs of two adjacent beams, as discussed in Sec. 5.3.2, resulting in a minimum gain of 10 dB.

The array dimensions are 6 by 33 inches. The width of the matrix feed behind the array may be greater than 6 inches. Examples of the patterns of an eight-element array fed with a Butler matrix are shown in fig. 29.

7.4 Antennas With 13.5-dB Gain

A 10- by 30-inch parabolic cylinder antenna, or a 15-inch helix antenna, will provide 13.5 dB gain. Use of either type of antenna is possible in the wing-root area (locations 5 and 6), but coverage to 35° aft of broadside cannot be obtained.

A 2 x 8 element, 50%-efficient conformal array mounted on the side fuselage so that the normal to the array points 25° above the horizon will satisfy a 13.5-dB gain requirement. The maximum gain of the array is 14.5 dB. The gain at ± 33° azimuth and 41° elevation is 13.5 dB. The principal-plane antenna beamwidths are 56° and 14°. The antenna dimensions are 10.2 by 35 inches.

Another possible array configuration is a 4 x 4 element array that would provide approximately the same gain. The principal-plane beamwidths of this antenna would be 28° in both azimuth and elevation. The array size would be 18.4 inches square.

A 4 x 5 element, 50%-efficient array mounted in a service door would have a maximum gain of 15.5 dB. The gain at ± 33° azimuth and 41° elevation is 13.8 dB. The principal plane beamwidths are 28° and 22°. The array size would be 18.4 by 22.5 inches.

A 2 x 9 element, 50%-efficient array mounted in a service door would have a maximum gain of 15 dB. The gain at ± 33° azimuth and 41° elevation is 13.3 dB. The principal-plane beamwidths are 56° and 12.4°. The array dimensions are 10.2 by 39.1 inches.

All of these arrays would require beam steering such that the beam maximum is pointing in the direction of the satellite.

7.5 Antennas With 18-dB Gain

A 10- by 74-inch parabolic-cylinder antenna and a 30-inch parabolic dish, or a four-element quad helix with 13.5-inch elements spaced 10 inches apart with a 16-inch-square ground plane (ref. 10) will provide 18 dB gain. However, none of the potential antenna locations provides sufficient swept volume for these antennas to obtain the azimuth and elevation coverage required for the experimental terminal.

Motorola end-fire arrays mounted at locations 7 and 8 (fig. 34) 36 inches in diameter and 10 inches deep would meet the 18-dB gain requirement. Because the array is linearly polarized, an additional 2-dB gain is necessary, as discussed in Sec. 2.2. Cooling would be difficult and relatively long transmission lines would be necessary for this installation.

A conformal 6 x 8 element, 50%-efficient phased array will satisfy the gain-coverage requirement if the array is mounted on the side fuselage in such a manner that the array normal points 25° above the horizon. The maximum gain of the array is 19.2 dB. The gain at ±33° azimuth and 41° elevation is 18.2 dB. The principal-plane beamwidths when the beam is normal to the array are 18.5° and 14°. The antenna dimensions are 26.5 by 35 inches. Continuous beam steering so that the beam maximum is always pointed at the satellite is required with this antenna.

Mounting an antenna in a service door would require vertical scanning from 9° to 41° from the array normal, resulting in a maximum pointing angle along the diagonal of the array of 47°. A 6 x 9 element, 50%-efficient array will satisfy this requirement. The maximum gain of the array is 19.7 dB. The gain at ±33° azimuth and 41° elevation is 18 dB. The principal-plane beamwidths are 18.5° and 12.4°. The antenna dimensions are 26.5 by 41 inches.

7.6 Surveillance Antennas

The surveillance requirement of communicating simultaneously with two satellites indicates the desirability of a nonsteerable antenna. The experimental aircraft-terminal configuration alternates discussed in vol. V reflect this desirability. The maximum surveillance gain considered for use with a 24-dBW satellite EIRP is 5.2 dB with a corresponding voice antenna gain of 18 dB. The three-element array described in Sec. 7.2 will provide the required surveillance gain. The three elements can be a subarray in the center of the 48-element, 18-dB-gain array described in Sec. 7.5. The three elements can be directly connected to the surveillance system without switching and with very little effect on the gain of the 48-element array.

A 0.7-dB surveillance gain can be attained with a single antenna mounted on the side, as described in Sec. 7.1. This antenna can be one element of the 16-element array that is necessary to provide the 13.5-dB voice gain required for configuration of a 24-dBW satellite EIRP and a paramp receiver on the airplane.

The other alternate configurations require a surveillance gain of -1 dB. This requirement is the design goal of the single top-mounted antenna that would provide coverage without the necessity of left-right switching.

8.0 RECOMMENDED EXPERIMENTAL-TERMINAL ANTENNA SYSTEM

Selection of the experimental-terminal antenna will depend on the satellite available for the experiment. Three alternate satellite configurations are discussed in vol. V. The use of a 10-watt satellite having an earth-coverage antenna (described as alternate 1) would require an airborne antenna gain of either 13.5 or 18 dB, depending on the preamplifier used on the airplane. Any of the high-gain antennas described in Secs. 7.4 and 7.5 represent a relatively high cost and complexity because two-dimensional beam steering is required.

Use of either a 20-watt or a 75-watt, regional-coverage satellite (alternate 2) will allow demonstration of the surveillance mode of operation with a single-top-mounted, low-gain antenna similar to the orthogonal-mode cavity discussed in Sec. 3.2. Determination of the operational performance of this class of antenna is desirable, because it represents an optimum antenna system from the viewpoint of the user. Thus, it is recommended that two airplane antenna systems that can be switched (fig. 36) be used with alternate 2 satellites.

If the 20-watt satellite is used, a side-fuselage-mounted, eight-element, Butler-matrix-fed array (Sec. 7.3) is recommended, because this type of beam-steering matrix is now virtually an off-the-shelf product. However, the series feed of fig. 27 may provide better experimental versatility and performance when it is developed. Thus, an experimental study of the properties of the series feed is recommended during phase II to determine the efficiency, typical phase errors, and the ease of beam-steering control of the feed. The development of this feed would make possible the use of a four-element array (Sec. 7.2).

The Butler-matrix array will provide multiple fixed beams with gains from 7.0 to 12.0 dB that can be predicted during a flight with the knowledge of the satellite and flight-path geometry and the roll of the airplane. The four-element series-fed array would provide continuous beam steering with a maximum gain of 9 dB.

If the 75-watt satellite is available, the two-element array described in Sec. 7.2 side-fuselage mounted with the array normal 38° above the horizon is recommended to demonstrate the voice capability. The minimum gain of the antenna over the required experimental coverage area is about 3 dB.

It is recommended that the specifications for the array element be determined during phase II by measuring the properties of an array of eight sleeve-dielectric-loaded, orthogonal-mode cavities (fig. 25). The pattern perpendicular to the line of the array will be used to specify the minimum beamwidth. The measured ellipticity and efficiency of the array will be specified as minimum requirements.

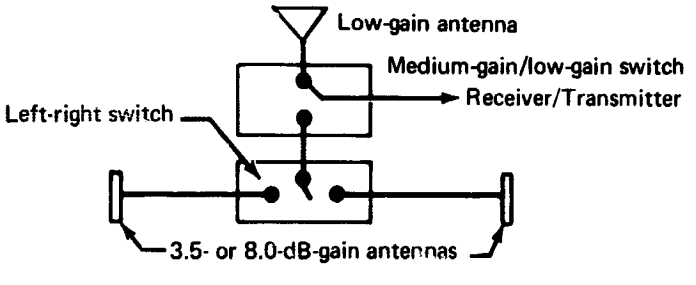

FIGURE 36.– RECOMMENDED EXPERIMENTAL ANTENNA SYSTEM

9.0 GROWTH TO OPERATIONAL TERMINAL

An operational system would require greater antenna coverage than that assumed for the experimental terminal. Ideally, complete upper-hemisphere coverage is desirable. Because there are many more airplanes than satellites, it appears cost effective to minimize the cost of the airplane terminal. However, a tradeoff study is needed to determine the optimum division of cost between the users and the satellite.

The ability to provide low-cost user systems is dependent on the availability of high EIRP on the satellite. Thus, both the satellite terminal and the airplane terminal are discussed in this section.

9.1 Satellite Systems With High Effective Radiated Power

Steerable satellite beam antennas are necessary to provide sufficient effective radiated power so that a low-gain airplane antenna system can be used. For example, satellite configuration alternate 3, shown in table 12 of vol. V, postulates 75 watts of transmitter power (18.7 dBW) and an antenna gain of 33.6 dB for three voice channels and surveillance using an antenna with -1 dB gain on the airplane. The IBM singing-array system discussed in Sec. 5.3.3 is an example of a system being developed to provide multiple high-gain beam capability on a satellite. RCA (ref. 31) also is developing a self-focusing satellite antenna system using a phased-array antenna consisting of subarrays of dipoles. The Boeing Company has also been performing analytical and experimental research on large-aperture phased-array antenna systems.

The prime objective of the Boeing study was to conceive and demonstrate a practical spacecraft array that is capable of forming many high-gain beams and compensate for spacecraft attitude variations and structural bending without user-originated pilot signals. The attainment of this objective was shown in March 1968 by the successful demonstration of an engineering model of a 10-module array of the Artificial Pilot Phased Array (APPA). A photograph of the model is shown in fig. 37.

The antenna phasing information is obtained from two earth stations by the formation of beams toward these stations using the conventional pilot tone techniques shown in fig. 38. Additional controlled beams are formed for either transmit or receive and are commanded to point in any selected direction by an artificial pilot signal in a manner similar to the pilot tone technique described in Sec. 5.3.3.

The advantages of an APPA system are summarized as follows:

(1) It is capable of forming many high-gain beams in any direction without user-pilot signals

(2) It yields high effective radiated power, although only low-level state-of-the-art rf amplifiers are required.

(3) It is capable of performing accurately under large attitude disturbances and/or deformation of the array structure.

(4) It maintains nominal performance as element failures occur.

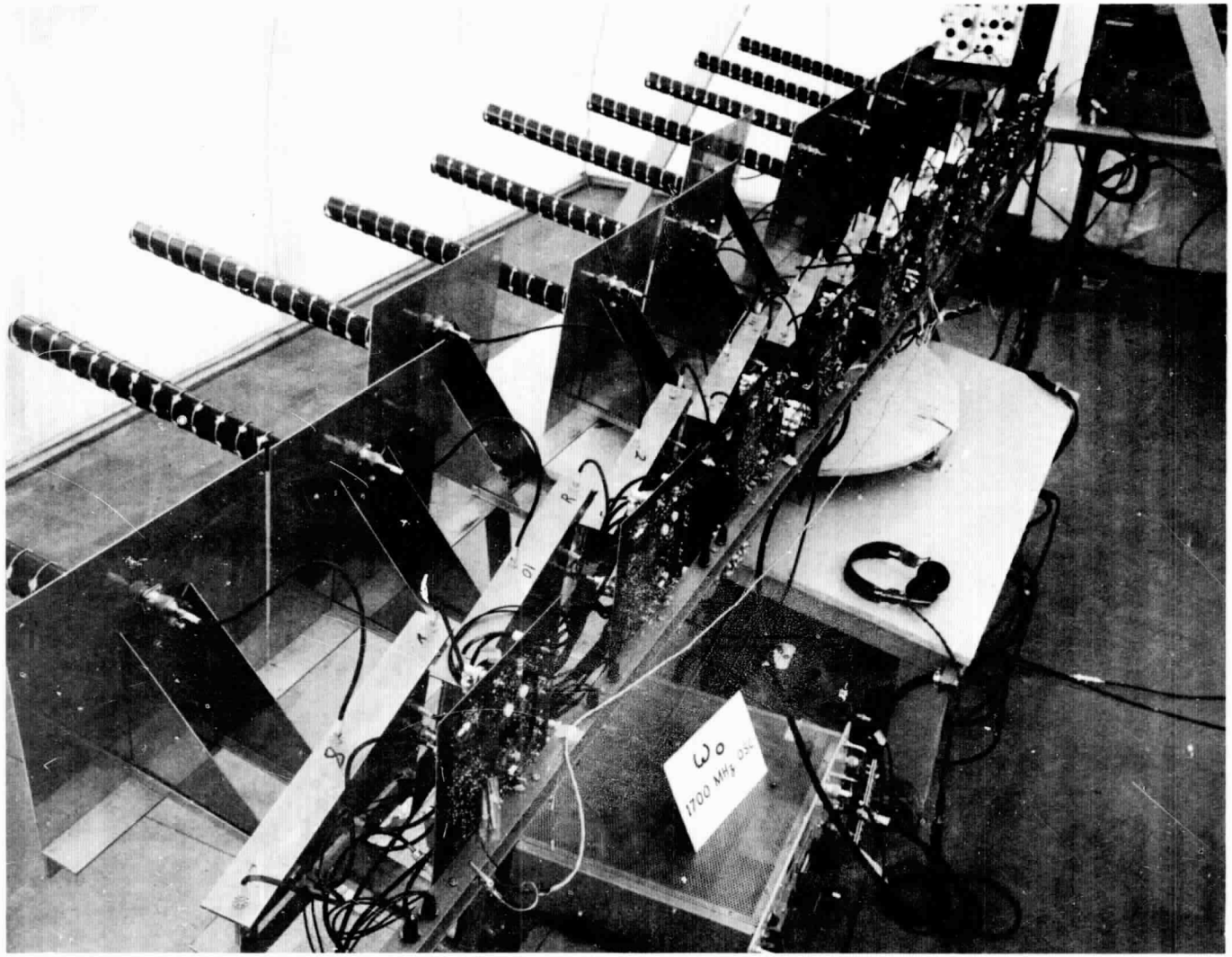

FIGURE 37.—DEMONSTRATION OF ARTIFICIAL PILOT PHASED ARRAY (APPA)

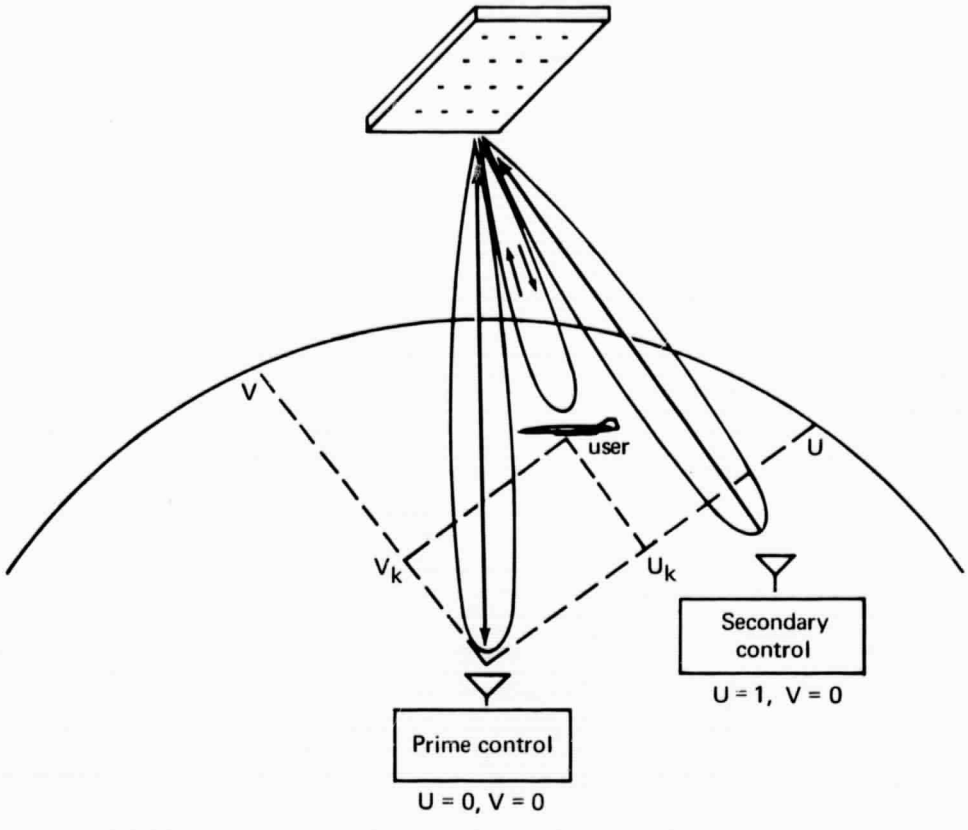

FIGURE 38.–ARTIFICIAL PILOT PHASED-ARRAY (APPA) CONCEPT

(5) It is capable of making maximum utilization of frequency and spatial diversity (multiplex) techniques.

(6) It uses easily implemented phase-control techniques.

(7) It is capable of being reprogrammed simply and quickly to establish communications channels where needed.

(8) It is independent of user modulation techniques.

(9) It does not rely upon complex rf switching matrixes or rf phase shifters for beam pointing.

9.2 Airplane Antennas

The high-ERP satellites discussed in Sec. 9.1 provide potential for an operational system using a single top-mounted simple antenna, similar to the orthogonal-mode cavity, that will provide a gain of about -3 dB throughout the entire upper hemisphere. The discussion of rf transmission-line characteristics in vol. V indicates the desirability of integrating the transmitter and receiver front-end into the antenna package so that rf transmission-line losses can be eliminated.

A cost tradeoff study may indicate desirability of a multiple-antenna installation with switching between elements for the operational system (figs. 39 and 40). The two-antenna system would provide a minimum of 3-dB gain within 10° of the horizon throughout the upper hemisphere, but it would require an increased fade margin of 4.5 dB (discussed in Sec. 2.3). Thus, the equivalent gain of the system is about 1 dB.

The three-antenna system will provide a minimum gain of 3 dB to within 5° of the horizon and ± 80° in azimuth with adequate multipath discrimination to limit the fade-margin requirements to 2 dB.

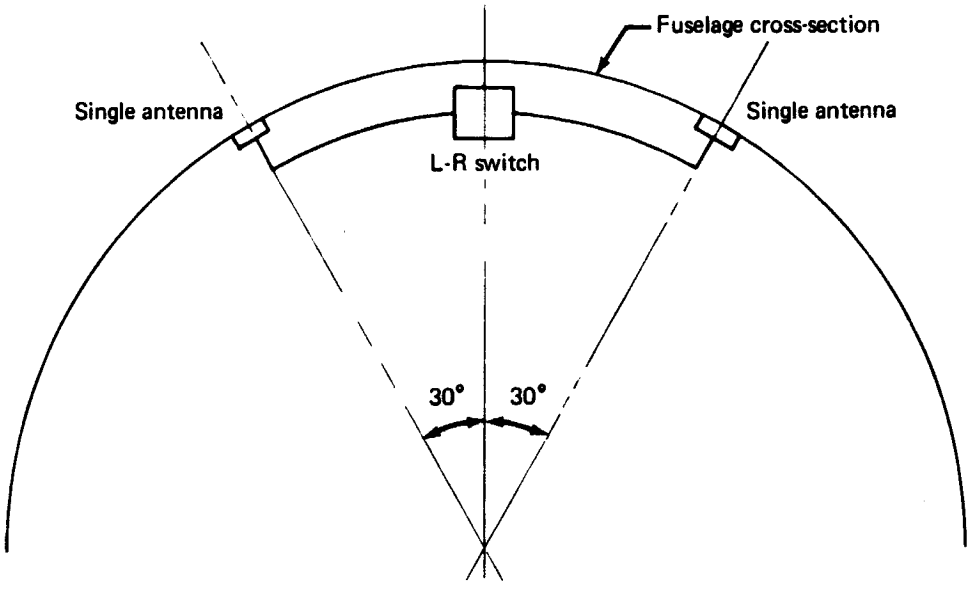

FIGURE 39.– SWITCHED TWO-ANTENNA OPERATIONAL CONFIGURATION

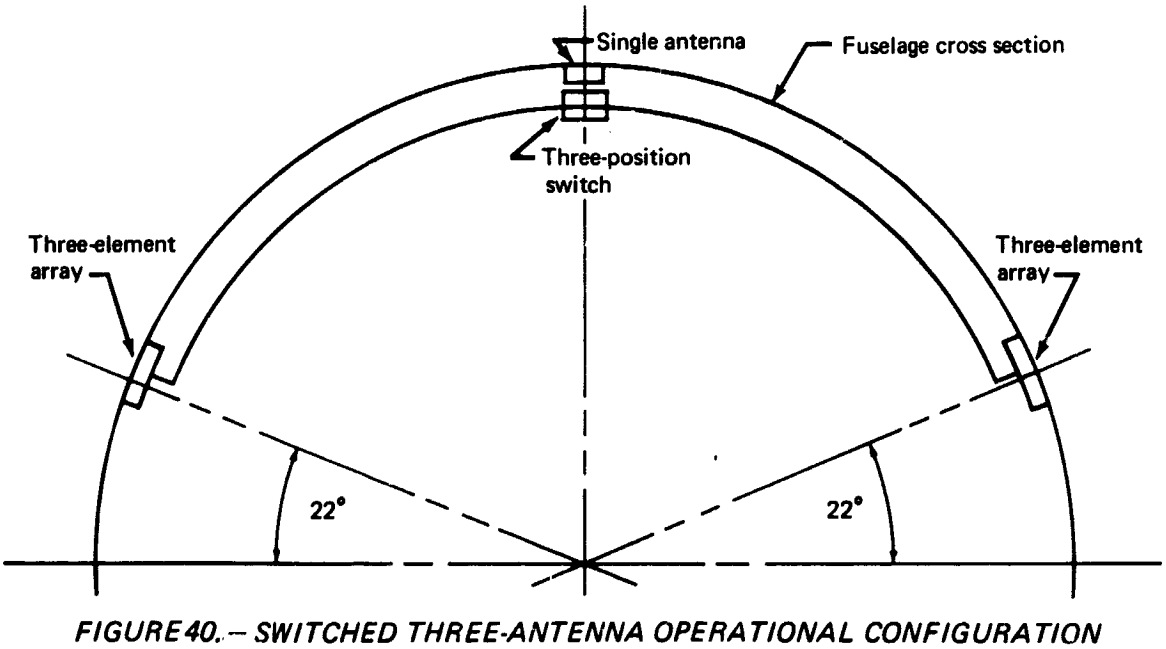

FIGURE 40.– SWITCHED THREE-ANTENNA OPERATIONAL CONFIGURATION

REFERENCES

1. Hartop: Power Loss Between Arbitrarily Polarized Antennas. Jet Propulsion Laboratory Technical Report No. 32-457, Sept. 1, 1964.

2. Stevens, Fred J.: Boeing Supersonic Transport Environment Criteria, D6A10496-1, The Boeing Company, April 25, 1967.

3. Majeau, H.: Antenna Research For Airborne Penetration Aids. Document D6-23451, The Boeing Co., 1968, Secret

4. State-of-the-Art Survey Discussion with J. Bohar, American Electronics Laboratories Inc., P.O. Box 552, Lansdale, Pa.

5. State-of-the-Art Survey Discussion with E. Bellee, Motorola, Government Electronics Division, Scottsdale, Arizona.

6. Kraus, J. K.: Antennas. McGraw Hill Book Co. Inc., New York, 1950 pp. 464-478.

7. Dyson, J. D.; and Mayes, P. E.: New Circularly Polarized Frequency–Independent Antennas with Conical Beam or Omnidirectional Patterns. IRE Transactions on Antennas and Propagation, vol. AP9, no. 4, July 1961, pp. 334-342.

8. Anon.: 1968 Product Data Sheet 322. Transco Products Inc., 4241 Glencoe Ave., Venice, Calif.

9. Jasik, H.: Antenna Engineering Handbook. McGraw-Hill Book Co., Inc., New York, 1961, Sec. 12.

10. Hatcher, E. C.: Endfire Antenna Research. Document D2-113430, The Boeing Co., 1966

11. Anon.: Annual Summary Report No. 1394-6, Ohio State University Research Foundation, Dec. 1, 1962.

12. Allen, John; et al: Phased Array Radar Studies. Lincoln Labs Technical Report No. 236, Nov. 1961.

13. Parad and Kruetal: Mutual Effects Between Circularly Polarized Elements. Antenna Arrays Section of the Abstracts of the Twelfth Annual Symposium on USAF Antenna Research and Development Program, University of Illinois, Oct. 1962.

REFERENCES–Continued

14. Tai, C. T.: The Optimum Directivity of Uniformly Spaced Broadside Arrays of Dipoles. Transactions of the IEEE, vol. AP12, no. 4, July 1964, pp. 447-454.

15. Meier, P. J.; and Wheeler, H. A.: Dielectric Lined Circular Waveguide with Increased Usable Bandwidth. Transactions of the IEEE, vol. MIT12, March 1964.

16. Meier, P. J.; Balfour, M. A.; and Wheeler, H. A.: Circular Waveguide Loaded with Dielectric Disks for Increased Usable Bandwidth. 1964 International Symposium of the Professional Group of Microwave Theory and Techniques Group Abstracts, p. 33.

17. Cappucci, J. D.: Lumped Element Circuit Components, Microwave Journal, Jan. 1968, p. 100-107.

18. Smith, J. K.: Antenna Array Phasing Device. Boeing Patent Disclosure No. 68-123, Feb. 19, 1968.

19. Butler, J.; and Lowe, R.: Beam Forming Matrix Simplifies the Design of Electronically Scanned Antennas. Electronic Design, vol. 9, April 12, 1961, pp. 170-173.

20. State-of-the-Art Survey Discussion with Don Venters, Sanders Associates, Microwave Division, Nashua, N. H.

21. Ross, G.; and Schwartzman, L.: Continuous Beam Steering and Null Tracking with a Fixed Multiple Beam Antenna Array System. Transactions of the IEEE, vol. AP12, Sept. 1964.

22. Bickmore, R. W.: Adaptive Antenna Arrays. IEEE Spectrum, Aug. 1964, pp. 78-88.

23. Cutler, C.C.; Kompfner, R.; and Tillotson, L.C.: A Self-Steering Array Repeater. Bell System Technical Journal, Sept. 1963, pp. 2013-2032.

24. Anon.: Ryan Integrated Antenna Programs. Ryan Electronic and Space Systems Div. Report No. 29174-99A, March 1, 1968 (and State-of-the-Art Survey Discussion with T. Witkowski).

25. State-of-the-Art Survey Discussion with E.L. Gruenberg, IBM Federal Systems Division, Thomas J. Watson Research Center, Yorktown Heights, N. Y.

REFERENCES–Concluded

26. Arnold, R. D.; et al: Microwave Integrated Circuit Applications to Radar Systems. The Microwave Journal, July 1968, pp. 45-52.

27. Sobol, H.: Extending IC Technology to Microwave Equipment. Electronics, March 20, 1967, pp. 112-124.

28. State-of-the-Art Survey Discussion with I.R. Colldeweih, Dalmo Victor, 1515 Industrial Way, Belmont, California

29. Anon.: Large High-Temperature Sandwich Structures Manufacturing Technology Development. Interim Engineering Progress Report IR-9-352 (VIII), Manufacturing Technology Division, Air Force Materials Laboratory, Air Force Systems Command, USAF, Wright-Patterson AFB, Ohio, Jan. 1968.

30. Wong, G. G.: Wide Angle Coverage Circularly Polarized Antenna for NAVSAT Application. Proceedings of the 20th National Aerospace Conference (NAECON), Dayton, Ohio, May 1968.

31. State-of-the-Art Discussion with J.D. Kiesling and M.W. Mitchell, RCA, Moorestown, N.J.